U.S. Department of Transportation
Federal Railroad Administration

Office of Research, Development and Technology
Washington, DC 20590

Automated Weld Repair of Manganese Frogs for Extended Service Life

DOT/FRA/ORD-24/29

Final Report | August 2024

REPORT DOCUMENTATION PAGE

Form Approved

OMB No. 0704-0188

1. AGENCY USE ONLY (Leave blank)	2. REPORT DATE	3. REPORT TYPE AND DATES COVERED
	November 2021	Technical Report (November 2018 – June 2020)

4. TITLE AND SUBTITLE

Automated Weld Repair of Manganese Frogs for Extended Service Life

5. FUNDING NUMBERS

Contract # DTFR53-16-C-00002

6. AUTHOR(S)

Seth Shira

7. PERFORMING ORGANIZATION NAME(S) AND ADDRESS(ES)

EWI
1250 Arthur E. Adams Dr.
Columbus, OH 43221

8. PERFORMING ORGANIZATION REPORT NUMBER

9. SPONSORING/MONITORING AGENCY NAME(S) AND ADDRESS(ES)

U.S. Department of Transportation
Federal Railroad Administration
Office of Railroad Policy and Development
Office of Research, Development, and Technology
Washington, DC 20590

10. SPONSORING/MONITORING AGENCY REPORT NUMBER

DOT/FRA/ORD-24/29

11. SUPPLEMENTARY NOTES

COTR: Cameron Stuart

12a. DISTRIBUTION/AVAILABILITY STATEMENT

12b. DISTRIBUTION CODE

13. ABSTRACT (Maximum 200 words)

EWI completed research and testing of an automated weld repair process for austenitic manganese steel railroad frogs. This report covers the second of two projects sponsored by the Federal Railroad Administration and EWI executed this research between March 2016 and June 2022. In this phase of work, EWI developed a metal-cored filler material and a pulsed gas metal arc welding process to repair two worn frogs, one for CSX and the other for NS. Revenue service testing of both frogs exceeded expectations for wear rates and longevity as compared to both new frogs and frogs repaired with traditional field techniques. This report documents EWI's weld repair process and field testing results; it also presents a conceptual view of a fully automated frog repair process. This research has demonstrated that an automated weld repair of frogs is feasible and can extend the service life of railroad frogs.

14. SUBJECT TERMS

Constant voltage, CV, flux-cored arc welding, FCAW, pulse gas metal arc welding, GMAW-P, radiographic testing, RT, ultimate tensile strength, UTS, yield strength, YS, rail frog, rail turnout, frog point, frog wings, solid state welding

15. NUMBER OF PAGES

98

16. PRICE CODE

17. SECURITY CLASSIFICATION OF REPORT	18. SECURITY CLASSIFICATION OF THIS PAGE	19. SECURITY CLASSIFICATION OF ABSTRACT	20. LIMITATION OF ABSTRACT
Unclassified	Unclassified	Unclassified	

NSN 7540-01-280-5500

Standard Form 298 (Rev. 2-89)
Prescribed by ANSI Std. 239-18
298-102

METRIC/ENGLISH CONVERSION FACTORS

ENGLISH TO METRIC	METRIC TO ENGLISH
LENGTH (APPROXIMATE)	**LENGTH (APPROXIMATE)**
1 inch (in) = 2.5 centimeters (cm)	1 millimeter (mm) = 0.04 inch (in)
1 foot (ft) = 30 centimeters (cm)	1 centimeter (cm) = 0.4 inch (in)
1 yard (yd) = 0.9 meter (m)	1 meter (m) = 3.3 feet (ft)
1 mile (mi) = 1.6 kilometers (km)	1 meter (m) = 1.1 yards (yd)
	1 kilometer (km) = 0.6 mile (mi)
AREA (APPROXIMATE)	**AREA (APPROXIMATE)**
1 square inch (sq in, in^2) = 6.5 square centimeters (cm^2)	1 square centimeter (cm^2) = 0.16 square inch (sq in, in^2)
1 square foot (sq ft, ft^2) = 0.09 square meter (m^2)	1 square meter (m^2) = 1.2 square yards (sq yd, yd^2)
1 square yard (sq yd, yd^2) = 0.8 square meter (m^2)	1 square kilometer (km^2) = 0.4 square mile (sq mi, mi^2)
1 square mile (sq mi, mi^2) = 2.6 square kilometers (km^2)	10,000 square meters (m^2) = 1 hectare (ha) = 2.5 acres
1 acre = 0.4 hectare (he) = 4,000 square meters (m^2)	
MASS - WEIGHT (APPROXIMATE)	**MASS - WEIGHT (APPROXIMATE)**
1 ounce (oz) = 28 grams (gm)	1 gram (gm) = 0.036 ounce (oz)
1 pound (lb) = 0.45 kilogram (kg)	1 kilogram (kg) = 2.2 pounds (lb)
1 short ton = 2,000 pounds (lb) = 0.9 tonne (t)	1 tonne (t) = 1,000 kilograms (kg)
	= 1.1 short tons
VOLUME (APPROXIMATE)	**VOLUME (APPROXIMATE)**
1 teaspoon (tsp) = 5 milliliters (ml)	1 milliliter (ml) = 0.03 fluid ounce (fl oz)
1 tablespoon (tbsp) = 15 milliliters (ml)	1 liter (l) = 2.1 pints (pt)
1 fluid ounce (fl oz) = 30 milliliters (ml)	1 liter (l) = 1.06 quarts (qt)
1 cup (c) = 0.24 liter (l)	1 liter (l) = 0.26 gallon (gal)
1 pint (pt) = 0.47 liter (l)	
1 quart (qt) = 0.96 liter (l)	
1 gallon (gal) = 3.8 liters (l)	
1 cubic foot (cu ft, ft^3) = 0.03 cubic meter (m^3)	1 cubic meter (m^3) = 36 cubic feet (cu ft, ft^3)
1 cubic yard (cu yd, yd^3) = 0.76 cubic meter (m^3)	1 cubic meter (m^3) = 1.3 cubic yards (cu yd, yd^3)
TEMPERATURE (EXACT)	**TEMPERATURE (EXACT)**
[(x-32)(5/9)] □F = y □C	[(9/5) y + 32] □C = x □F

QUICK INCH - CENTIMETER LENGTH CONVERSION

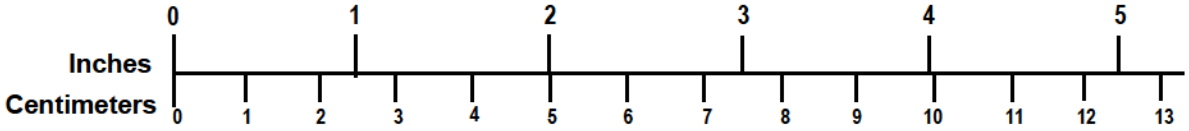

QUICK FAHRENHEIT - CELSIUS TEMPERATURE CONVERSIO

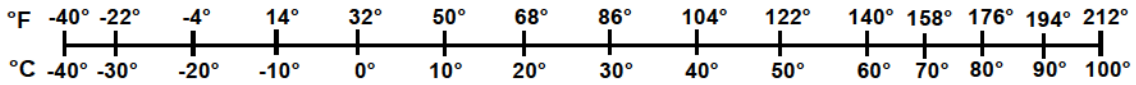

Contents

Illustrations

Tables

Executive Summary

EWI completed Federal Railroad Administration (FRA)-sponsored research and testing of an automated weld repair process for austenitic manganese steel (AMS) railroad frogs. This report documents the second of two projects, sponsored by the Federal Railroad Administration, to investigate automated frog repair methods that can improve the service life of these components. EWI executed this research from March 2016 through June 2020.

Special trackwork components, including AMS turnout frogs, are safety-critical elements in railroad track. They are subjected to high-impact forces due to their unique construction and functional requirements, and their wear rate is much higher than normal-running rail surfaces. Railroads have developed repair procedures for these items which effectively restore the running profile of the rail but do not provide the same service life as new components. Worn or damaged frogs in freight and shared corridors can have a detrimental effect on ride quality and can increase the life cycle costs of track and rolling stock systems. Repair processes that can extend the service life of frogs will improve the safety and efficiency of rail operations.

EWI developed and tested a robot-based, automated weld repair process for AMS frogs. The project work included a baseline study of current manual repair processes, the use of off-the-shelf flux-cored arc welding wire with robotic motion for repair, and the development of a metal-cored wire for use with pulsed gas metal arc welding and robot motion. These new materials and techniques reduced weld heat input during the repair process while improving weld deposition rates and overall weld quality. EWI also developed a crack mitigation strategy for welds that tie into a work-hardened frog running surface. Researchers repaired and tested three frogs using the new process. One frog was tested at the U.S. Department of Transportation's Transportation Technology Center (Phase 1), and two frogs underwent revenue service tests with support from CSX and Norfolk Southern Railway (Phase 2). All in-track testing of frogs repaired by EWI resulted in a longer service life than the average first-time weld repair, and the performance of the two revenue service frogs exceeded the average service of a new frog before requiring a weld repair.

This report documents EWI's weld repair process and field testing results; it also presents a conceptual view of a fully automated frog repair process. This research has demonstrated that an automated weld repair of frogs is feasible and can extend the service life of railroad frogs.

1. Introduction

From March 2016 to June 2020, EWI completed Federal Railroad Administration (FRA)-sponsored research and testing of an automated weld repair process for austenitic manganese steel (AMS) railroad frogs. This report documents the second phase of research to investigate automated frog repair methods that can improve the service life of these components.

In the first phase, EWI investigated methods of improving quality and increasing productivity via the use of automation and the flux-cored arc welding (FCAW) process [1]. Phase 1 concluded with a successful field test of a repaired frog at the Transportation Technology Center (TTC) in Pueblo, Colorado. This next phase of work advances the automated welding technique using pulsed gas metal arc welding (GMAW-P) technology and a metal-cored electrode and documents the long-term in-service performance of repaired frogs. This research and development effort was made possible with the support of CSX and Norfolk Southern Railway (NS).

1.1 Background

Worn or damaged special trackwork rolling surfaces can be repaired to extend their lifetime, but current repair methods typically cannot achieve original durability. This is particularly true for AMS turnout frogs. Welding AMS is challenging, as it requires rapid cooling rates, low heat inputs, and minimal heating of the base material to retain the mechanical properties that result in high toughness and wear resistance. Manual or semi-automatic field repair of AMS frogs must resolve the inherent conflict between stringent limits on inter-pass temperature and the productivity level required to minimize track downtime. Time constraints often mean that only a portion of the frog can be repaired, and the resulting rail surface height mismatch leads to further damage before a full repair can be completed. Traditional repair processes are shielded metal arc welding and semi-automatic (manually applied) self-shielded FCAW. Special techniques are used to limit heat buildup.

The application of modern welding materials and techniques to this repair operation may provide advantages in both productivity and component service life. Automated arc welding processes have a track record of improved weld quality, reduced heat input, and increased productivity when compared to manual welding processes.

1.2 Objectives

The objective of this project was to build on the success of the first phase and advance the automated weld repair technology and technique through improved materials, processes and field testing of additional frogs. EWI investigated the use of a metal-cored electrode to increase weld quality and to simplify the automated system by eliminating weld slag and the need for inter-pass weld cleaning. EWI tested the efficacy of the modified processes through field testing of 2 repaired frogs, one installed in CSX track and the other on NS track. EWI completed regular inspections of these frogs while in service and performed a detailed post-service inspection of the CSX frog. A post-service inspection of the NS frog was not possible during the period of performance of this project, but is planned.

1.3 Overall Approach

The project scope included the development of a new welding electrode, the repair and testing of two worn frog assemblies, post-test analysis of one repaired frog, and a conceptualization of a fully automated repair process. These work items are briefly described below.

Metal-Cored Electrode Development

Working with a supplier, Devasco International, Inc. (Devasco), EWI developed a metal-cored welding electrode designed to eliminate the need to perform inter-pass weld slag cleaning and to enhance the work hardening properties of the repaired frog. EWI tested and compared the material characteristics and performance of the new electrode against the performance from the FCAW process employed in the earlier program.

CSX Frog Repair

EWI completed inspection, preparation, weld repair, and final inspection on a worn #20, flat-top frog supplied by CSX. This work was conducted at EWI facilities in Columbus, Ohio.

CSX Frog Revenue Service Testing

CSX installed the repaired frog in mainline track at Decatur Junction in northern Alabama. EWI and CSX performed routine inspections of the frog for 13 months. These inspections included a mix of visual inspection, profile measurement, hardness measurement, and dye penetrant inspection. CSX completed maintenance grinding as required.

CSX Frog Post-Test Analysis

CSX removed the repaired frog from track after 13 months and approximately 68 MGT of service. CSX returned the frog to EWI and EWI performed a thorough analysis of the worn condition.

NS Frog Repair

NS supplied a worn welded boltless manganese (WBM) conformal top frog to EWI for automated weld repair. EWI used the same repair process on this frog as with the CSX frog.

NS Frog Revenue Service Testing

NS installed the repaired WBM frog in a heavy-haul line near Nicholasville, Kentucky. NS provided traffic (MGT) and grinding information to EWI for the test period. EWI and NS visited the frog five times to collect hardness data and perform penetrant inspection in the repaired areas. The project period of performance expired before this frog reached the end of its service life.

Concept of a Fully Automated Repair Process

The repair process detailed in this report is partially automated. Only the welding part of the process is fully automated. All other steps in the process from initial inspection to post-weld grinding are manual. In this task, EWI develop a conceptual design for a fully automated frog repair process that can be performed on site, or at a welding plant.

1.4 Scope

The project's major task milestones are listed in Table 1. All the work proposed was performed by EWI, CSX, and NS in accordance with the work breakdown structure (WBS), shown in Figure 1.

Table 1. Major task milestones

WBS No.	Task Description	Milestone Completion Week
1	**Development of a Custom Metal-Cored Electrode**	16
1.1	Chemistry Analysis and Custom Electrode Procurement	12
1.2	Metal-Cored Buildup and Evaluation	12
1.3	Interim Report	16
2	**CSX Frog Repair**	24
2.1	Repair of Supplied Frog	22
2.2	Interim Report	24
3	**CSX Frog Revenue Service Testing**	105
3.1	Site Visits	105
3.2	Testing and Monitoring	105
4	**CSX Revenue Service Post-Test Wear Analysis**	123
4.1	Nondestructive Evaluation	108
4.2	Destructive Evaluation	112
4.3	Mechanical Testing	116
4.4	Interim Report	123
5	**NS Frog Repair**	212
5.1	Repair of Supplied Frog	130
5.2	Interim Report	212
6	**NS Frog Revenue Service Testing**	224
6.1	Site Visits	220
6.2	Testing and Monitoring	220
6.3	Final Report	225

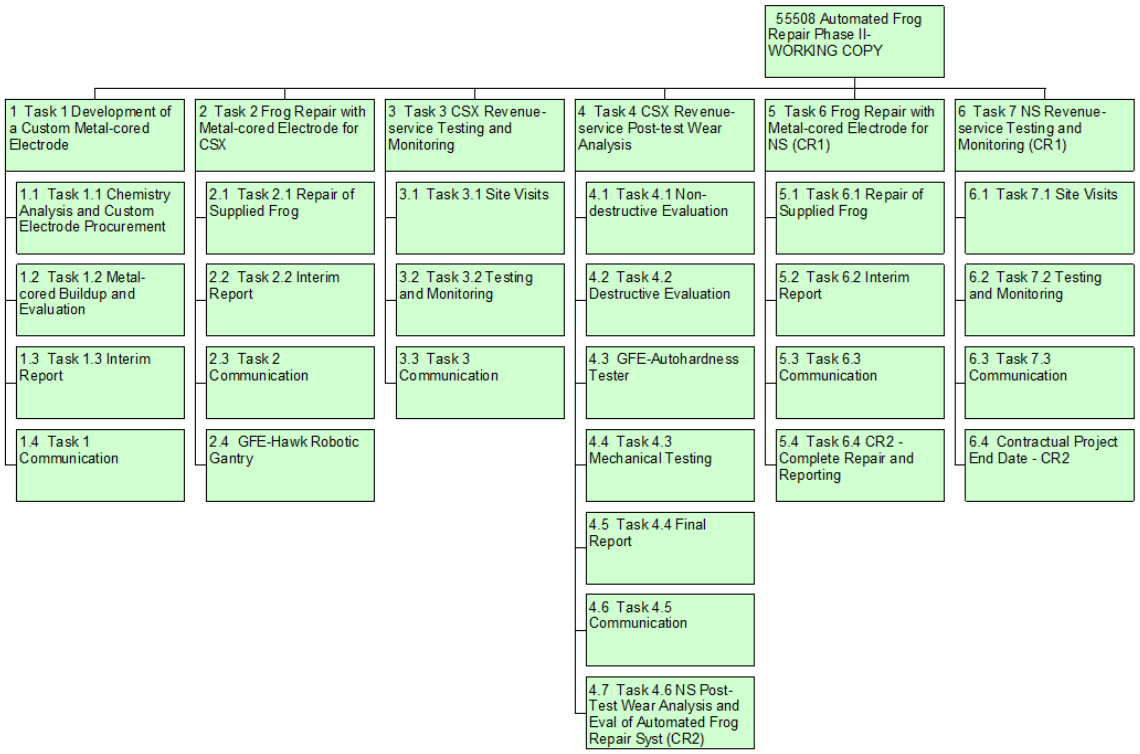

Figure 1. Work breakdown structure

1.5 Organization of the Report

This report is organized to match the chronology of the project. Section 2 documents the development and testing of the metal-cored electrode and GMAW-P welding process. Section 3 details the repair of the CSX frog. Section 4 presents the field test data collected during the service life of the repaired CSX frog. Section 5 covers the post-service inspection of the CSX frog. Section 6 documents EWI's repair of the NS-supplied WBM frog. Section 7 presents the field test data from NS through the end of the project. Finally, Section 8 highlights the conclusions from the effort, including an overview of a fully automated repair concept. Appendix A contains more details on the fully automated repair concept.

2. Development of a Custom Metal-Cored Electrode

The FCAW process generates a slag that must be removed prior to depositing subsequent weld beads. If slag is not properly removed, it can result in linear inclusions in the weld metal that will negatively affect the mechanical properties and performance of the repair. To avoid the risk of slag inclusions from the FCAW process, alternative wires and processes can be evaluated. One such approach is the use of metal-cored wire. Metal-cored electrodes are widely used and known to provide high-quality welds. They use a powdered core that allows the manufacture of custom electrodes in smaller batches than traditional wires. Additionally, metal-cored electrodes can be made to chemistries that are highly work-hardenable, such as the high-manganese steel electrode chemistry commonly used for AMS frog repair. Metal-cored electrodes produce a weld deposit that does not produce slag and does not require the same level of cleaning as flux-cored wire.

2.1 Technical Approach

The technical approach for this phase of the project included: 1) procure the required base materials and consumables to create a sample buildup using flux-cored wire, 2) evaluate the chemistry and mechanical properties, and 3) develop a metal-cored wire based on the results. EWI created welding mockups using 2-inch-thick sections of actual frog material donated by TTCI during Phase 1. The mockups were approximately 2 inches wide by 8.5 inches long, and were welded to a carbon-steel baseplate using 308 stainless steel electrodes (Figure 2, Figure 3). This material was waterjet-cut and ground smooth prior to welding. The approach produced a buildup using the same flux-cored wire and the same welding parameters, bead sequence, and stacking techniques as used in Phase 1[1]. The process ensured the temperature of the base material was kept below 500°F at a distance of 1 inch from the weld. The buildups were sized to accommodate all necessary testing, including three sub-scale tensile specimens, three Charpy V-notched (CVN) specimens, one metallographic section, and one chemistry test.

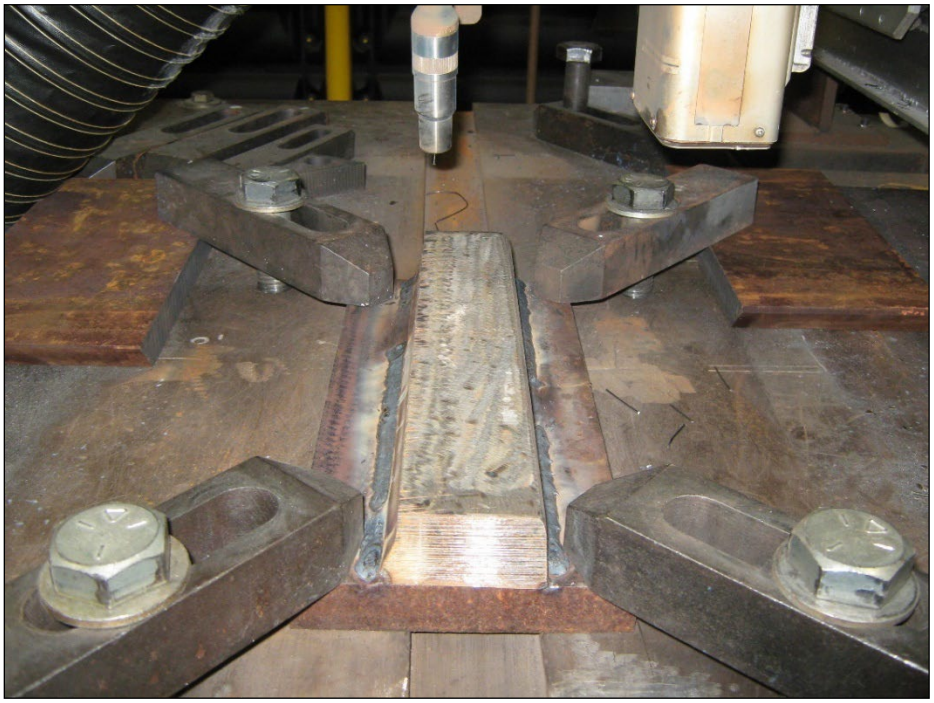

Figure 2. Mockup configuration

Figure 3. Buildup marked for testing

EWI completed the testing, selected the appropriate chemistry, and communicated these requirements to Devasco. The company uses sophisticated in-house manufacturing equipment and processes to meet the precise requirements for its custom welding wire. Based on the chemistry requirements, Devasco then used their internal methods to formulate, create, and test a metal-cored wire. EWI also evaluated the results to ensure the chemistry fell within the necessary requirements.

Weld parameters were developed with the metal-cored wire to produce similar bead-stacking characteristics as with the flux-cored wire. The goal of this effort was to ensure the mechanical properties, as well as chemistry, met or exceeded that of the flux-cored wire.

2.2 Weld Buildup with FCAW

EWI produced the flux-cored buildup using the same parameters and bead-stacking techniques used in Phase 1 (Table 2, Table 3). When repairing a frog, weld beads must be deposited on the corner of the point as well as in the middle. These two scenarios present different challenges from a welding standpoint. As illustrated in Figure 4, welds placed on the corner of the point are at risk of "drooping" due to the force of gravity. After the two corner beads are deposited, center beads can be deposited without fear of drooping (Figure 5). In this case, a higher heat input parameter can be used for increased productivity. EWI developed two welding parameter sets during Phase 1 to address these different scenarios. A lower-heat input (cold) parameter was developed to allow weld beads to be deposited on a corner without drooping (Table 3). A high-heat input (hot) parameter was developed for use on center beads to create a flat weld bead that would allow for adequate tie-

in when welding in the middle of the mock-up and to provide adequate heat to reduce slag inclusions (Table 3). The mockup was allowed to cool below 250°F between weld beads.

Table 2. FCAW equipment

Power Supply	Lincoln Powerwave 455
Mode	91
Wire	0.045 Stulz XL
Shielding Gas	75% Ar/25% CO_2 @ 45 CFH
Tip-to-Work	0.625 in.
Travel Angle	15° drag

Table 3. FCAW welding parameters

	Cold (for edges)	**Hot (for interior)**
Wire Feed Speed (ipm)	240	400
Arc Voltage (V)	21	28
Travel Speed (ipm)	15	15
Arc Current (A)	140–150	200–215

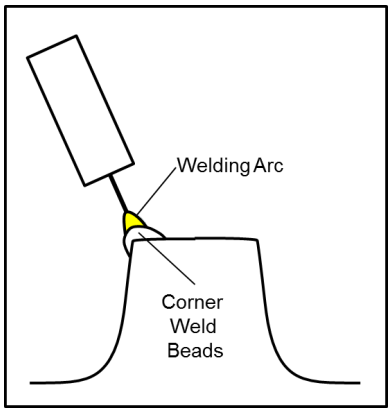

Figure 4. Corner/edge bead welding

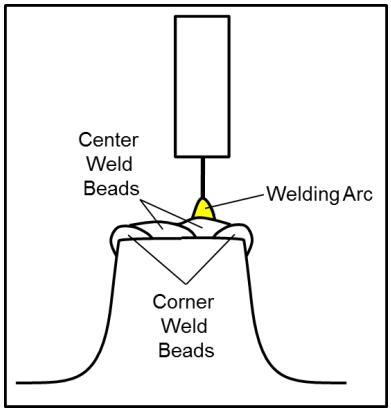

Figure 5. Center bead welding

These welding parameters resulted in a buildup that was seventeen layers high with seven beads on each layer, producing a 1.5-inch-tall deposit (Figure 6). Slag was removed from each weld bead using a chipping hammer and wire brushed to ensure there was no remaining slag prior to depositing the next weld bead.

Figure 6. FCAW macrograph

2.3 Evaluation of Flux-Cored Buildup

EWI evaluated the FCAW buildup by testing tensile specimens, CVN testing, and chemistry analysis. EWI extracted specimens from the build through machining at the approximate locations shown in Figure 7. The tensile specimens were prepared and tested per ASTM E8. The size and dimensions are shown in Figure 8. The CVN specimens were prepared and tested per ASTM E23. The size and dimensions are in Figure 9.

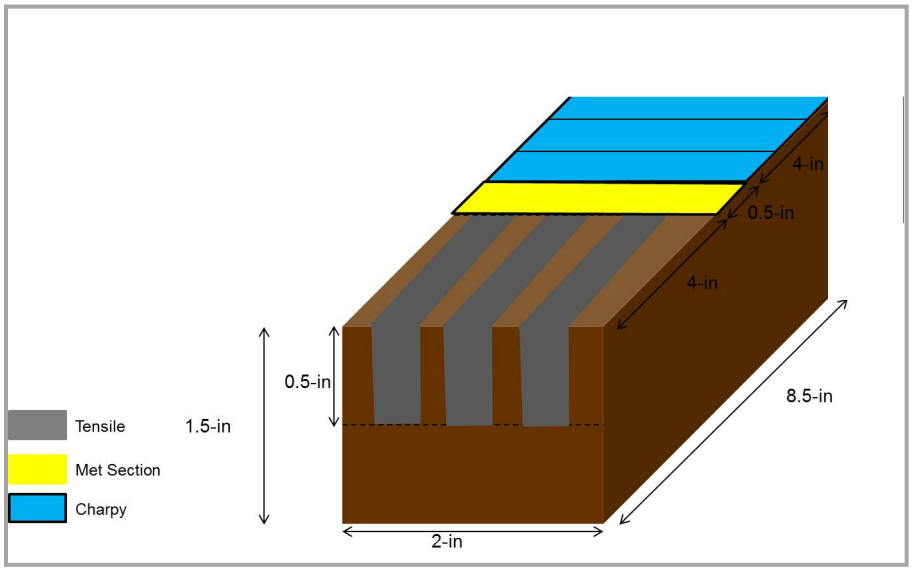

Figure 7. Weld buildup test specimen locations

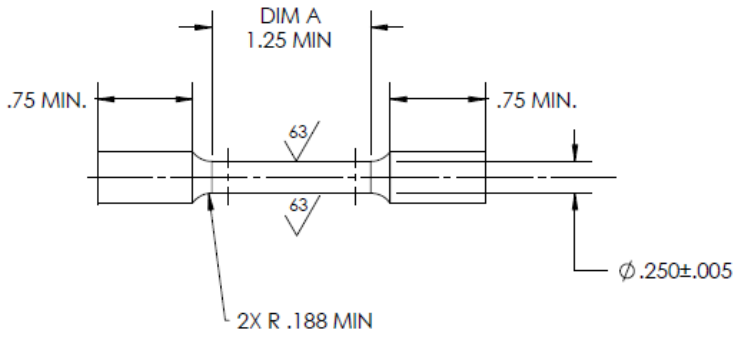

Figure 8. ASTM E8 specimen configuration

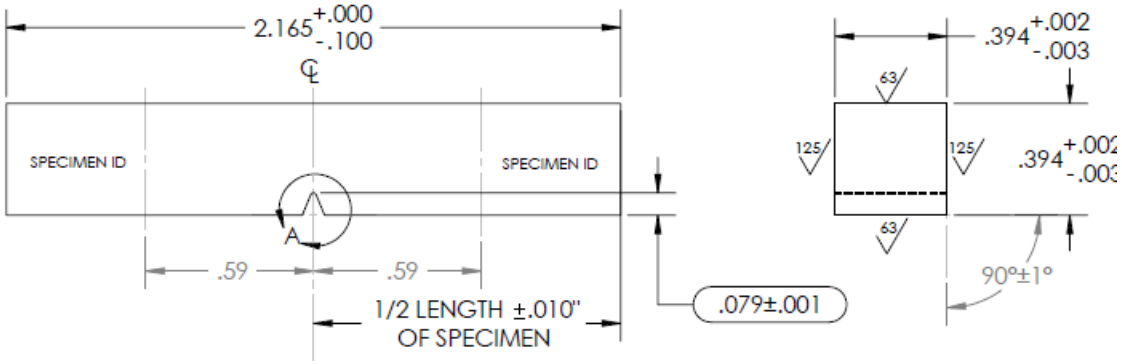

Figure 9. CVN specimen configuration

Coincident with EWI's work, Devasco created its own buildup, using the same flux-cored wire and the same parameters, but with a different buildup size. This second specimen provided an additional chemistry composition dataset for comparison. Table 4 compares the results from Phase 1, the EWI test, and the Devasco test of flux-cored buildups. Some of the elements in the weld chemistry are more critical to weld quality and durability than others. The critical elements are carbon, manganese, nickel, and chromium. Carbon increases mechanical strength, manganese increases hardenability and tensile strength, nickel increases ductility and toughness, and chromium provides corrosion resistance. These elements affect the performance of the weld material and the life of the repair. The results shown in Table 4 indicate that the flux-cored buildups performed at EWI and at Devasco produced similar results as the earlier project.

Table 4. FCAW electrode chemistry comparison

Element	Phase 1 FCAW	EWI FCAW	Devasco FCAW
C	0.86	0.82	0.84
Mn	14.38	16	14.93
Ni	0.59	0.58	0.62
Cr	4.31	4.89	4.13
Cu	0.05	0.038	0.08
P	0.008	0.021	0.016
S	0.01	0.012	0.009
Si	0.04	0.061	0.02
Al	0.01	0.003	<0.01
V	0.03	0.026	0.01
Ti	0.05	0.029	0.02

Mechanical testing was also performed on the same flux-cored buildup to get a baseline. The tensile results are shown in Table 5 and CVN results are in Table 6.

Table 5. Phase 1 and Phase 1I FCAW tensile testing results

Phase 1 FCAW Tensile Testing Results		Phase 1I FCAW Tensile Testing Results	
Ultimate Strength (ksi)	0.2% Yield Strength (ksi)	Ultimate Strength (ksi)	0.2% Yield Strength (ksi)
108.6	73.8	133.4	80.3
112.3	74	132.3	81.5
115.5	73.3	135.6	80.8

Table 6. Phase 1 and Phase 1I FCAW CVN testing results

Phase 1 FCAW Charpy Testing Results		Phase 1I FCAW Charpy Testing Results	
Test Temp (°C)	Absorbed Energy (ft-lbs)	Test Temp (°C)	Absorbed Energy (ft-lbs)
-35	30	-35	42
-35	32	-35	41
-35	33	-35	39

2.4 Metal-Cored Electrode Development

Based on the results from testing the flux-cored buildup chemistry, EWI instructed Devasco to develop a metal-cored electrode. The requirements are shown in Table 7. Devasco suggested using a 0.052-inch-diameter metal core, larger than the 0.045-inch-diameter, flux-cored electrode. The larger diameter allows the wire to be formed more easily and cost efficiently. In addition, the larger diameter enables more consistency in the product.

Table 7. Metal-cored wire chemistry requirements

Element	Devasco MC1 (%)
C	0.7–0.10
Mn	13.9–15.9
Ni	0.45–0.75
Cr	3.1–5.2
Cu	0.04–0.20
P	0.02 max
S	0.015 max
Si	0.05 max
Mo	0.03 max
Al	0.03 max
V	0.03 max
Ti	0.05 max
W	0.03 max

Devasco manufactured 100 lbs of 0.052-inch-diameter, metal-cored electrode and evaluated the chemistry against EWI's requirements. The actual resulting values fell within the specified range (Table 8).

Table 8. Devasco metal-cored electrode chemistry results

Element	Min.	Max.	Actual
C	0.7	0.10	0.86
Mn	13.9	15.9	14.38
Ni	0.45	0.75	0.59
Cr	3.1	5.2	4.31
Cu	0.04	0.20	0.05
P		0.02	0.008
S		0.015	0.010
Si		0.05	0.04
Mo		0.03	0.01
Al		0.03	0.01
V		0.03	0.03
Ti		0.05	0.05
W		0.03	0.02

2.5 Constant Voltage Weld Buildup and Evaluation

For comparison purposes, EWI developed metal-core electrode welding parameters like those used with the flux-cored wire. However, the wire feed speed was lower due to the larger-diameter material (Table 9). The parameters resulted in a buildup 19 layers high, with 7 beads on each layer, and produced a 1.5-inch-tall deposit that can be seen in Figure 10. The initial buildup width was less than the desired 2 inches. To achieve this width, EWI rotated the buildup 90° and deposited two layers of weld material. These extra passes can be seen on the right side of the buildup in Figure 10.

Table 9. FCAW vs. metal-cored wire parameters

Parameter	FCAW		MC1	
	Cold	Hot	Cold	Hot
CTWD (in.)	0.625	0.625	1	1
Travel Angle (°)	15 (drag)	15 (drag)	14 (drag)	14 (drag)
Shielding Gas	75% Ar/25% CO_2	75% Ar/25% CO_2	75% Ar/25% CO_2	75% Ar/25% CO_2
WFS (ipm)	240	400	180	280
Voltage (volts)	21	28	21.1	27.7
Travel Speed (ipm)	15	15	15	15
Current (amps)	140–150	200–215	163	237

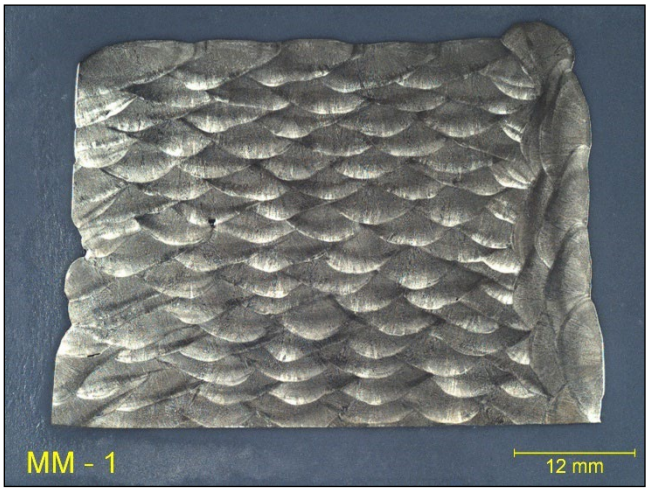

Figure 10. Metal-cored wire macrograph (CV parameters)

The metal-core build (MC1) was tested in the same manner as the flux-cored build. Tensile specimens, CVN test specimens, and chemistry tests were performed in locations represented in (Figure 7). The results are in Table 10, Table 11, and Table 12.

Table 10. FCAW and metal-cored wire chemistry comparison

Element	Phase 1 FCAW	EWI FCAW	EWI MC1
C	0.86	0.82	0.85
Mn	14.38	16	14.6
Ni	0.59	0.58	0.57
Cr	4.31	4.89	4.18
Cu	0.05	0.038	0.013
P	0.008	0.021	0.016
S	0.01	0.012	0.01
Si	0.04	0.061	0.099
Al	0.01	0.003	0.015
V	0.03	0.026	0.016
Ti	0.05	0.029	0.062

Table 11. Metal-cored wire tensile testing results (CV parameters)

Specimen Number	Ultimate Strength (ksi)	0.2% Yield Strength (ksi)
MC1-1	122.7	76.8
MC1-2	125.1	80.1
MC1-3	121.5	80.2

Table 12. Metal-cored wire CVN testing results (CV parameters)

Specimen Number	Test Temp (°C)	Absorbed Energy (ft-lbs)
MC1-1	-35	43
MC1-2	-35	45
MC1-3	-35	48

The chemistry, tensile, and Charpy results from MC1 tests are comparable to the flux-cored electrode baseline. However, even though these parameters proved successful from a mechanical and chemistry testing standpoint, the welding parameters may not lend themselves well to automation. Due to the 1-inch contact tip-to-work distance (CTWD), there is more chance of the electrode wire wandering over long distances – potentially creating improperly located weld beads. Over short distances, such as the 8-inch-long sample buildup, the parameters were consistent, but in an actual frog repair, they may not be. Accurate placement of weld beads is critical to the success of automating this repair process. Therefore, EWI developed more precise parameters.

2.6 GMAW-P Parameter Development

The initial metal-cored welding parameters were designed to run in CV mode with spray transfer. In this mode, the spray arc propels small molten droplets of the electrode onto the workpiece. It produces enough current to send a constant stream of metal off the electrode and usually results in high deposition rates, good penetration, strong fusion, and good weld appearance. GMAW-P offers advantages over spray arc CV mode. Pulse welding is effectively midway between spray transfer and the short-circuit transfer mechanism. In short-circuit transfer, the wire contacts the base metal surface and short circuits to the workpiece, causing the electrode metal to transfer to the workpiece. This happens 20–200 times per second. This process uses relatively low amounts of energy and works well for thin material, 0.25 inch or less, and for welding out of position. In spray transfer, the wire transfers across the arc in small droplets that can form and detach at the rate of several hundred per second. This creates relatively spatter-free welds with high deposition. However, this mode is used mostly in the flat and horizontal positions because it is hotter (more energy) and produces a larger weld puddle. In pulse mode, the power supply cycles between a high current and low background current. This allows for faster cooling of the weld pool during the background cycle, making it ideal for welding thicker sections where more heat is needed, but for which spray transfer is still too hot. GMAW-P can produce a comparatively lower heat input. With the right parameters, it also produces a stable arc, suitable for controlling bead placement during the automation of this process [2][1].

EWI developed a set of both cold (lower energy) and hot (higher energy) pulsed welding parameters (Table 13).

Table 13. Metal-core wire welding parameters (pulsed)

Parameter	Pulsed MC1	
	Cold	Hot
Pulse Program	84	84
CTWD (in.)	0.625	0.625
Travel Angle (°)	10 (push)	10 (push)
Shielding Gas	75% Ar/25% CO_2	75% Ar/25% CO_2
WFS (ipm)	180	280
Voltage(volts)	18.3	24.0
Travel Speed (ipm)	15	15
Current (amps)	164	234

With these parameters, the deposition rate was higher than both the flux-cored and constant-voltage metal core parameters (Table 14). The CTWD was reduced to 0.625 inch. Compared to the 1-inch

[1] For further information on pulsed GMAW, please consult the American Welding Society handbooks.

CTWD used previously, this shorter CTWD will ensure better arc stability and more accurate placement of weld beads.

Table 14. Deposition rate comparison

	FCAW	MC1 CV	MC1 Pulse
Cold Passes	3.9 lbs/hr	5.7 lbs/hr	6.2 lbs/hr
Hot Passes	5.6 lbs/hr	8.2 lbs/hr	9.7 lbs/hr

Using these weld parameters, EWI produced a buildup 15 layers high with 8 beads on each layer and produced a 1.5-inch-tall deposit (see Figure 11).

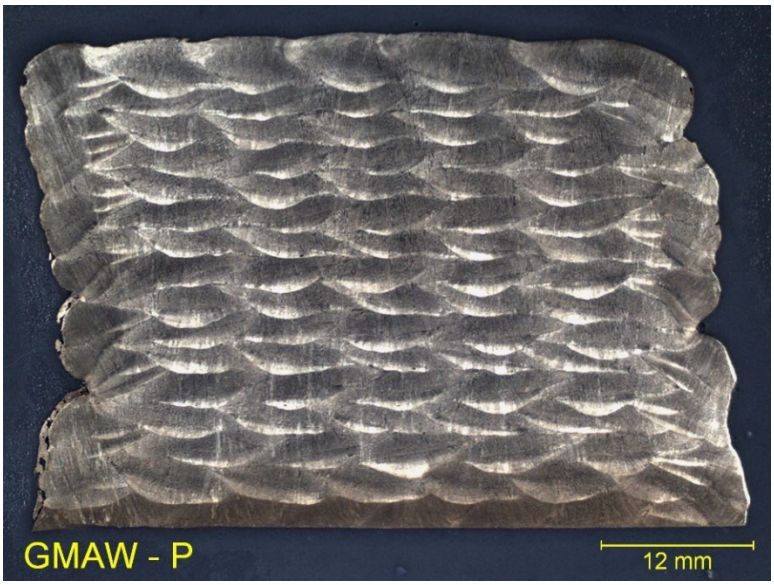

Figure 11. Metal-cored electrode macrograph (GMAW-P)

2.7 GMAW-P Buildup Evaluation

EWI tested the metal-core, GMAW-P buildup in the same manner as the flux-cored tests. Tensile specimens, CVN testing, and chemistry tests were performed in locations shown in Figure 7. The results are in Table 15, Table 16, and Table 17. The average tensile and CVN results between all buildups are shown for comparison in Table 18. The GMAW-P process, combined with the metal-cored electrode produces superior results.

Table 15. Chemistry comparison among all buildups

Element	Phase 1 FCAW	EWI FCAW	EWI MC1	EWI MC1 GMAW-P
C	0.86	0.82	0.85	0.82
Mn	14.38	16	14.2	14.2
Ni	0.59	0.58	0.55	0.64
Cr	4.31	4.89	4.18	3.92
Cu	0.05	0.038	0.011	0.011
P	0.008	0.021	0.013	0.014
S	0.01	0.012	0.01	0.010
Si	0.04	0.061	0.099	0.079
Al	0.01	0.003	0.015	0.016
V	0.03	0.026	0.016	0.014
Ti	0.05	0.029	0.062	0.068

Table 16. GMAW-P tensile testing results

Specimen Number	Ultimate Strength (ksi)	0.2% Yield Strength (ksi)
MC1-1P	117.6	78.8
MC1-2P	116.3	80.3
MC1-3P	127.4	79.6

Table 17. GMAW-P CVN results

Specimen Number	Test Temp (°C)	Absorbed Energy (ft-lbs)
MC1-1P	-35	52.9
MC1-2P	-35	51.5
MC1-3P	-35	62.4

Table 18. Tensile and CVN comparison among all buildups

	Phase 1 FCAW	EWI FCAW	EWI MC1	EWI MC1 GMAW-P
Average Ultimate Strength (ksi)	112.1	133.7	123.1	120.4
Average 0.2% Yield Strength (ksi)	73.7	80.9	79	79.6
Average CVN (ft-lbs)	31.6	40.6	45.3	55.6

3. CSX Frog Repair

EWI used the metal core electrode and GMAW-P weld process parameters to repair a full-size, #20, traditional, flat-top frog section provided by CSX. The frog was prepared in a manner representative of repairs in the field. The repair depth, location, and approach were similar to that used in Phase 1; however, in Phase 1, only the point and one wing were repaired. For the CSX frog, EWI repaired the point and both wings. Pre-weld and post-weld inspection tests were conducted to ensure the base material and weld deposit were free of cracks and other defects. CSX visited EWI and performed the required finish grinding.

3.1 Technical Approach

The objectives of this portion of the project were to: 1) select a #20 traditional, flat-top frog for repair; 2) identify and mark out the repair area; 3) prepare and repair the frog with the metal-cored electrode and GMAW-P parameters detailed in Section 2; and 4) grind the repaired frog to final dimensions. EWI received two #20, traditional, flat-top frogs from CSX (Figure 12) and prepared and weld repaired the frog in a manner similar to Phase 1.

Figure 12. #20 Flat-top frogs delivered to EWI

3.2 Frog Selection and Repair Plan

CSX sent EWI two, #20, traditional flat frogs. Both were in reasonably good condition, with very little surface deformation. Of the two, the frog labeled “20-136RE 48B” (Figure 13) was selected for repair, as it was in the best overall condition. If this frog were repaired in the field, one of the following approaches might be used:

- Light grind (0.25 in.) on the point and a two-layer repair
- Light grind (0.1875 in.) and one- or two-layer repair on upper wing

- Deeper grind (0.375 in.) and three-layer repair on lower wing

Figure 13. Frog selected for repair – 20-136RE 48B

EWI had not tested or evaluated light repairs (one- or two-layer repairs) made with the automated FCAW or metal-cored GMAW-P welding processes. To accurately compare the new process to the phase 1 process, EWI decided to limit the variables between the repairs. The depth of repair on both wings and the point should be comparable to the frog repaired in Phase 1. Therefore, EWI and CSX selected the following approach:

- Wings ground to approximately 0.75-inch depth.
- Point ground to approximately 1-inch depth.

In future research, additional tests to look at the influence of dilution on chemistry and performance should be evaluated. Mechanical and chemical tests can help determine the minimum number of weld layers before dilution has a negative impact on weld quality. This testing was outside the scope of this project.

3.3 Preparing Frog Surfaces for Repair

EWI prepared both the wings and the point using the same methodology as in Phase 1. The surfaces were initially carbon-arc-gouged to remove the bulk of the material (Figure 14). An electric grinder made the final dimensions and smoothed out the surfaces. In the future, this operation could be carried out with robotic automation, using grinders that would keep the grind profiles more consistent as well as reduce any safety concerns with the manual work.

Figure 14. Frog surface prepared

EWI inspected the prepared surfaces for cracks prior to welding. EWI attempted magnetic particle inspection, but the rail surface did not magnetize well making this process ineffective. EWI chose

eddy current testing as an alternative for detecting surface cracks (Figure 15). The eddy current setup consisted of a Nortec model 600 portable eddy current instrument with a Hocking NDT model 800P01 cross-point 100-KHz probe. A piece of AISI 4340 steel was used to calibrate the system. The calibration sample contained three electrical discharge machined (EDM) notches to simulate surface cracks. The notches were 0.2-, 0.5-, and 1.0-mm deep. An image of the eddy current equipment and calibration sample is in Figure 16. An image of the eddy current response for each EDM notch is in Figure 17. Following calibration, the entire excavated and ground area was manually scanned using the eddy current cross-point probe. No cracks were detected during this inspection.

Figure 15. Prepared frog with eddy current equipment

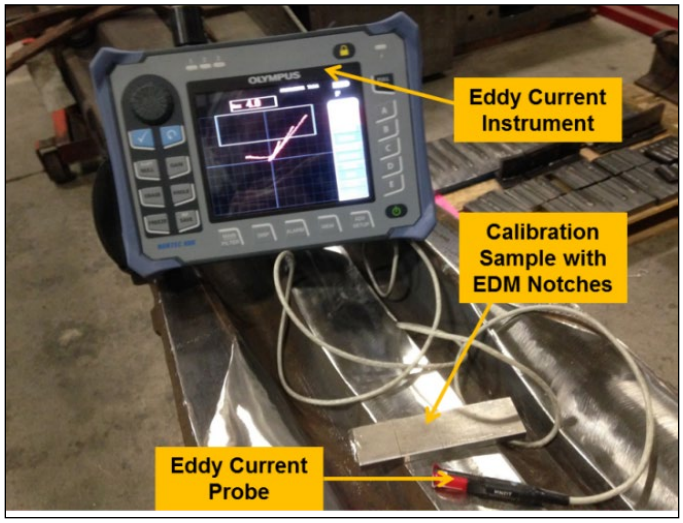

Figure 16. Eddy current equipment setup

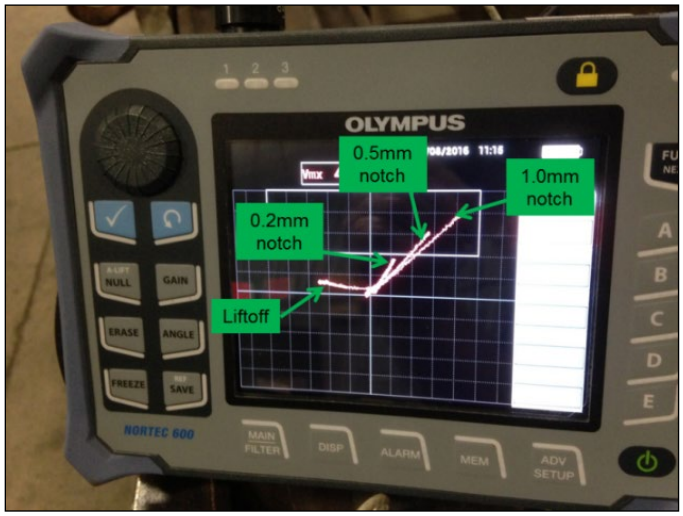

Figure 17. Eddy current response from calibration notches

3.4 Weld Repair of CSX Frog

Following successful eddy current inspection, EWI set up the frog for weld repair. The same Fanuc robot and Lincoln PowerWave 455 power supply used during Phase 1 were also used for this project (Figure 18).

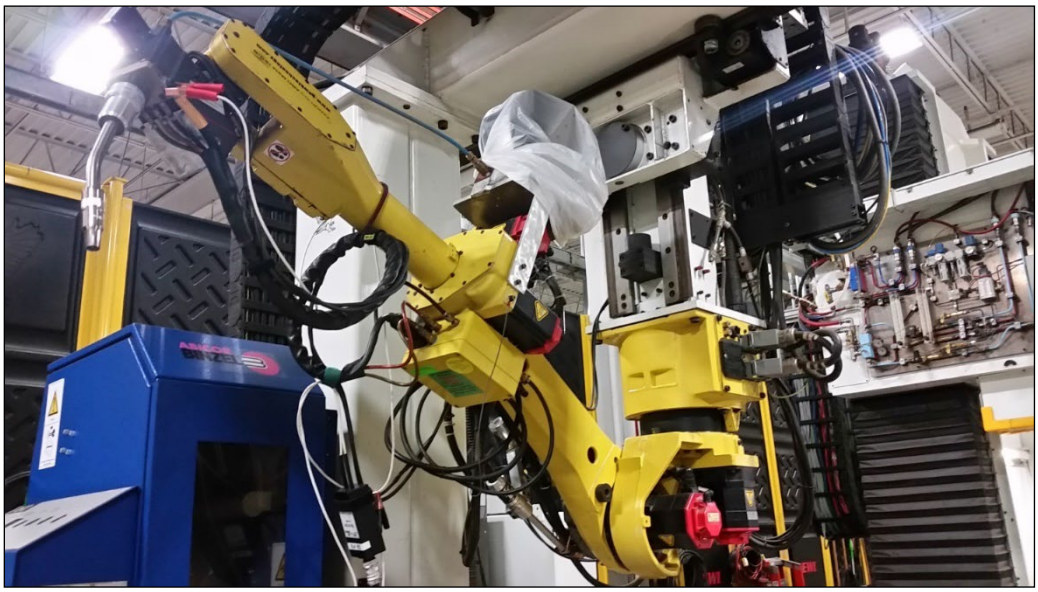

Figure 18. Fanuc robot utilized for welding

During Phase 1, EWI created a robot control program that consisted of various points along the length of the point and wing to allow technicians to program each layer and adjust parameters at the starts and stops. In Phase 2, EWI made some modifications to the points to accommodate the different length of repair needed on the CSX frog. The point area of the frog was addressed first, as this is typically the more challenging area and requires more time (Figure 19).

Figure 19. Programming point for repair

Nine layers of weld, each with approximately eight to nine beads, were required to build up the point. While welding the points, the maximum recorded inter-pass temperature was 248°F, as measured 1 inch from the weld.

There was excessive spatter within the nozzle observed during the point welding process (Figure 20). EWI had some concerns about the weld spatter negatively impacting the weld characteristics and quality, especially considering that the wing repairs would be significantly longer passes. To evaluate the effect of spatter on weld quality, EWI executed a test weld on a carbon steel base plate, welding three beads across and three layers high over a 47-inch length (Figure 21). The entire length was subjected to radiographic testing that revealed zero pores and no lack of fusion. The spatter was not affecting the weld quality.

Figure 20. Spatter collection on nozzle

Figure 21. Spatter collection test beads

Excessive spatter may be a negative factor in a production-type automated welding process. Frequent nozzle cleaning would be necessary, thus reducing the productivity of the system. Considering this, EWI made a few changes to the process to minimize spatter collection. The first change was the nozzle material. The GMAW torch nozzle was a standard brass shroud. This is typically sufficient for most applications. However, copper shroud nozzles are also available and typically used for more heavy-duty applications. Copper has high thermal conductivity and spatter does not collect as easily on this surface. The second change was to the contact tip and nozzle diameter. The setup used a recessed contact tip position which increases the chance of spatter collection (Figure 22). EWI changed the setup to use an extended-contact tip position and a larger-diameter nozzle (Figure 22, Figure 23).

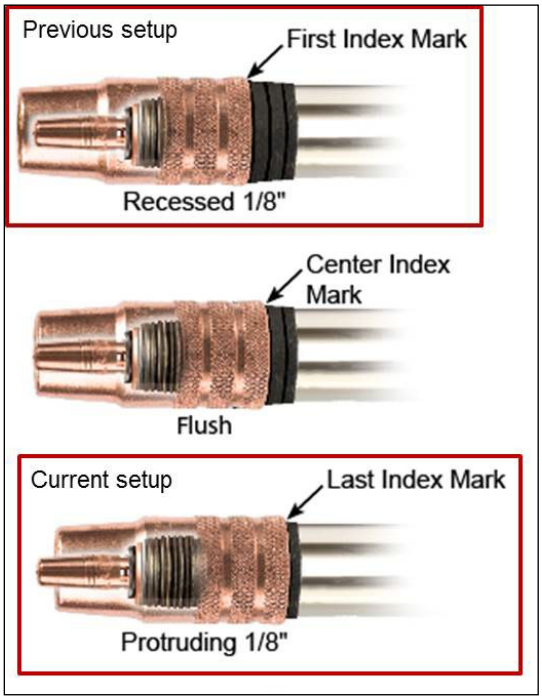

Figure 22. Contact tip position comparison

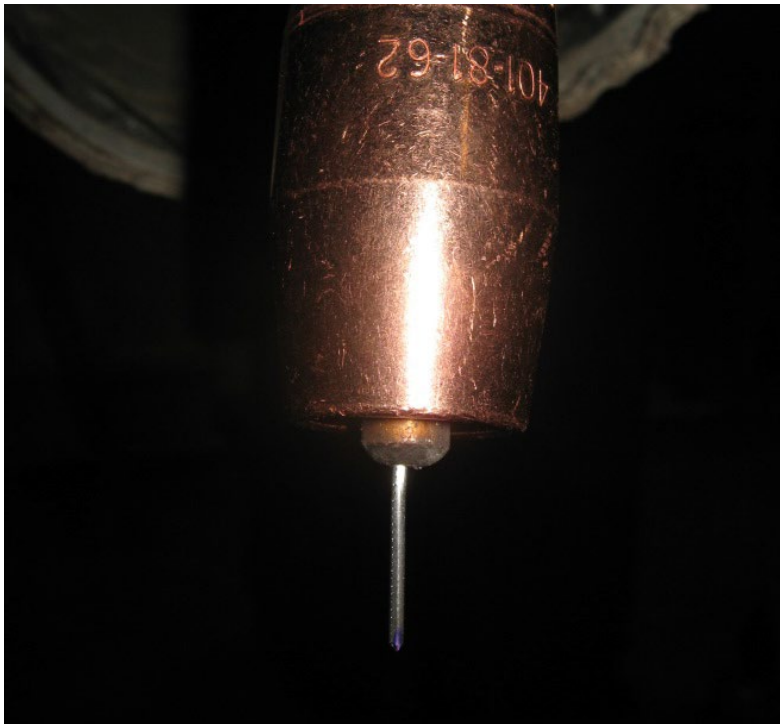

Figure 23. Extended contact tip position

EWI ran additional tests to verify the changes resulted in less spatter collection. The tests showed the changes produced a significantly less spatter collection within the nozzle. Figure 24 shows the difference in spatter collection once these changes were implemented, where a “1” represents the spatter with the previous setup, and a “2” represents the spatter with the changes implemented.

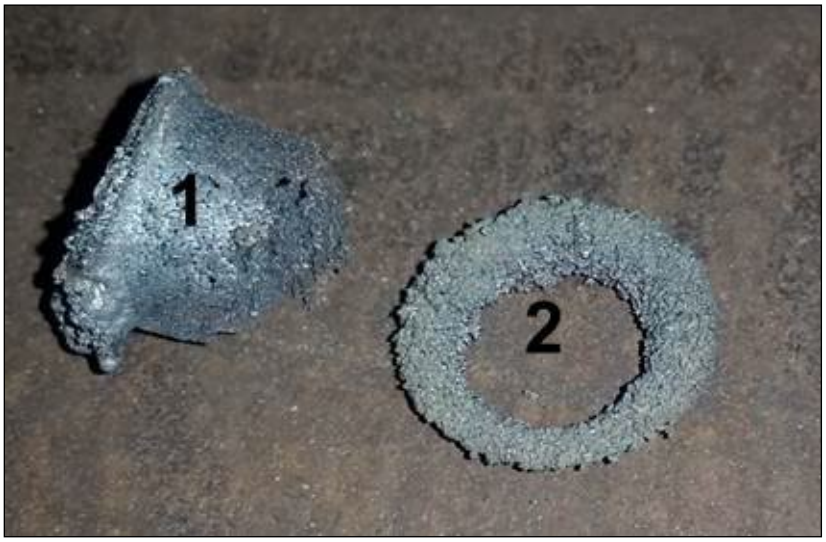

Figure 24. Spatter collection comparison

Proceeding with the weld repair, EWI repaired the lower wing first (Figure 25). A total of eight layers were required to build up the wing (Figure 26). Layers 1–6 were deposited in the same direction. Once the end of Layer 6 was reached, the weld deposit was approximately 0.125 inch below the work-hardened surface. Layers 7 and 8 were then welded from the opposite direction and started on top of the work-hardened base material surface. The upper wing was repaired in the same manner as the lower wing. The final repair is shown in Figure 27.

Figure 25. Upper and lower wing locations

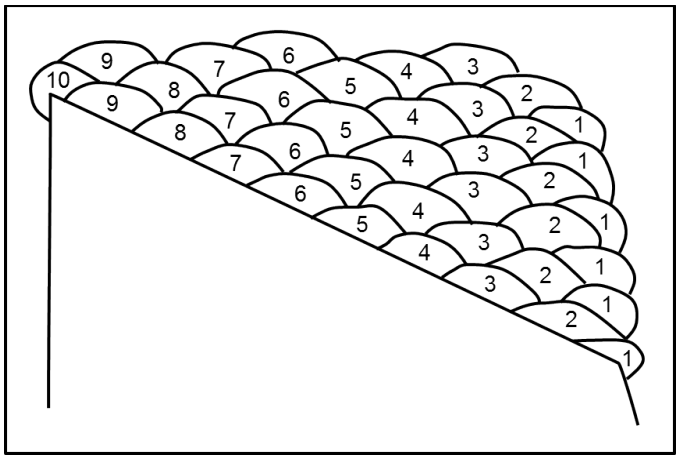

Figure 26. CSX frog wing repair welding sequence

Figure 27. Both wings and point repaired

3.5 CSX Frog Grinding and Inspection

A CSX team visited EWI to grind the frog to final shape. A hydraulic grinder was used to grind the bulk of the material and an electric grinder was used to smooth out the edges of the repair (Figure 28).

Figure 28. Grinding of repaired CSX frog

Both wings were ground to final dimensions and part of the point was finished. However, during final grinding, the point appeared to be slightly lower than the 0.1875-inch requirement (Figure 29). During initial layout of the repair, the point exhibited the correct height, but the additional thickness of repair on the wings was not taken into consideration. To bring the point back to the correct height, CSX recommended that EWI add additional weld material in the area shown in Figure 30, which extended 14 inches back from the point. EWI deposited eight layers of weld material in this area to bring up the height (Figure 31).

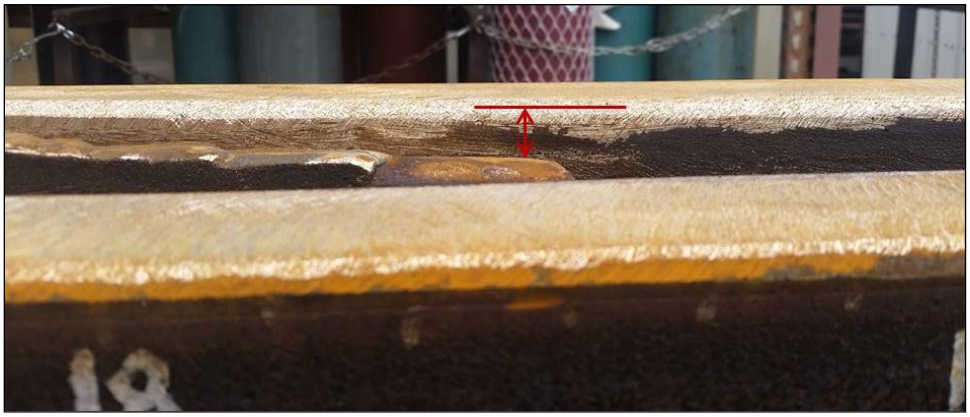

Figure 29. Point-to-wing height difference

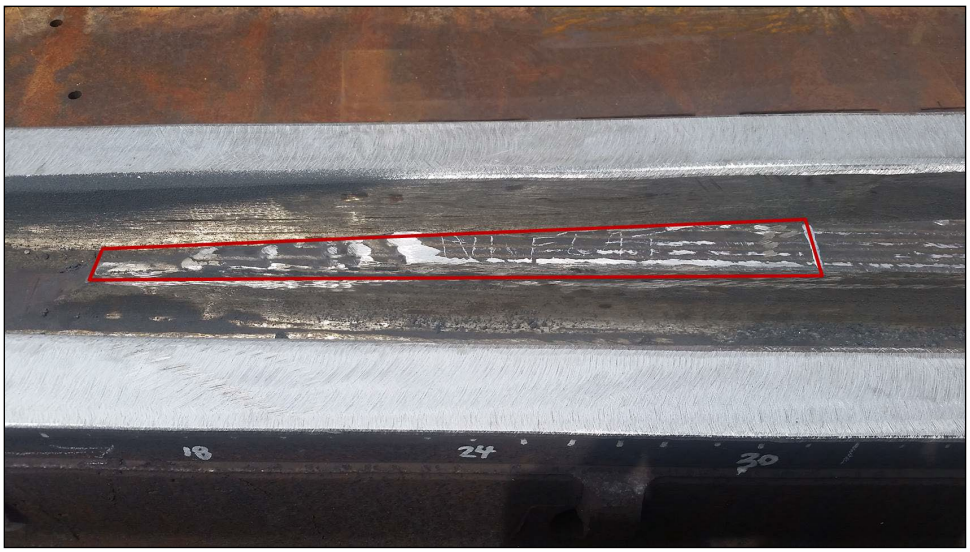

Figure 30. Area on point needing additional deposit

Figure 31. Additional weld material deposited

Once EWI completed depositing additional material on the point, the CSX team revisited EWI to complete the grinding on the additional point weld deposit. During grinding, CSX noticed an area on the point, outside of the repaired area, that showed some signs of wear on the straight side (Figure 32, Figure 33). After consideration, CSX decided that this slight wear was not a concern. CSX later sent a representative from Lincoln Electric to complete the final grinding on the frog (Figure 34)

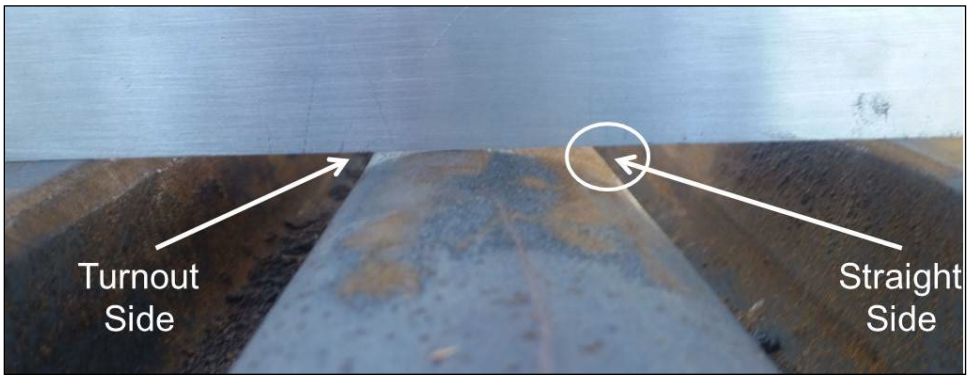

Figure 32. Area on point with uneven deformation

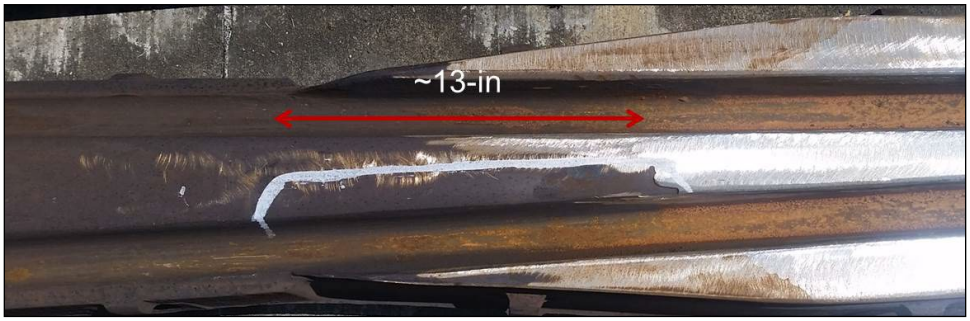

Figure 33. Area on point, outside of repaired area, with uneven deformation

Figure 34. Final grinding

EWI completed post-grind dye penetrant (PT) and ultrasonic (UT) inspections. The UT setup consisted of an Olympus Epoch model 650 portable ultrasonic instrument and two, 0-degree, longitudinal wave probes. Two scans were performed on the repaired area to detect discontinuities in the weld deposit layers and interface. For the first scan, a 5-MHz, 0.25-inch-diameter delay line probe was used to detect discontinuities up to 0.5 inch deep. For the second scan, a 5-MHz, 0.5-inch-diameter probe was used to detect discontinuities up to 1.5 inches deep. EWI used a NAVSHIPS carbon steel calibration block with 0.046875-inch-diameter, side-drilled holes for calibration. An image of the UT equipment is in Figure 35. No discontinuity indications were detected during the inspections.

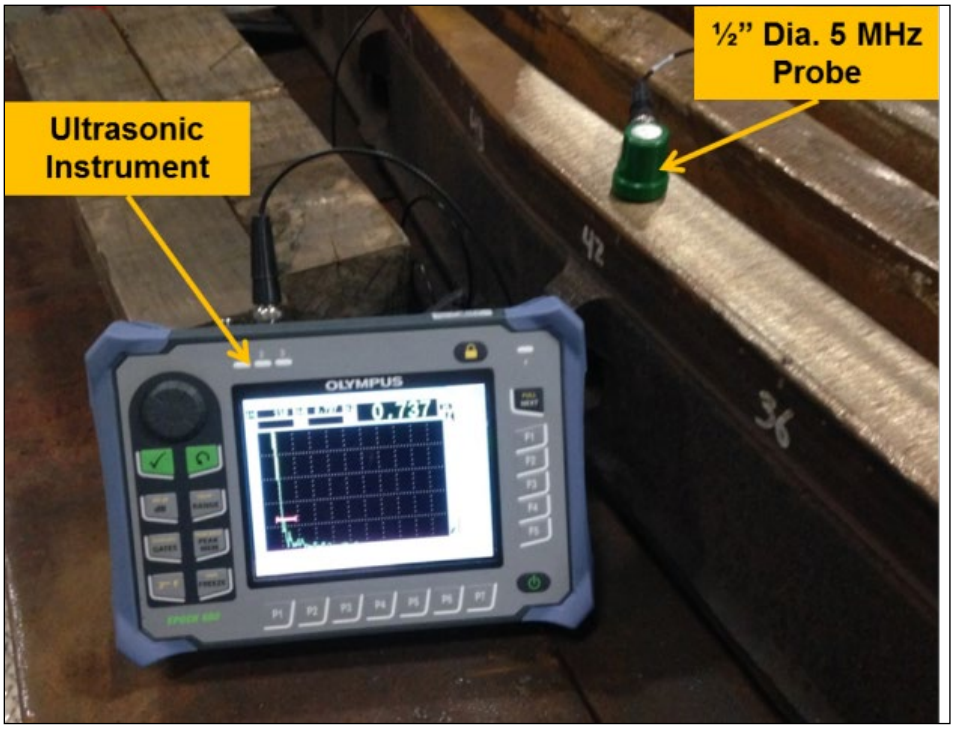

Figure 35. Ultrasonic equipment used for the inspection

4. CSX Frog Revenue Service Testing and Monitoring

CSX installed the EWI-repaired frog on November 1, 2016, on the Alabama Division A Line where the railroad crosses the Tennessee River at Decatur Junction. NS owns and operates the A Line, but CSX is responsible for maintaining the turnout at Decatur Junction (Figure 36). Speeds at this junction are typically 35 mph. In 2015, accumulated traffic for CSX and NS across the junction was 70.3 MGT. Traffic is split between NS (straight side of switch) and CSX (diverging side of switch) 60 percent/40 percent, respectively.

Figure 36. Frog installation location

4.1 Condition Monitoring

CSX and EWI jointly monitored the frog as it accumulated service tonnage. A CSX welder/helper team inspected the frog, measured it for wear, and performed maintenance grinding monthly, as required. EWI visited the frog with CSX roughly once per quarter and completed dye penetrant inspection and running surface hardness tests. Excluding installation and removal, the frog was visited 13 times while in service. Table 19 provides the dates of inspection, the calculated service tonnage, and the inspection activities for each visit.

Table 19. CSX frog monitoring timeline

Visit	Date	Tonnage (MGT, Calc.)	Visual Inspection	Profile Measurement	Hardness Measurement	Penetrant Inspection	Maintenance Grinding
Installed	11/1/2016	0.0	X	X			
1	11/17/2016	2.5	X	X			X
2	12/7/2016	5.6	X	X	X	X	X
3	1/12/2017	11.1	X	X			
4	1/20/2017	12.4	X	X			
5	2/8/2017	15.3	X	X	X	X	
6	2/24/2017	17.8	X	X			
7	3/14/2017	20.5	X	X			
8	4/3/2017	23.6	X	X			
9	5/9/2017	29.2	X				
10	6/20/2017	35.7	X	X	X	X	X
11	8/31/2017	46.8	X	X			
12	11/1/2017	56.4	X	X			X
13	12/5/2017	61.6	X	X			
Removed	12/15/2017	63.0					

4.2 CSX Frog Profile Measurements

CSX measured the frog profile at the following locations relative to the point: -16, -8, +0.5, +2, +8, +16 , and +22 inches. (Figure 37). Negative numbers denote measurements taken ahead of the point and positive numbers denote measurements taken after the point. Profile measurements were taken using a straightedge and taper gauge.

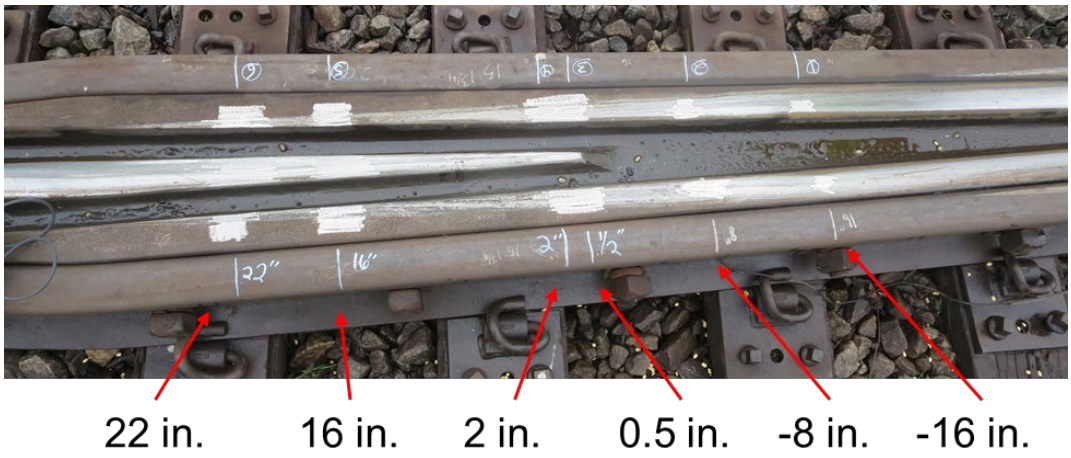

Figure 37. Profile measurement locations on the frog

Detailed profile measurement data is provided in Table 20 and images of the frog at installation, midpoint, and end of test are shown in Figure 38. CSX and EWI estimated the frog's service load reached 63 MGT over its 13-month service life – roughly 125 percent of the life of an average first-time repair on a frog, as reported by field personnel. Per CSX, the frogs installed at Decatur Junction often required more frequent weld repairs than average, sometimes once per month. CSX qualified the frog's wear as minor, aside from the breakout near the point tip (described below). Only minimal grinding was needed to remove plastic metal flow from the point and wings. The final profile measurements show a maximum wear of 0.3125 inch at an isolated location. The average wear was 0.125 inch over the wings and point. The wear criteria for weld repair is 0.375 inch.

Table 20. Profile or wear measurement table

		Position of the tip of the point											
		-16-in		-8-in		+0.5-in		+2-in		+16-in		+22-in	
Date	Traffic (MGT's)	Taper Gauge Measurement	Amount of Wear from Original Surface	Taper Gauge Measurement	Amount of Wear from Original Surface	Taper Gauge Measurement	Amount of Wear from Original Surface	Taper Gauge Measurement	Amount of Wear from Original Surface	Taper Gauge Measurement	Amount of Wear from Original Surface	Taper Gauge Measurement	Amount of Wear from Original Surface
Measurements prior to install	0.0	Flush	0	Flush	0	3/16-in	0	1/8-in	0	Flush	0	Flush	0
11/1/2016 (installation)	0.0	Flush	0	Flush	0	3/16-in	0	1/8-in	0	Flush	0	Flush	0
11/17/2016	2.5	Flush	0	Flush	0	3/16-in	0	1/8-in	0	<1/16-in	<1/16-in	Flush	0
12/8/2016	5.6	Flush	0	Flush	0	1/4-in	1/16-in	1/8-in	0	<1/16-in	<1/16-in	Flush	0
1/12/2017	11.1	Flush	0	Flush	0	1/4-in	1/16-in	1/8-in	0	<1/16-in	<1/16-in	Flush	0
1/20/2017	12.4	Flush	0	Flush	0	1/4-in	1/16-in	1/8-in	0	<1/16-in	<1/16-in	Flush	0
2/8/2017	15.3	1/16-in	1/16-in	3/32-in	3/32-in	1/4-in	1/16-in	3/16-in	1/16-in	<1/8-in	<1/8-in	1/8-in	1/8-in
2/24/2017	17.8	1/16-in	1/16-in	3/32-in	3/32-in	1/4-in	1/16-in	3/16-in	1/16-in	<1/8-in	<1/8-in	1/8-in	1/8-in
3/14/2017	20.5	1/16-in	1/16-in	3/32-in	3/32-in	1/4-in	1/16-in	3/16-in	1/16-in	<1/8-in	<1/8-in	1/8-in	1/8-in
4/3/2017	23.6	1/16-in	1/16-in	3/32-in	3/32-in	1/4-in	1/16-in	3/16-in	1/16-in	<1/8-in	<1/8-in	1/8-in	1/8-in
6/20/2017	35.7	1/8-in	1/8-in	1/8-in	1/8-in	1/4-in	1/16-in	3/16-in	1/16-in	1/8-in	1/8-in	1/8-in	1/8-in
8/31/2017	46.8	1/8-in	1/8-in	1/8-in	1/8-in	1/4-in	1/16-in	3/16-in	1/16-in	1/8-in	1/8-in	1/8-in	1/8-in
11/1/2017	56.4	1/8-in	1/8-in	1/8-in	1/8-in	1/4-in	1/16-in	3/16-in	1/16-in	1/8-in	1/8-in	1/8-in	1/8-in
12/5/2017	63.0	1/8-in	1/8-in	3/16-in	3/16-in	1/4-in	1/16-in	1/4-in	1/8-in	1/8-in	1/8-in	1/8-in	1/8-in

Figure 38. Frog profile over the revenue service life

4.3 CSX Frog PT and Surface Hardness Monitoring

EWI completed four PT inspections of the repaired frog, 3 inspections during the frog's service life and 1 inspection after CSX removed the frog from track (Figure 39). EWI found crack indications on the running surface of the point during each inspection. Crack indications near the side of the point were obscured by material flow that held excessive amounts of penetrant. Areas of surface spalling and surface cracks grew in size during the frog's service life.

EWI observed a roughly 4-inch-long section of the point broken out 10 inches from the tip during the final visit on December 5, 2017 (Figure 43). The depth of this broken-out area was greater than allowable, 0.375 inch, and CSX removed frog from service to facilitate a detailed inspection by EWI. See Section 5 for more information on this post-test inspection.

The wings of the frog had no crack indications, aside from isolated pores and one surface crack that formed after the point breakout occurred.

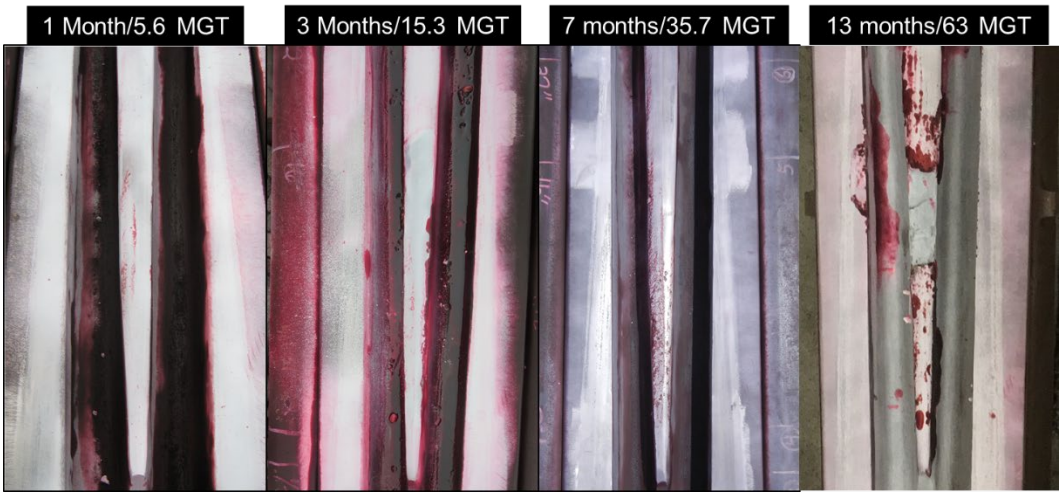

Figure 39. Penetrant inspection on repair area

Using a Proceq Equotip 550 Leeb D hardness tester, EWI measured surface hardness on the frog running surface three times while it was in service and once post-service (Figure 40). EWI

measured the hardness at the same points along the frog where the profile measurements were made. Measurements were taken on both wings and the point at the locations shown in Figure 40. A traverse of 10 to 12 individual hardness measurements were taken across the running surface at each location. The individual hardness traverses were statistically analyzed by the Proceq tester. The mean value for each measurement location and set is shown graphically in Figure 41. The repaired area quickly work-hardened. To gage the rate of work hardening, EWI collected measurements from the repaired area, but outside the running surface. These areas had an average as-welded hardness of 283 Brinell (BNH). Hardness measurements taken at the running surface after a little more than 5 MGT had an average of 464 BNH, confirming a rapid work-hardening in the repaired areas.

Figure 40. Hardness measurements in each of the red oval locations: Proceq hardness tester (top-right) and measurements from the CSX frog (bottom-right)

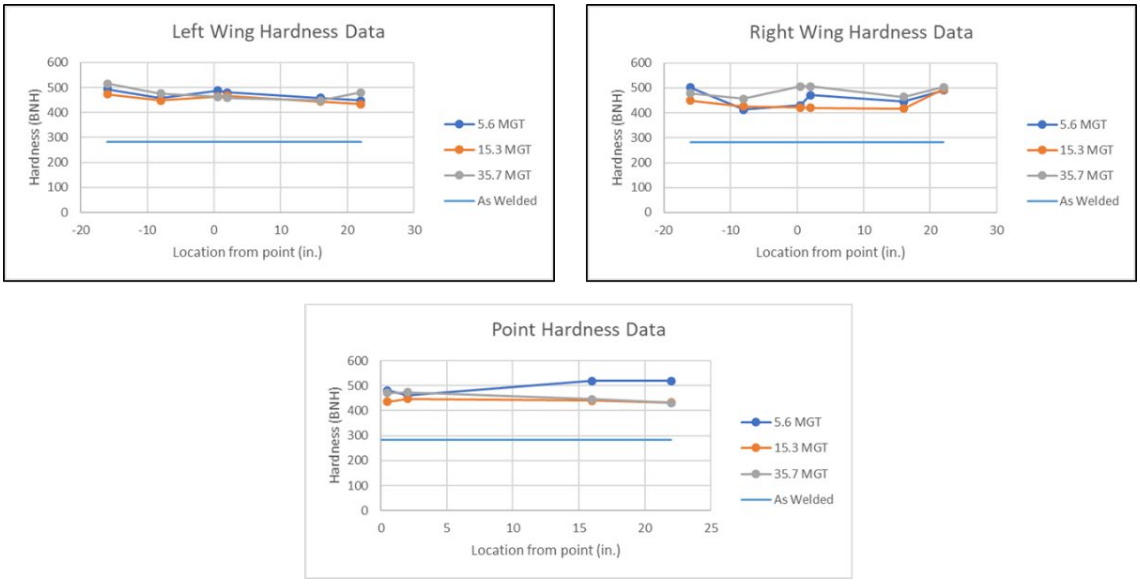

Figure 41. Hardness measurements in repair areas of the CSX frog

Material flow is common during running surface hardening (Figure 42). CSX reported some roll-over material during its inspections and performed grinding to remove the plastic meAtal flow four times during the service test.

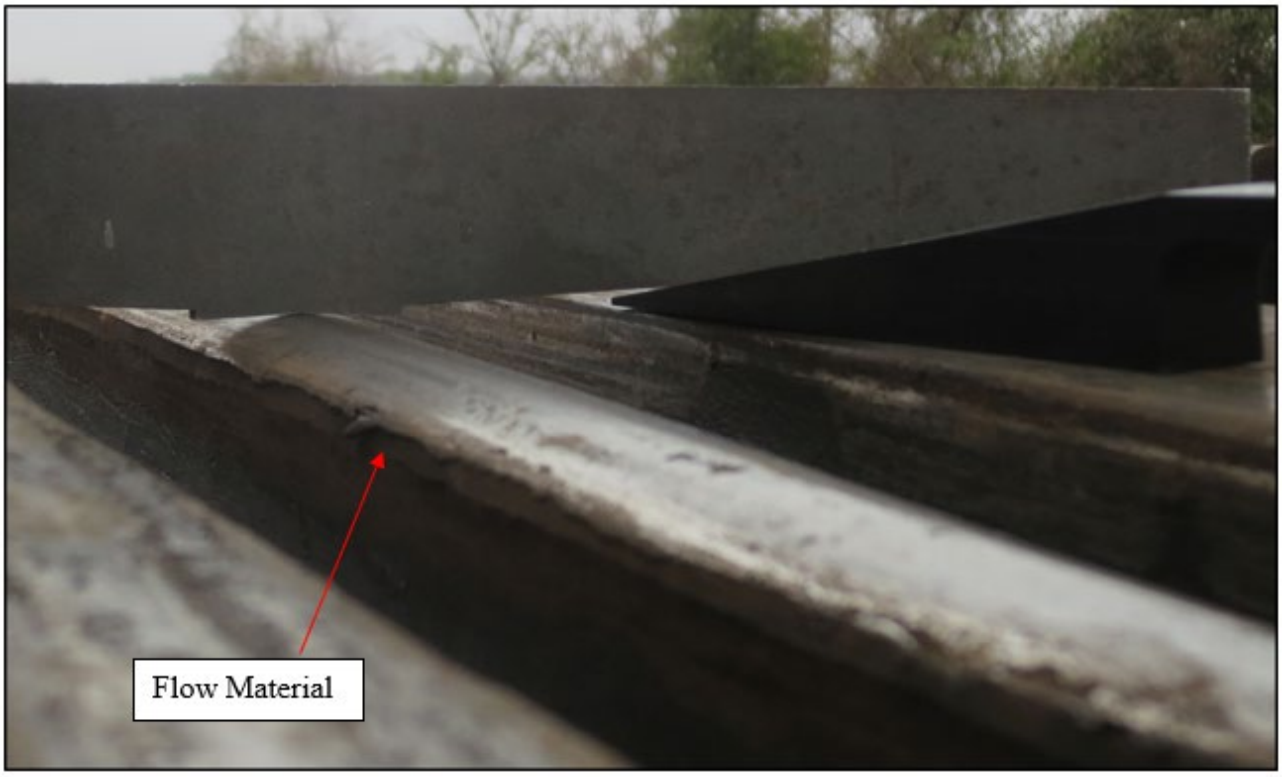

Figure 42. Point with unground flow material during a profile measurement

5. CSX Frog Post-Test Inspection and Analyses

CSX shipped the frog back to EWI for post-test inspection at the conclusion of the test. EWI completed final wear measurements, surface hardness measurements, ultrasonic testing (UT), and cross-section hardness, tensile, and Charpy tests. EWI's analysis was broken into two investigations to: 1) determine how revenue service affected the repaired areas for comparison to the results from Phase 1 [1], and 2) determine if the automated weld repair influenced the broken-out section along the frog point. EWI cut cross-sections out of the frog point and completed metallurgical evaluations around the breakout area to determine if the automated weld repair contributed to this failure.

5.1 CSX Frog Point Break-Out

EWI observed a roughly 4-inch-long section of the point broken out 10 inches from the tip during the final visit on December 5, 2017 (Figure 43). In general, small areas of material loss are tolerable. However, due to the size and depth of this breakout, a weld repair would be required to keep the frog in service. The team decided to end the revenue service test at this service level (63 MGT).

Figure 43. Frog with break-out on point during final in track inspection

5.2 Ultrasonic Inspection

EWI cleaned the repair area of the frog in preparation for UT. Solvent was used to remove oils, and a sanding pad on a grinder was used to smooth rough areas. The UT inspection used a single crystal, straight-beam technique (Figure 44). This is the same technique used to inspect the as-repaired frog.

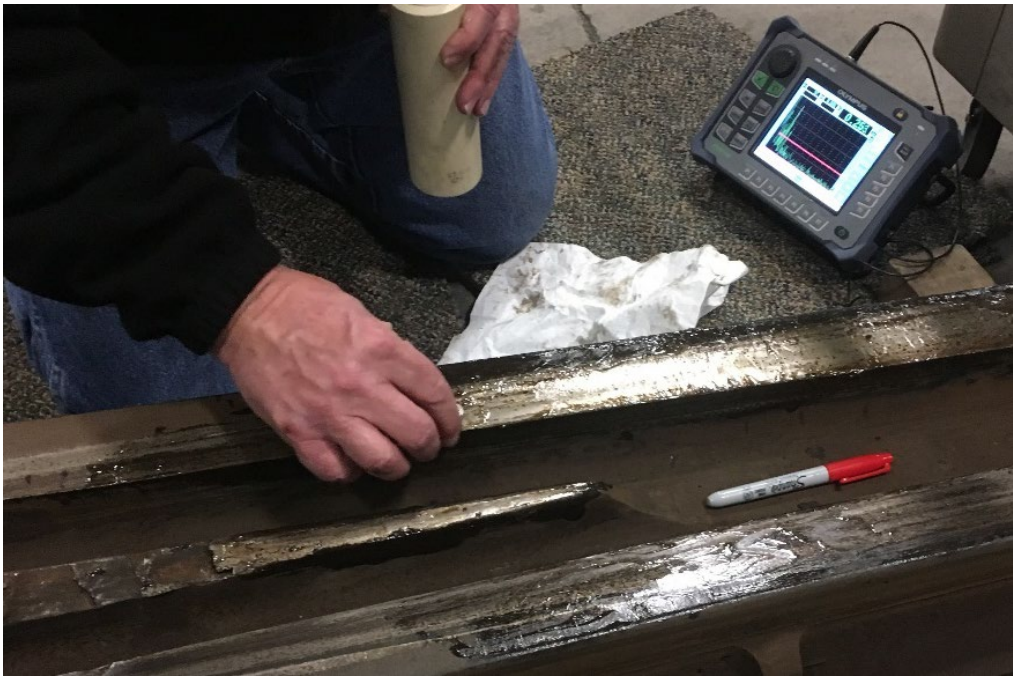

Figure 44. UT inspection with a single crystal probe

The UT inspection found 19 notable crack indications at various depths from the running surface. All UT crack indications were located within the running surfaces. Welding repair areas outside the running service (no wheel contact) had no indications. The depth of the indications from the running surface ranged from 0.125 inch to 0.650 inch. The indications were isolated, and there were no clusters of indications. The longest indication was roughly 2 inches in length. EWI mapped the locations (Figure 45) and documented their depths and positions relative to the frog point (Table 21).

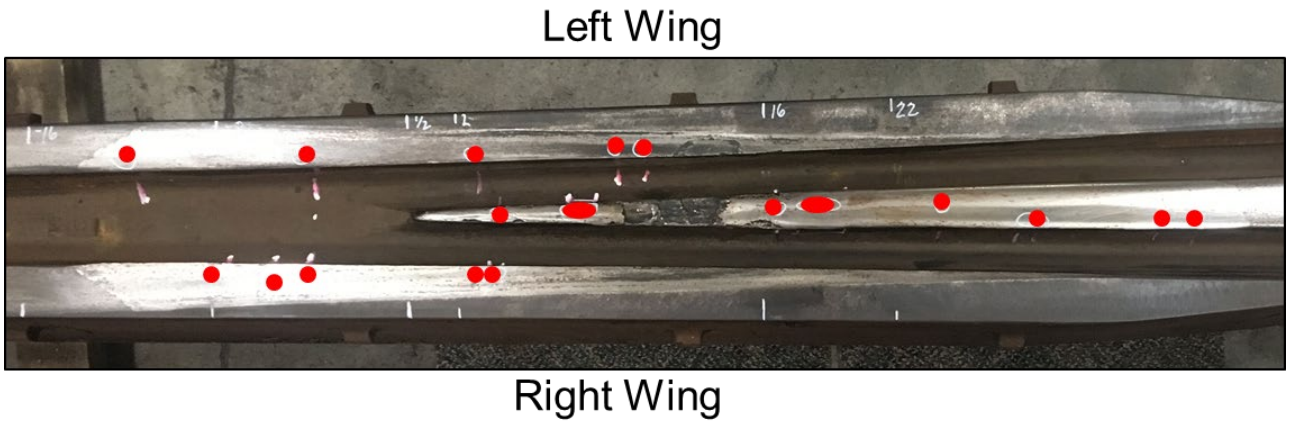

Figure 45. UT indication map

Table 21. UT indication location from point and depth

Left Wing		
ID	Location (in.)	Depth (in.)
L1	-11.75	0.33
L2	-4.25	0.36
L3	2.5	0.50
L4	9.5	0.48
L5	11	0.48

Point		
ID	Location (in.)	Depth (in.)
P1	3.75	0.50
P2	5.75	0.52
P3	7	0.60
P4	8.25	0.33
P5	16	0.40
P6	18-20	.65-.37
P7	24	0.39
P8	28-29	Shallow
P9	34	0.38
P10	35.5	0.13

Right Wing		
ID	Location (in.)	Depth (in.)
R1	-8	0.30
R2	-6	0.30
R3	-4.25	0.33
R4	3.25	0.25
R5	3.75	0.36

5.3 Penetrant Inspection

EWI completed a PT inspection that confirmed the visual results. Two areas were noted (Figure 46). An area near the point breakout location (area A in Figure 46) exhibited excessive penetrant bleed-out, indicating a deep void. This finding supported the UT results in this area. Further along the point (area B in Figure 46), surface spalling indications were accompanied by excessive rollover or material flow.

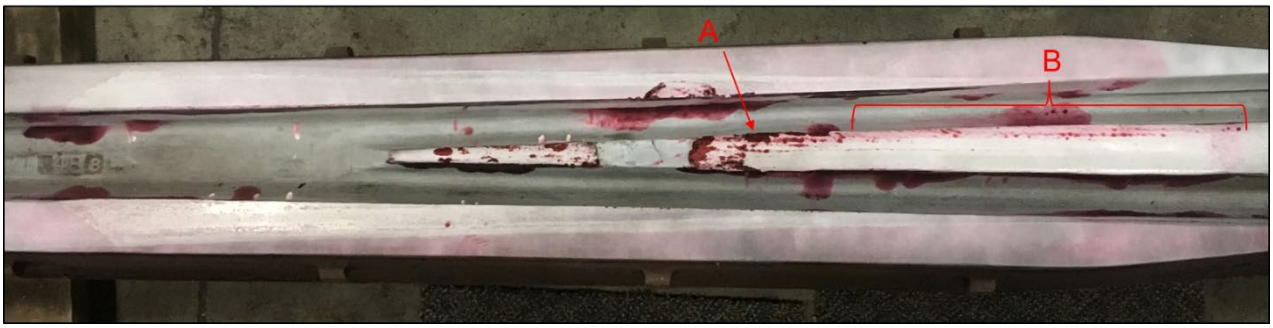

Figure 46. PT results on CSX frog

5.4 Surface Hardness

After PT was complete, EWI cut the frog into sections with an oxyfuel torch near the ends of the repair for ease of handling. A grid area (approximately 1×1-inch) was drawn over the repair area (Figure 47). A technician acquired four hardness measurements in each box and the results were statistically analyzed by the Proceq tester. The mean values were plotted on graphs for comparison to hardness measurements taken while the frog was installed at Decatur and to the frog repaired during Phase 1 (Figure 48). The hardness data plots focus on the left wing and point since there was no repair on the right frog wing Phase 1. EWI gathered hardness data from the CSX frog's right wing and is comparable the left wing. The hardness levels for the CSX and Phase 1 (labelled "TTCI" in figure) frogs were very close in value. Both were in the desirable range for AMS in-service material. The Phase 1 frog was welded with commercially available FCAW wire, while the CSX frog was welded with a custom metal-cored wire based on the FCAW wire. The parity between the hardness results indicates the new metal-cored electrode and GMAW-P process did not reduce the hardenability of the weld material. The hardness measurement taken near the tip of the

point (~0 in.) after 63 MGT on the CSX frog was notably lower than the other readings taken at that location. This was likely due to subsurface cracking in that area. The Proceq hardness tester uses a rebound-style probe to measure hardness. This style of test requires the material to have a minimum level of stiffness; the measurement system will produce erroneous results when the test area is flexible. Subsurface cracks, discussed later in this section, will reduce the local stiffness of the assembly.

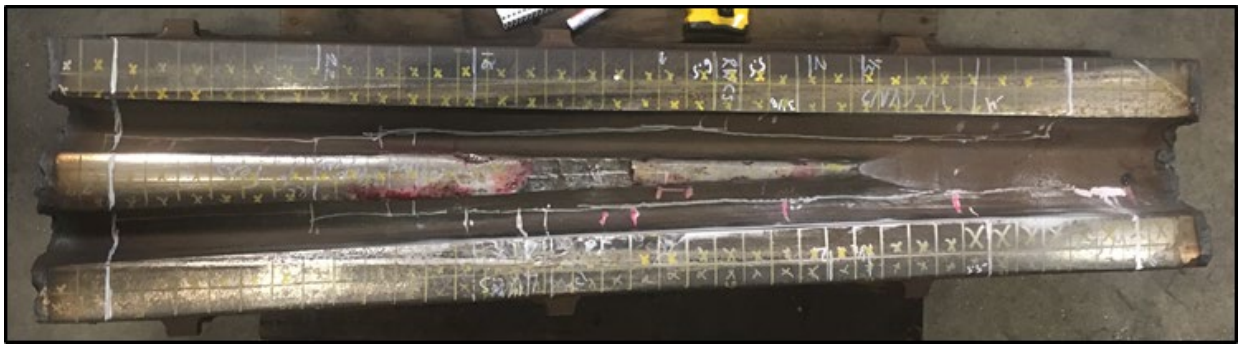

Figure 47. CSX frog with hardness grid layout

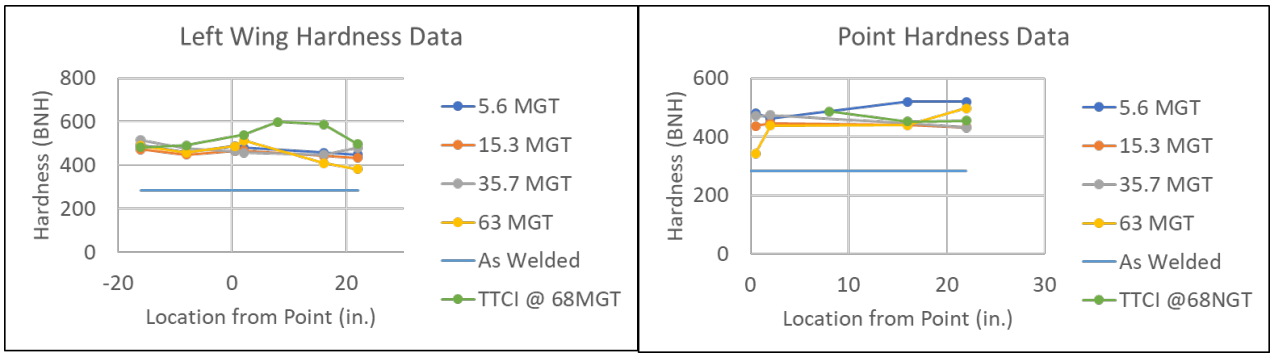

Figure 48. Comparison plot of hardness measurements

5.5 CSX Frog Wing Cross-Section Hardness

EWI cut cross-sections from the wings of the CSX frog for hardness mapping, labelled LW and RW in Figure 49.

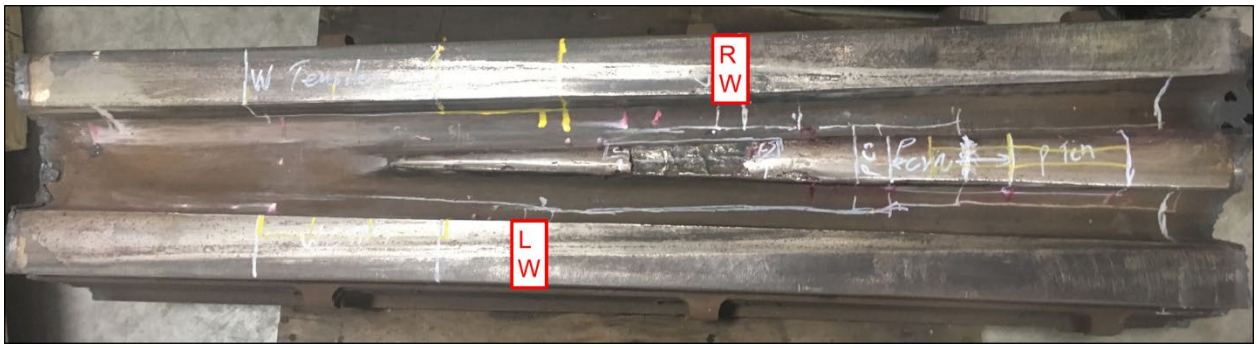

Figure 49. Wing cross-section locations

The cross-sections for both wings were taken from the running surface (wheel contact area) in the frog transition zone where the wheel load is partially carried by the point. The full width of the wing was excised down to approximately 1.5 inches below the running surface (Figure 50 and Figure 51). EWI completed hardness mapping with an automatic micro-harness system using a 500g load. Indents were made 0.057 inch apart.

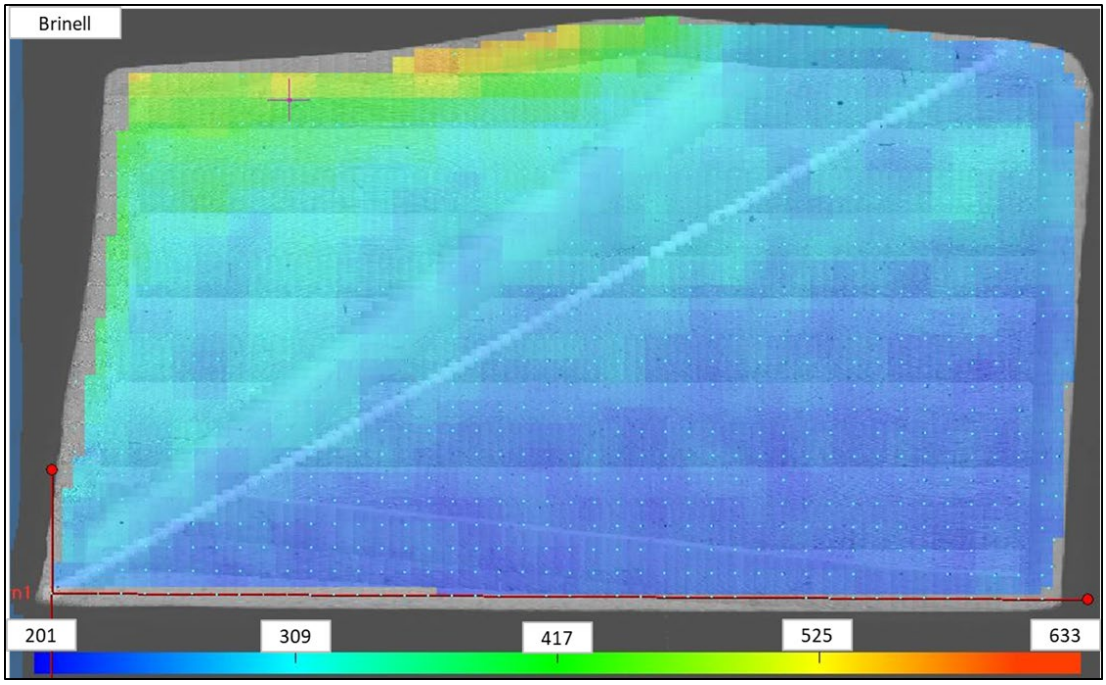

Figure 50. Left wing cross-section with hardness map

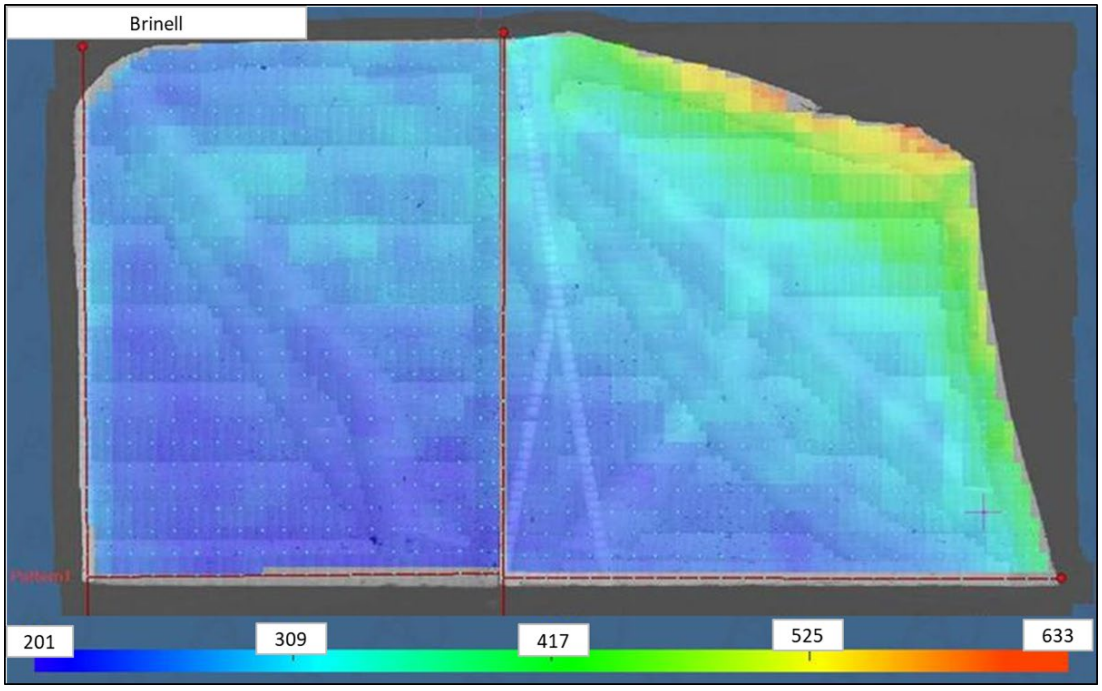

Figure 51. Right wing cross-section with hardness map

These maps clearly show the depth of hardening that occurred due to the wheel loads. The section of wing taken from the left side had an average hardness near the running surface of 543 BNH (Figure 50) – similar to the hardness measured at the surface (Figure 48). Hardness in the as-welded areas of the build averaged 296 BNH. New premium frogs are explosion depth-hardened on their running surfaces to approximately 352 BNH, and the hardened depth extends approximately 0.5 inch below the running surface. On the left wing section of the CSX frog, hardness decreased to 352 BNH at the depth of 0.35 inch. The right wing section had an average hardness near the running surface of 515 BNH (Figure 51). The as-welded area had an average hardness of 260 BNH. The depth to reach 352 BNH from the running surface on this wing was 0.29 inch.

5.6 CSX Frog Point Cross-Section and Metallurgical Analyses

EWI excised three cross-sections from the frog point area as shown in Figure 52. Technicians were careful while cutting the point to preserve the fracture face of the breakout and surrounding areas.

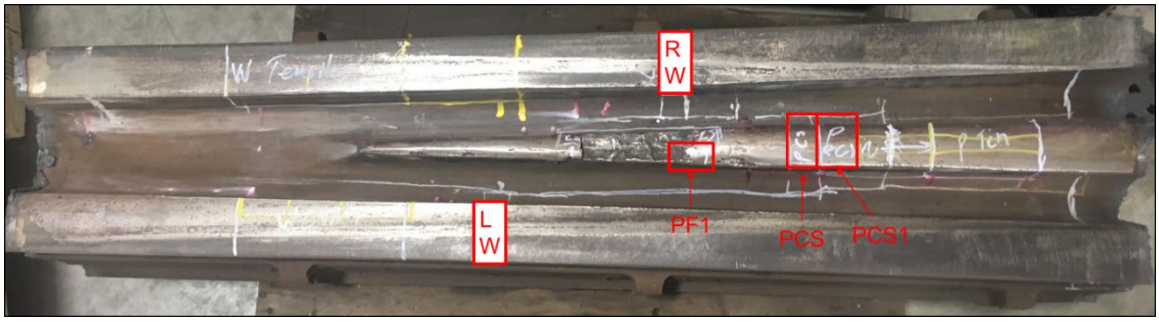

Figure 52. Cross-section cut lay out

Cross-section PF1 cut into the side of the point. The section in Figure 53 is parallel to the point centerline. This section displays the edge of the breakout and part of the remaining point surface. The cross-section shows the cracking which led to the breakout. The crack lines do not follow the layers of the repair welds. After a high-magnification examination of the weld repair in this area, EWI concluded that there was no clear indication of discontinuity in the microstructure that would lead to a weld repair failure.

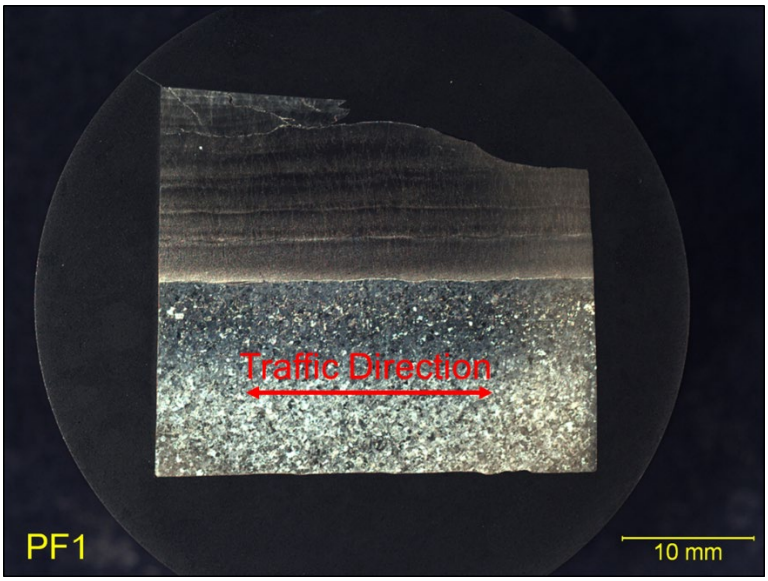

Figure 53. Cross-section PF1

Cross-sections PCS and PCS1 were located adjacent to each other. EWI intended to mount and polish both samples, but once they were removed for the frog cross-section PCS was found to be cracked through the entire point, revealing a fractured face (Figure 54). One side of the point had a section of material that had been broken out, leaving a notch. This notch appeared to be the initiation point of a fatigue crack that propagated through the repair to the other side of the point. Both sides appeared to have plastic material flow that was not completely removed by grinding.

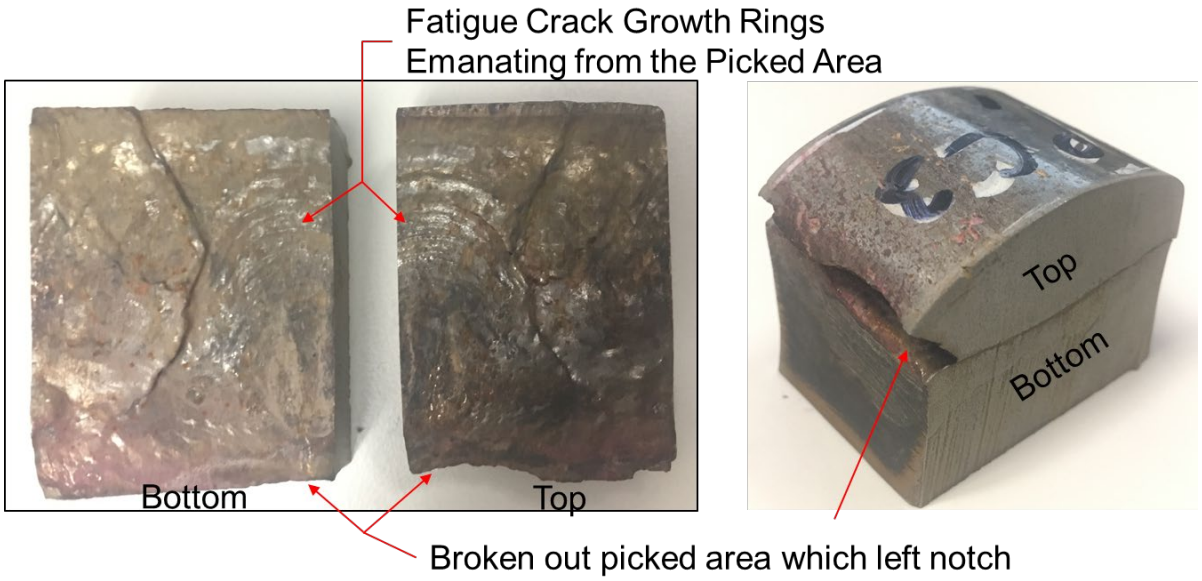

Figure 54. PCS cross-section with fracture face

Cross-section PCS1 contained the same crack but it did not propagate through the entire point. One side of the cross-section contains a notch next to some unground material flow (Figure 55, left). The opposite side of the point had a small area of partly ground flow with a small crack visible. The remaining area had well-ground flow and no visible cracks (Figure 55, right).

Figure 55. PCS1 cross-section

The waterjet-cut face of PCS1 was polished and etched for metallurgical examination (Figure 56). Overall, the weld cross-section looked good. There was no porosity or indication of issues at the bond line between the weld and casting. At the top, a roughly 0.1875-inch crack was visible and open to the running surface. This is likely due to shear stress caused by the passing train wheels. The crack running through the weld repair from one side of the point to the other did not appear to follow any metallurgical features.

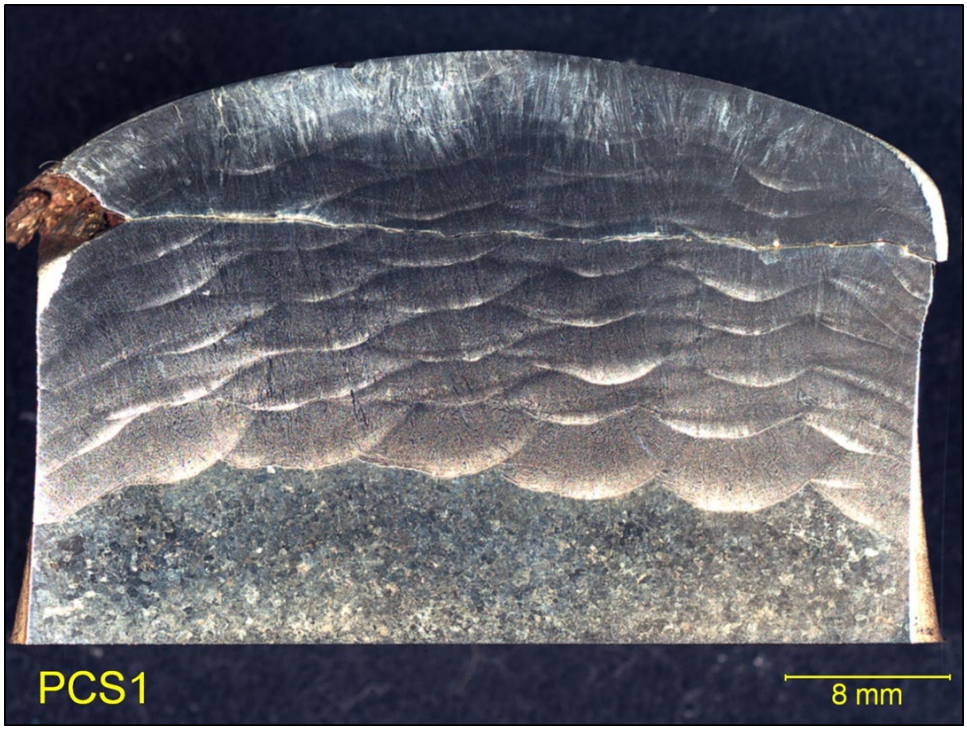

Figure 56. Weld cross-section from the point, PCS1

EWI performed a high-magnification examination of the PCS1 cross-section. Some strain bands are visible near the running surface of the point (Figure 57, left). These were straight, dark, parallel lines that cover the polished surface, occasionally changing orientation. Strain bands are caused by work-hardening as wheels roll over the point. An examination of the microstructure further from the running surface, just above the crack, shows fewer strain bands (Figure 57, right).

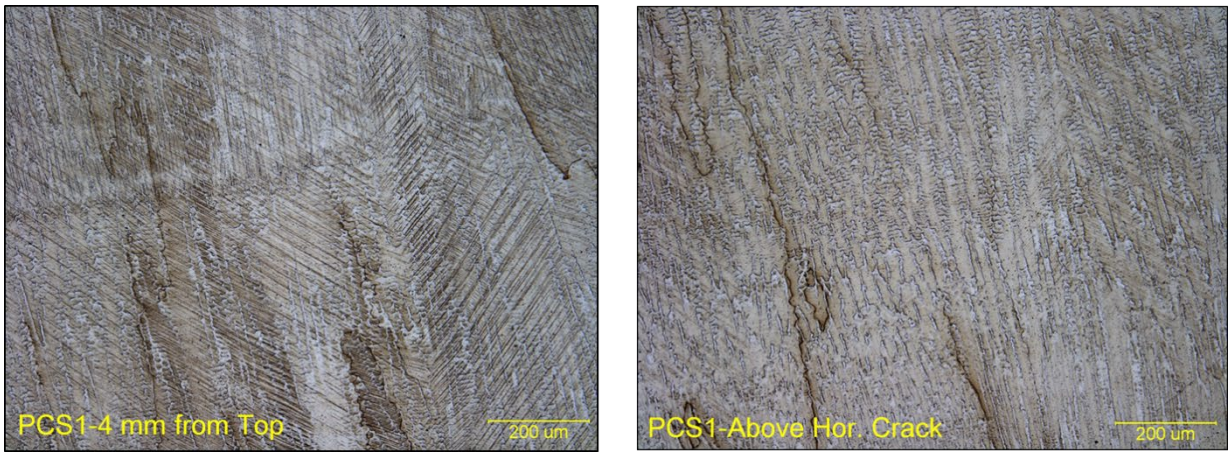

Figure 57. High-magnification images of the point microstructure

EWI also examined the cross-sections taken from the wings and found no indications of microstructural issues. Both wing cross-sections had clear areas of strain bands where the deformation was highest (Figure 58 and Figure 59). On the right wing a crack was visible on the running surface. This location corresponded with the breakout area on the point. When the wheel fell into the breakout, it landed on the wing, which is a likely cause for this crack.

Figure 58. Left wing cross-section

Figure 59. Right wing cross-section

5.7 Mechanical Testing

EWI excised specimens for tensile bar and CVN tests from the CSX frog using a waterjet (Figure 60). Three samples of each specimen type were machined from each area shown in Figure 60. The specimens were cut from as close to the running surface as possible.

Figure 60. Mechanical test specimen cut plan, tensile bars from red areas, and CVN specimens from blue areas

EWI machined tensile bars to ASTM E8 dimensions for a round gauge section, 0.35 inch in diameter (Figure 61). EWI tested tensile bars from the left wing and the point at room temperature (Table 22). The ultimate strength was within the typical range for cast AMS material (100 to 150 ksi). The yield strength was higher than the cast AMS range (50 to 57 ksi), likely due to the work-hardening the weld repair received in service.

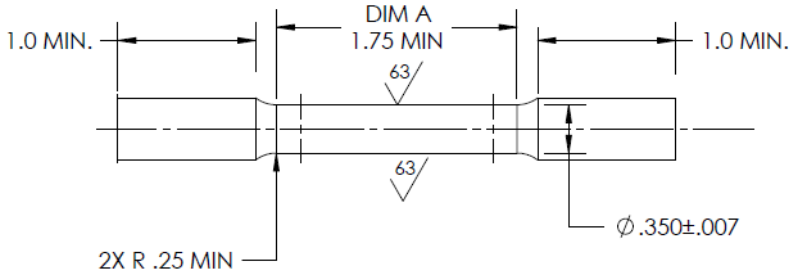

Figure 61. ASTM E8 round tensile dimensions

Table 22. Tensile test results for CSX frog

Specimen ID	Location	Ultimate Strength	Yield Strength	Elongation
		psi	psi	%
PT-1	Point	116,000	100,300	4
PT-2	Point	137,000	83,800	32
PT-3	Point	117,100	104,100	6
WT-1	Left Wing	127,800	93,500	11
WT-2	Left Wing	123,500	86,300	20
WT-3	Left Wing	131,500	111,600	4

EWI machined Charpy V-notch samples to ASTM E23 dimensions (Figure 62). Samples were cut from the right wing and point. The V-notch was cut into the side of the sample facing the running surface. For example, Figure 63 shows where the Charpy samples were cut from the point.

The Charpy tests were made at two temperature levels, 73°F and -29°F. In Phase 1, cast AMS base material was cut from a frog into ASTM E23 CVN samples and impact-tested. On average, these tests yielded 97 ft-lbf when tested at 73°F and 70 ft-lbf when tested at -30°F. The CSX frog impact tests averaged 33 ft-lbf at 73°F and 30 ft-lbf at -29°F (Table 23). The impact test that resulted in 73 ft-lbf at -29°F was considered an anomaly and dropped from the average.

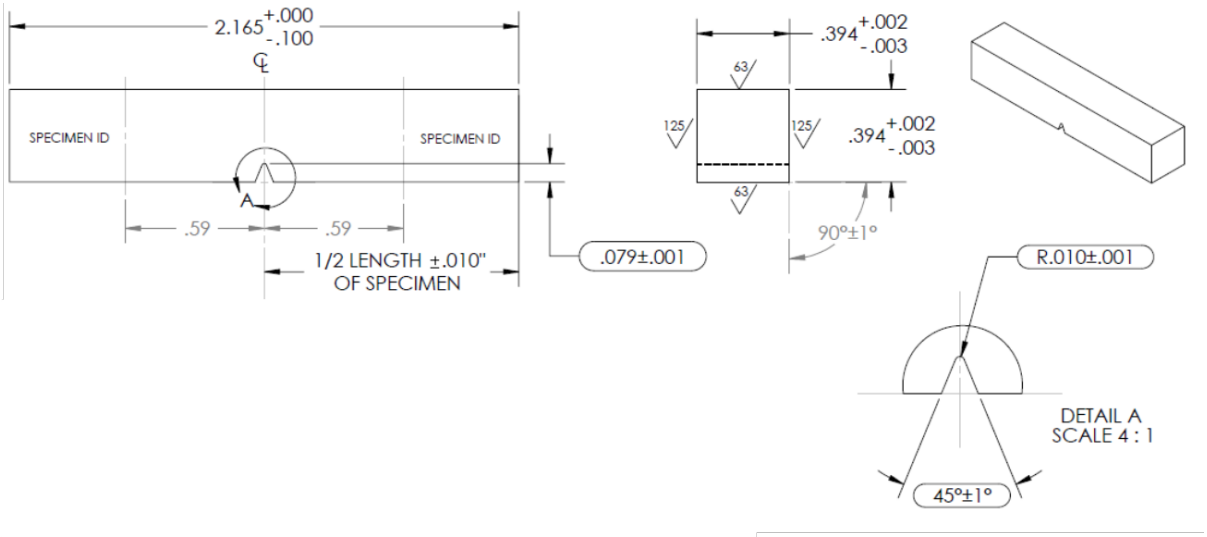

Figure 62. ASTM E23 CVN specimen dimensions

Figure 63. Charpy sample location for point

Table 23. Charpy impact test results for CSX frog

Specimen ID	Location	Temp	Abs. Energy
		°F	ft-lbf
WC-1	Point	73	22
WC-2	Point	73	38
WC-3	Point	73	40
PC-1	Right Wing	-29	28
PC-2	Right Wing	-29	31
PC-3	Right Wing	-29	73

5.8 Conclusion of Post-Test Analysis

Overall, the CSX frog performed well in this revenue service test, exceeding the average life of a first-time field repair. The wear condition of the wings after 63 MGT was comparable to the test frog run at TTC (Phase 1) after similar amounts of traffic (Figure 64). The Phase 1 test frog profile was measured as part of TTCI's test while it was in service. The CSX frog profile was measured after revenue service using a laser scanner. The scale is not the same for the graphs, but the profile measures show roughly 0.110 to 0.120 inch of deformation due to wear at 5 to 6 inches from the point after 63 to 68 MGT.

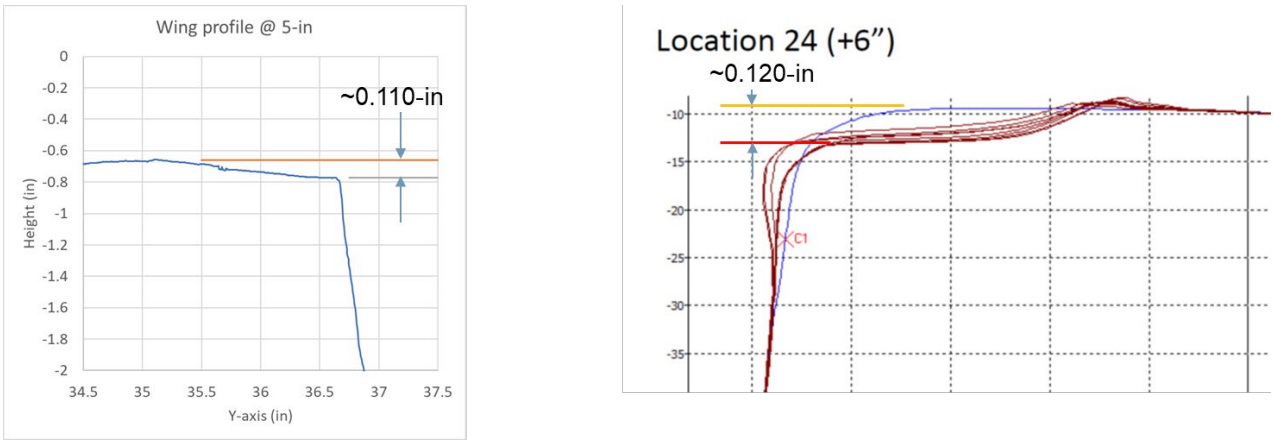

Figure 64. Comparison of wear: Phase 1 (left) and CSX frog (right)

EWI and CSX ended the revenue service test at 63 MGT after the material breakout in the point, but the profile measurements indicate that the CSX frog was wearing similarly to the Phase 1 frog. EWI ended the Phase 1 frog test at 118 MGT due to contractual obligations. This frog was still fit for service at the conclusion of the test.

The UT and cross-section examinations of the CSX frog point around the breakout found additional subsurface cracks that may have led to further material breakouts. These cracks and the breakout were not a direct result of the automated weld repair, but may have been the result of mechanical forces acting through lip of material that was not ground (see Section 5.6).

The mechanical test properties of the automated weld repair changed during service but not in any unexpected ways. The hardness of the weld material under the running surface increased to levels that are common for in-service AMS frogs. The tensile strength properties stayed close to those

found in as-welded development buildups (EWI MC1 GMAW-P) and the CSX frog after testing (Table 24). The increase in yield strength and drop in impact toughness are consistent with an increase in the hardness that occurred during service.

Table 24. Comparison of mechanical properties

	Typical Casting	EWI MC1 GMAW-P	CSX Frog Post
Average Ultimate Strength (ksi)	100–150	120.4	125.5
Average 0.2% Yield Strength (ksi)	50–57	79.6	96.6
Average CVN (ft-lbf) @~-30°F	~70.0	41.0	26.6

6. NS Frog Repair

EWI used GMAW-P with metal-cored wire parameters to repair a WBM frog section provided by NS. The frog was prepared in a manner representative of repairs in the field. The repair depth, location, and approach were all consistent with those during Phase 1 and the CSX frog repair. EWI repaired the point and both wings of the NS frog. For the CSX frog, a bead-by-bead programming method was used for the robot paths. For the NS frog, a layer-by-layer approach was taken. EWI completed pre-weld and post-weld inspection tests to validate the base material and weld deposit quality. NS visited EWI and performed the required finish grinding.

6.1 Technical Approach

The objectives of this repair were to: 1) inspect the provided WBM frog from NS; 2) identify and cut out the areas to be repaired, including previous field repairs; 3) repair the frog with the metal-cored wire using a layer-by-layer path plan; and 4) with help from NS, grind the repaired frog to final dimensions. EWI received a #20, WBM, conformal top frog from NS (Figure 65, Figure 66) and prepared and weld-repaired it in a manner similar to the frog tested by CSX.

Figure 65. #20 WMB frog as delivered to EWI

Figure 66. #20 WMB frog as delivered to EWI (with visible damage marked)

6.2 NS Frog Preparation

The NS #20 WBM frog was part of an experimental lot provided by Nortrak to NS in 2013 and had a heavy point (wider than standard) and conformal wings (designed to carry wheel loads over a greater area). NS removed the frog from service in Kentucky after 366 MGT over more than 4 years. During that time, NS weld-repaired the frog in the field 14 times (Figure 67). The frog was destined for scrap but was instead re-directed to this automated weld repair program.

Figure 67. #20 WMB frog with evidence of field repairs indicated

The NS frog was significantly more worn than the Phase 1 or CSX frogs. Approximately 1 inch of material removal was required to prepare the frog for the weld repair process. Per NS, some of the damage to the wings of the frog was caused by a height mismatch between the wings and point. For the train wheel to smoothly transition from the wing to point, or vice versa, both must be at the same height where the load is transferred. According to NS, some frogs with this conformal wing design have had wings roughly 0.25 inch above the point. This mismatch resulted in the wheel

climbing or falling off the wing during the transition. This climbing and falling action caused severe wear on the wing and caused impact damage to the point where the wheel landed (Figure 68).

Figure 68. Wing damage due to wheel climb

The WBM frog provided to EWI was not the only frog that suffered from excessive damage due to wing height mismatch in NS service. To address this issue, NS engaged a program to grind the wings of all affected frogs in the system. EWI and NS agreed that completing this grinding process before the automated weld repair was essential to achieving the correct final wing heights after repair. NS sent a crew to grind the frog in EWI's laydown area (Figure 69), which included a mechanized and manual grinding process.

Figure 69. Mechanized grinding system to lower frog wings

After NS completed grinding, EWI laid out the repair area in a fashion similar to the previous frogs. One unexpected effect of grinding the wing and point surfaces was it allowed the easy identification of prior field repair locations. A light coat of rust formed on the freshly ground surfaces, causing the field repairs to pop out due to less rust forming in these areas. This is due to the filler material used for field repairs which contains a small amount of chromium that the base frog material does not, making the weld-repaired areas more corrosion resistant (Figure 70). With the field repairs visible, EWI chose to extend the total repair area to roughly 54 inches to remove as many field repairs as possible.

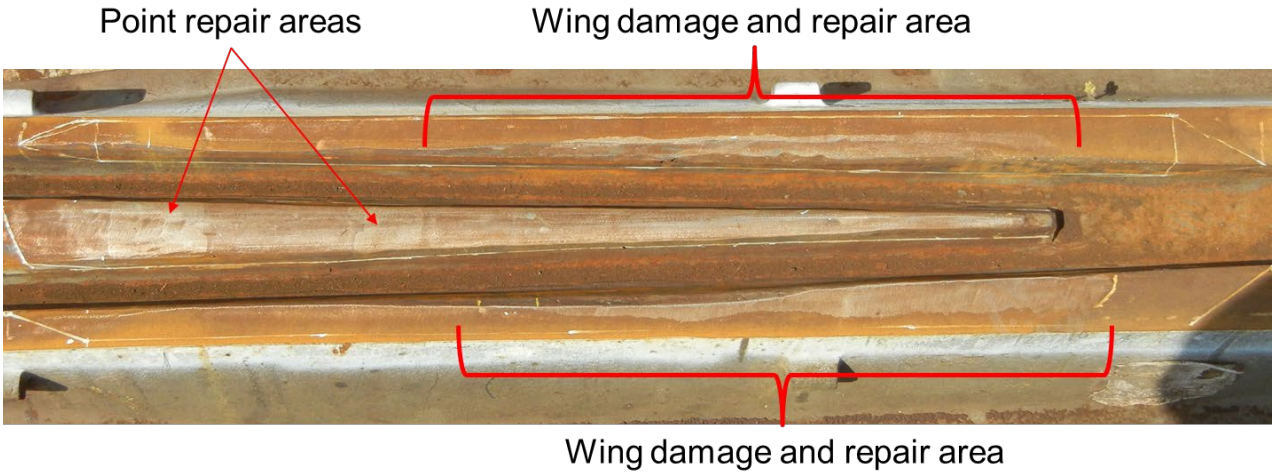

Figure 70. Field repair areas pop out visibly due to light rust formation

6.2.1 Wing Repair Geometry

The Phase 1 and CSX frogs were a rail-bound design, not WBM. Rail-bound frogs have a consistent wing width through the transition area. WBM frogs, however, have a tapered wing width in the transition area, with the wing narrowing from full rail head width as the wheel transfers to the point (Figure 71). The weld repair area for the wings had a triangle-shaped cross-section (Figure 72). The dimension from the outside edge of the wing to the repair area was 0.25 inch, and the repair depth from the wing running surface (flangeway side) was 1 inch. Since these two dimensions were fixed and the wing running surface varied along the length of the repair, the angle and width of the repair face also varied (Figure 73). At the narrow end of the wing, the repair face was 1.76 inches wide, at a 34.7° angle. At the wide end of the repair, the repair face was 2.79 inches wide, at a 20.99° angle.

Figure 71. WBM varying wing width along the repair area

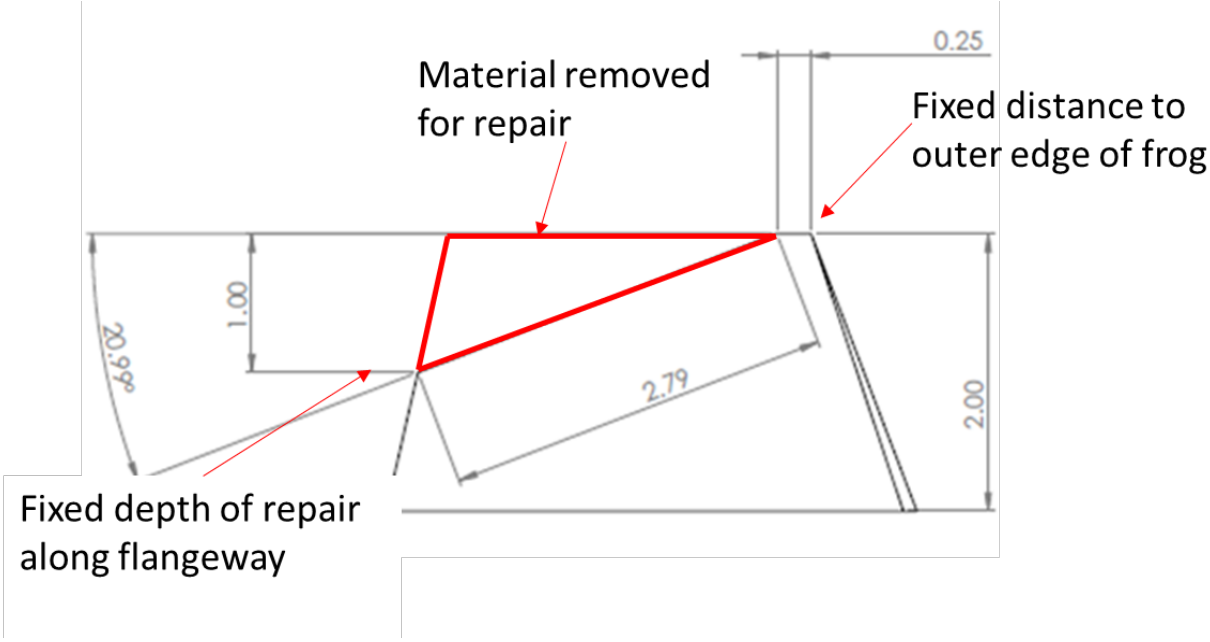

Figure 72. Drawing of a wing cross-section showing material to be replace during an automated repair

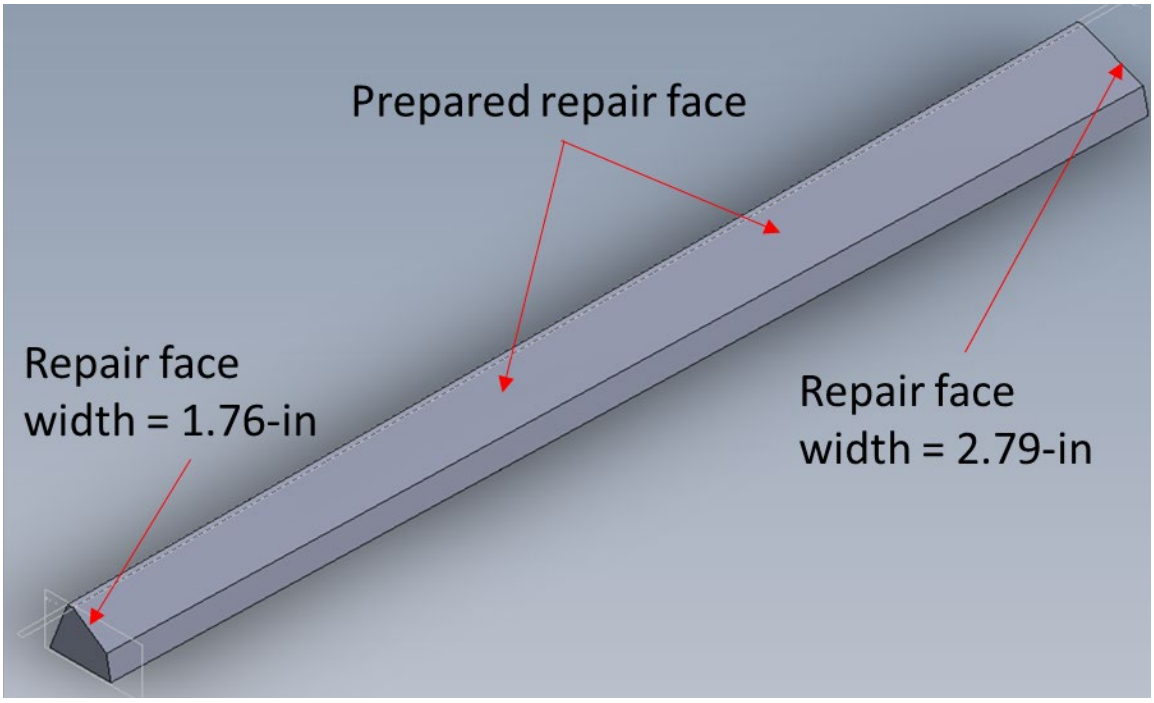

Figure 73. Model of a WBM wing prepared for automated repair

The width of the repair face changed over its length by nearly 1 inch. This tapered face required EWI to modify the welding conditions. EWI developed a method to taper the weld bead width by adjusting the travel speed along the wing repair. A test plate was laid out with the narrow and wide end dimensions of the wing repair face. Welding travel speed was broken into seven segments along the length. Each subsequent segment was welded 2 ipm faster than the previous. The first

segment used 14 ipm travel speed and the last segment used 26 ipm travel speed (Figure 74). Weld bead alignment was maintained by the first pass following the straight or outer wing edge, and the remaining beads used offsets of the transverse position's first pass (Figure 75).

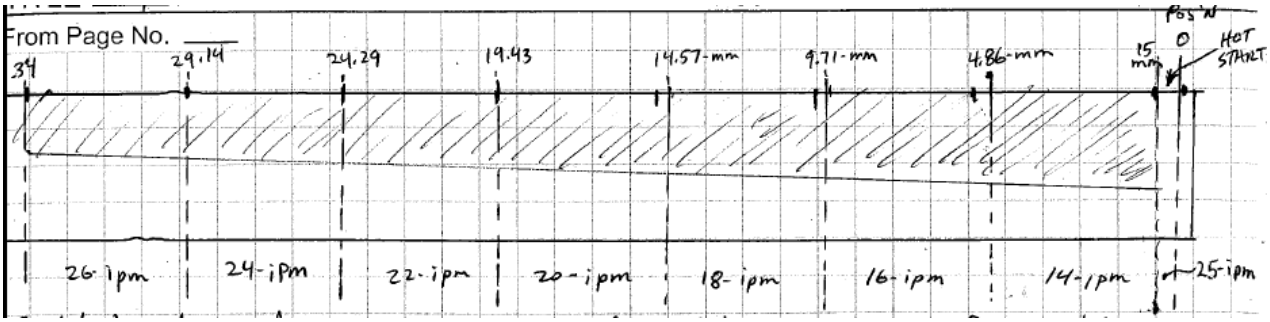

Figure 74. Travel speed segments for tapered wing welding

Figure 75. Tapered bead test plate with varied travel speed to narrow build area

After the test plate trail, EWI tested the method on a practice frog. A rail-bound frog was the only design available, and one wing was laid out with the same dimensions planned for the WBM wing repair (Figure 76 and Figure 77).

Figure 76. Practice rail-bound frog with simulated WBM wing repair cut

Figure 77. Practice rail bound frog with automated weld repair

6.2.2 Preparing the Frog Surfaces for Repair

EWI manually carbon-arc-gouged the worn frogs to remove the bulk of the material (Figure 78). After gouging, a crack was found in the point near the end of the repair (Figure 79).

Figure 78. WBM frog after gouging repair area

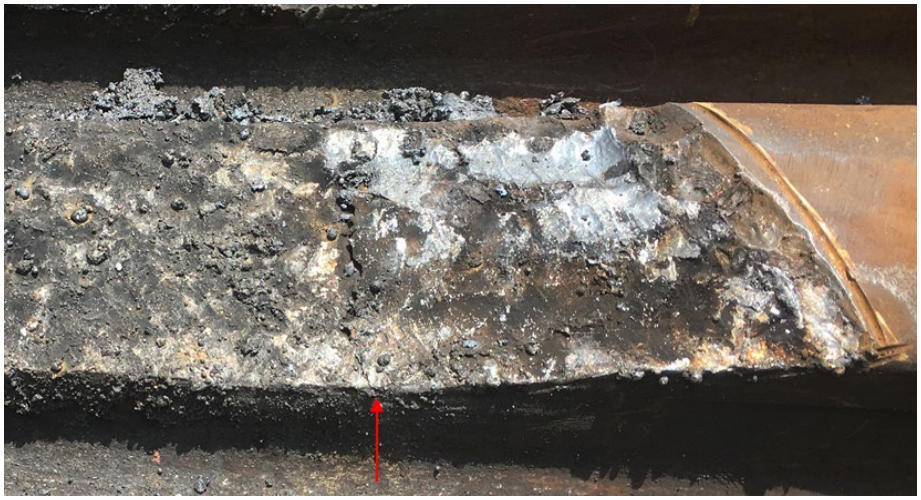

Figure 79. Crack in point found after gouging WBM frog, red arrow

EWI ground a groove on the point to remove the crack found after grinding. An electric grinder was used to achieve the final dimensions and to smooth the surfaces. To inspect the ground repair area a PT was performed (Figure 80), revealing deep cracks in the point that were areas subject to prior filed repairs. Shallow cracks were also found in the wings, many of which would be consumed by the weld repair penetration.

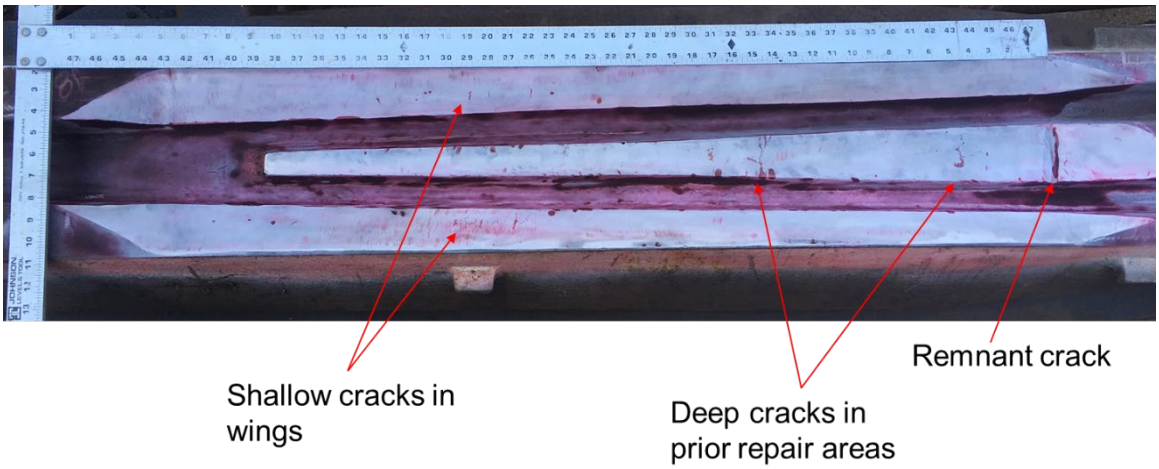

Figure 80. Repair area in WBM frog after penetrant test

EWI employed acid etching to highlight any additional areas where prior repairs were made. The composition of the field repair filler material etched differently than the frog AMS, revealing four notable areas (Figure 81). All areas except area 1 shown in Figure 81 received additional grinding to remove nearly all the remnant field repair material. Area 1 was left in place because it's narrow and fully contained within the wing width. In contrast, area 2 was ground and welded because it had one edge that extended to either edge of the wing.

Figure 81. Acid etched repair area in NS frog with field repairs labeled

EWI addressed field repair areas 2–4 using the following procedure. First, the field repair and adjacent area was ground out an additional 0.25 inch in depth. This area was then acid etched to

verify how much of the prior repair had been removed. If an acceptable amount was removed, the area was welded to height using the automated weld procedure (Figure 82). After the weld repair, the new buildup was ground flush with the adjacent surfaces.

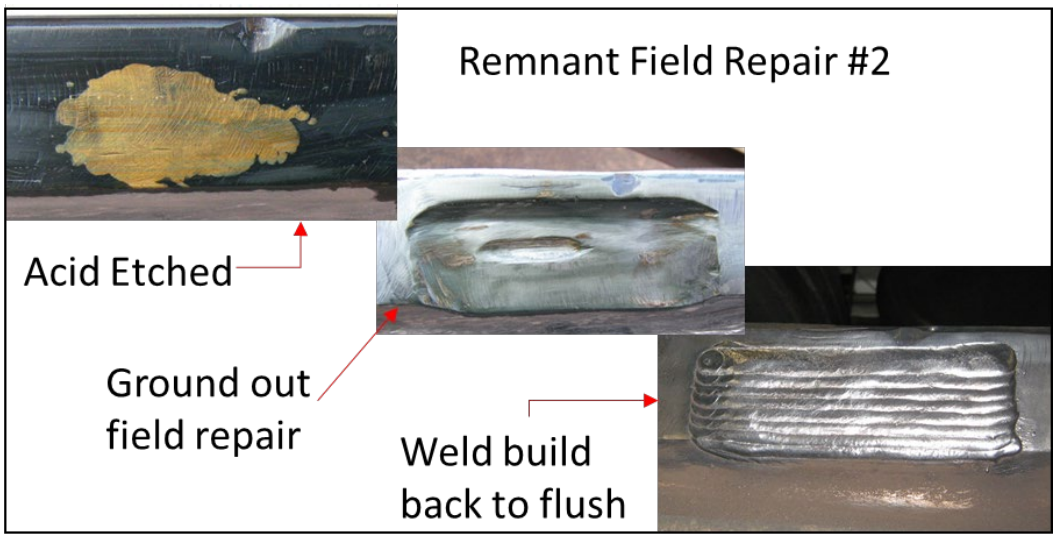

Figure 82. Example of field repair removal and automated weld repair buildup

The final step in preparation before robot programming and welding was to check the hardness of the joint face. Areas of the joint face adjacent to the running surface of the frog had a hardness gradient ranging from above 500 BNH to roughly 250 BNH (Figure 83). When repairing AMS frogs in the field, cracks often form on the running surface adjacent to repairs. Field personnel mitigate this cracking risk by peening each bead. For the automated repair process, EWI used bead sequencing to help mitigate cracking. The hardness data was used to determine bead placement and sequences to minimize cracking. The weld beads were not stopped at the edge of the joint face in areas of higher hardness. Instead, the beads were broken into two sections, so the final termination was in the center of the repair joint face (Figure 87). Weld beads were only started on joint faces that had been affected by work hardening to minimize stress caused by weld shrinkage and the potential for cracking.

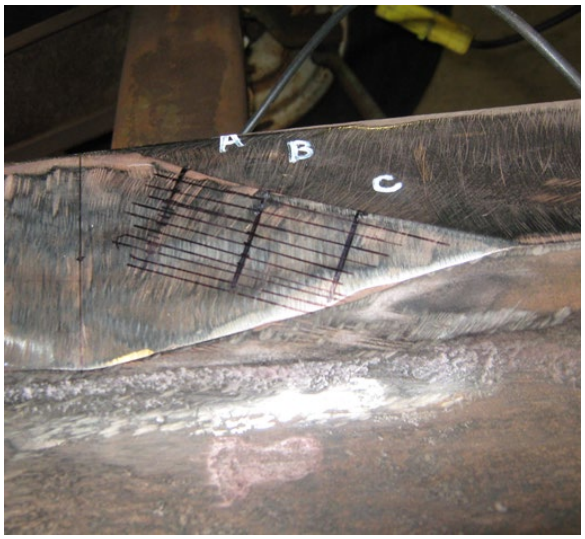

Figure 83. Map of hardness measurements taken on the point joint face

6.3 NS Frog Weld Repair

EWI's welding process was continuously improved as more frogs where welded. The Phase 1 process applied automated welding techniques with a commercially available flux-cored wire. As part of Phase 2, a metal-cored wire was developed, allowing the use of GMAW-P for the CSX frog, further improving weld quality. In preparation to weld the NS frog, EWI updated the power supply on the robotic system and the shielding gas was changed to improve weld stability and reduce spatter.

The same Fanuc robot used to weld the previous frogs was also used for this project (Figure 84). The welding power supply was updated to a Lincoln Power Wave S500. This is a new generation power supply with faster processing speeds which can produce a more stable arc.

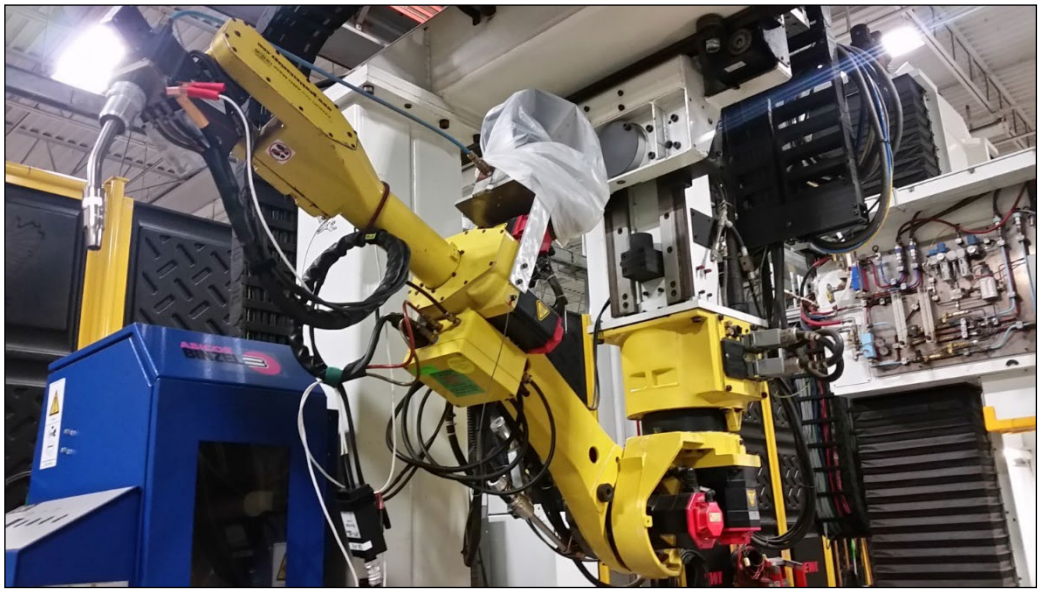

Figure 84. Fanuc robotic welding system used for automate weld repair

Spatter generation and collection on the gas nozzle was an issue during the CSX frog repair. A consistent flow of shielding gas is essential to producing high-quality weld repairs. The shielding gas used for all automated frog repairs in this program had been 75 percent argon/25 percent CO_2. This gas is recommended for use with the flux-cored wire used in Phase 1, and it was carried over during the CSX frog repair. GMAW-P shielding gasses with higher CO_2 content tend to generate more spatter than those with less. However, less CO_2 can lead to a lack of fusion as well as an unstable arc, depending on the GMAW-P conditions. To test the effect of CO_2 content on weld quality, EWI made small weld pads with shielding gasses of various CO_2 content using welding conditions from the CSX frog. Technicians tested and evaluated 5, 10, 15, and 20 percent CO_2 with an argon balance for arc stability and spatter. They concluded that 15 percent CO_2 provided the best balance of arc stability and spatter reduction.

6.3.1 Automated Weld Repair Process Parameters

Two weld repair conditions were used for the automated frog repair. A cold or corner/edge condition was used for weld repair near a corner or at locations with geometry features that could affect bead shape (Figure 85). A hot or center weld repair condition was used for all other areas and was designed to maximize deposition (Figure 86).

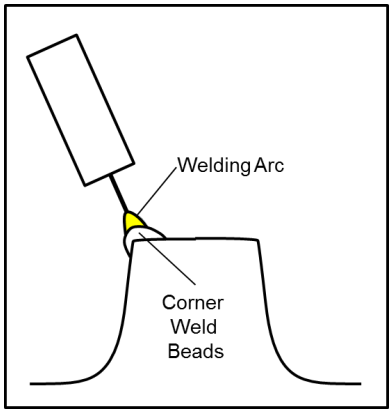

Figure 85. Corner/edge bead welding

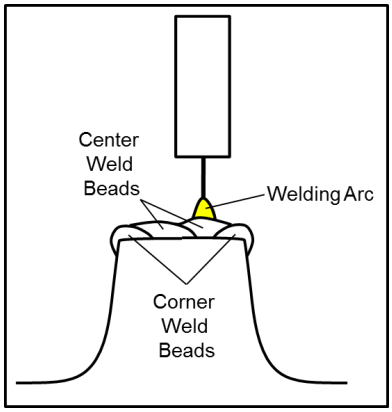

Figure 86. Center bead welding

The Lincoln Power Wave S500 power supply has built-in GMAW-P modes specifically designed for different filler wire types/diameters and shielding gases. The mode used for both the hot and cold bead welding conditions was #26, designed for 0.052-inch-diameter steel wire with an argon/CO_2 mixed shielding gas. The welding parameters used for hot and cold bead welding conditions are listed in Table 25.

Table 25. Welding conditions used to repair NS frog

Fixed Conditions		Welding Parameters		
		Variables	Cold	Hot
Wire Electrode	DEV MC1 .052	Wire Feed Speed (IPM)	170	270
Shielding Gas	85% Ar/15% CO_2 @ 40 CFH	Current (A), Avg.	146	240
Travel Angle	Push 10°	Trim (#)	1.000	1.030
CTWD	0.625 in.	Voltage (V), Avg.	24.5	27.3
Power Supply	Lincoln S-500	Ultimarc (#)	0.00	0.00
Weld Mode	Mode 26 (GMAW-P)	Travel Speed (IPM)	15	14-26

EWI programmed the robot sequence bead-by-bead for the prior frog repairs. This method allowed for a high level of control in bead placement but was very time-consuming. For the NS frog, EWI programmed the weld beads by layer. Figure 87 shows a bead plan by layer for a wing. The layer welding sequence included a hold at the end of each bead to allow the inter-pass temperature to be checked. If the temperature was below 500°F, the operator would start the next pass.

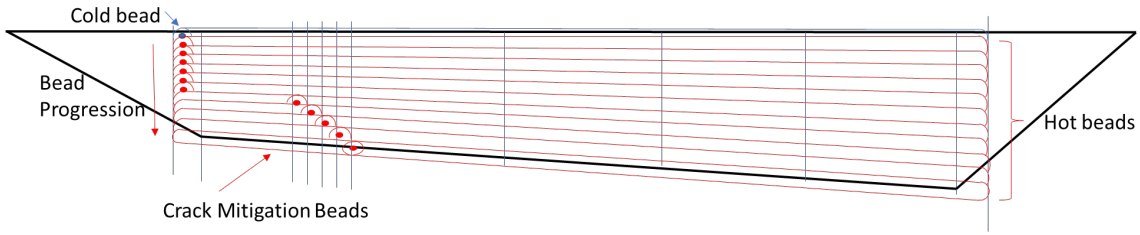

Figure 87. Bead layout for a weld repair layer on a wing

Figure 87 is a sketch of a program layer for a wing repair. The shape of the wing joint face is outlined in black. Each bead is represented by a red outline with a red spot for the stop location, except the first bead. The first bead was a cold bead placed at the top of the wing; its stop location is represented by a blue dot. All subsequent passes were made with the hot bead weld parameters and subsequent beads progressing down the joint face. The blue vertical lines represent the location of points along the programmed weld path. Path point locations were predetermined by calculating their location in a spreadsheet and moving the robot incrementally. The precise location of the path points was needed to ensure proper bead spacing and travel speed changes for the tapered joint face. The final five beads were made using the crack mitigation technique developed on previous frog repairs to locate the weld termination in the center of the repair joint face.

The weld repair used roughly 90 lbs of filler material to build up the wings and point. In total, nearly 500 beads were needed to create the 8 layers each for the wings and 11 layers for the point (Figure 88). EWI monitored inter-pass temperatures closely, with an average temperature at 154°F and a max of 220°F. Due to the distortion created from weld shrinkage, the frog would move; these movements required monitoring and shifting the weld paths. These position checks and position shifts led to longer pauses between beads than expected and influenced the inter-pass temperatures.

Figure 88. Fully welded frog repair joint

Other process techniques were used to keep the part temperature low. The direction of travel for each layer was alternated. Odd-numbered layers started on the right and traveled left, while even-numbered layers started on the left and traveled right, relative to the paths shown in Figure 88. The layer locations were rotated by layer. The left wing would have a layer built, then the right wing, then the point and back to the left wing. In a production environment, this technique would allow one area to cool while another is welded.

6.3.2 Nondestructive Evaluation of the Weld Repair

EWI ground the bead surface smooth for nondestructive evaluation (NDE). The first test was a phased-array ultrasonic test (PAUT) that inspected the entire volume of weld repair material. A sonogram-like visualization of inspection area was used to look for discontinuities in the weld (Figure 89). The weld repair was found to only have three notable discontinuities, as listed in Table 26 below.

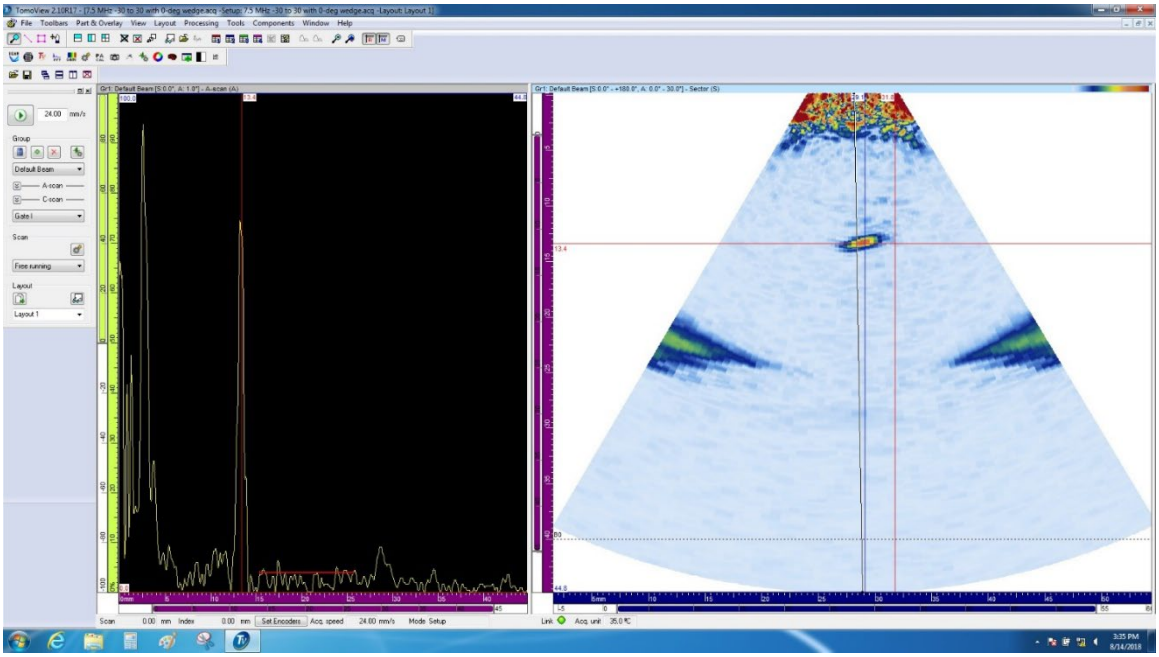

Figure 89. Example of a PAUT scan with discontinuity in sonogram

Table 26. Discontinuity location and size as detected by PAUT

Ultrasonic Inspection Data		
Location	Position from Point	Diameter
Left Wing	-8 in.	<0.5 in.
Right Wing	43 in.	<0.5 in.
Point	42 in.	<0.5 in.

EWI performed PT on the repaired areas after profile grinding by NS (see next section). The PT technique used was a solvent-removable, visible process performed for information only by a trained but not certified technician. No indications were found in the repaired area. However, an area with surface cracking was found nearly 50 inches from the point, just outside the repaired area (Figure 90). This was likely a subsurface defect created during service that was opened during profile grinding and the stresses created by the weld repair.

Figure 90. Surface crack found with PT outside the weld repair area

6.3.3 Repair Area Grinding to Profile

The frog's profile is an essential part of its functionality. The NS grinding crew returned to EWI to grind the repaired and adjacent areas back to a usable profile. This was accomplished by using a rail mounted, mechanized grinding system to set the height of the frog's running surfaces, and electric hand grinders to create the slopes and rounded corners. Profile gauges and straightedges were used to ensure the proper contours were ground (Figure 91).

Figure 91. NS grinding of repaired areas back to profile

NS technicians completed additional point grinding after the frog arrived at a preinstallation yard near Danville, Kentucky. A profile gauge inspection performed by the welding crew in Danville showed the end of the point was at the same height relative to the wings. In the first 10 inches, the point was to taper from 0.3125 inch below the wings to even with the wings (Figure 92). The welding crew in Danville used an electric grinder to modify the point profile to the proper taper.

Figure 92. Point before (left) and after (right) taper was ground to the proper profile

7. NS Frog In-Service Monitoring and Testing

Norfolk Southern installed the automated weld repair frog near the RJ Corman headquarters in Nicholasville, Kentucky, on December 10, 2018 (Figure 93). EWI was not present for the installation. This location has an average speed near 50 mph and sees estimated traffic of 75.6 MGT per year. During the monitoring period, the automated weld repair frog received an estimated 113.4 MGT of traffic. This is 112 percent of the average MGT before a weld repair for a new frog and 290 percent of the average MGT life of a frog with a first-time field repair [1].

Figure 93. Satellite image of frog location in central Kentucky

In the 18 months after installation, EWI visited the frog five times. Penetrant inspection, wear measurements, and running surface hardness testing was performed during most visits. The NS welding crew also visited the frog six additional times during this period to visually inspect for damage, and to grind material flow and weld repair areas as needed. Maintenance grinding was conducted seven times to remove material flow and help prevent subsurface cracking like that seen on the CSX frog.

7.1 NS Frog Inspections

EWI collected profile and wear data at 11 locations along the repaired area of the frog using a straightedge and taper gauge (Figure 94). Negative positions denote measurements taken ahead of the point, while positive positions denote measurements taken after the point.

Figure 94. Wear measurements being taken with a straightedge and taper gauge

EWI measured profiles during each of the five visits made by EWI. There were no profile measurements taken at the time of installation. The first measurements were collected after the frog had been in service for 6.3 MGT and had received a maintenance grind. The maximum wear measured between visits at any location was 0.0625 inch. No location had worn more than 0.0625 inch over the entire monitoring period. Table 27 contains the taper gauge measurements taken during each visit. The areas labeled BU indicate the surface was built up in the field during the last visit.

In addition to profile measurements and visual inspections during the visits, EWI inspected with PT four times (Figure 95). PT was not performed during the final visit due to the need for weld repairs. Crack indications were found on the running surface of the point during each of the last three inspections. Most areas of surface spalling and surface cracks grew between the second and third visit (October 2019 to January 2020). There were no indications of cracking that required repair during the final PT. The wings had no crack indications aside from isolated pores.

Figure 95. Frog PT

Table 27. Profile or wear measurement table

Position of the tip of the point, All measurements in inches

			-12-in		-4-in		0.5-in		4-in		8-in		12-in		16-in		24-in		32-in		40-in		48-in	
Date	Traffic (MGT's)	Area	TGM	Wear	TGM	Wear	TGM	Wear	TGM	Wear	TGM	Wear	TGM	Wear	TGM	Wear	TGM	Wear	TGM	Wear	TGM	Wear	TGM	Wear
1/3/2019	6.3	Point	N/A	N/A	N/A	N/A	1/4	N/A	1/4	N/A	3/16	N/A	1/8	N/A	1/16	N/A	1/16	N/A	1/16	N/A	1/16	N/A	1/4	N/A
		Wing T1	<1/16	N/A	<1/16	N/A	1/16	N/A	1/16	N/A	1/16	N/A	1/16	N/A	<1/16	N/A	<1/16	N/A	<1/16	N/A	<1/16	N/A	<1/16	N/A
		Wing T2	<1/16	N/A	<1/16	N/A	<1/16	N/A	<1/16	N/A	<1/16	N/A	1/16	N/A	<1/16	N/A	<1/16	N/A	<1/16	N/A	<1/16	N/A	<1/16	N/A
4/23/2019	29.3	Point	N/A	N/A	N/A	N/A	1/4	N/A	1/4	N/A	3/16	N/A	1/8	N/A	1/8	1/16	1/8	1/16	1/8	1/16	1/16	N/A	1/4	N/A
		Wing T1	<1/16	N/A	<1/16	N/A	1/16	N/A	1/16	N/A	1/16	N/A	1/16	N/A	1/16	<1/16	<1/16	N/A	<1/16	N/A	<1/16	N/A	<1/16	N/A
		Wing T2	<1/16	N/A	<1/16	N/A	<1/16	N/A	<1/16	N/A	1/16	<1/16	1/16	N/A	1/16	<1/16	1/16	<1/16	<1/16	N/A	<1/16	N/A	<1/16	N/A
10/3/2019	63.0	Point	N/A	N/A	N/A	N/A	1/4	N/A	1/4	N/A	3/16	N/A	3/16	1/16	1/8	1/16	1/8	1/16	1/8	1/16	1/16	N/A	1/4	N/A
		Wing T1	<1/16	N/A	<1/16	N/A	1/16	N/A	1/16	N/A	1/16	N/A	1/16	N/A	1/16	<1/16	<1/16	N/A	<1/16	N/A	<1/16	N/A	<1/16	N/A
		Wing T2	<1/16	N/A	<1/16	N/A	<1/16	N/A	<1/16	N/A	1/16	<1/16	1/16	N/A	1/16	<1/16	1/16	<1/16	<1/16	N/A	<1/16	N/A	<1/16	N/A
1/9/2020	75.6	Point	N/A	N/A	N/A	N/A	1/4	N/A	1/4	N/A	3/16	N/A	3/16	1/16	1/8	1/16	1/8	1/16	1/8	1/16	1/16	N/A	1/4	N/A
		Wing T1	<1/16	N/A	<1/16	N/A	1/16	N/A	1/16	N/A	1/16	N/A	1/16	N/A	1/16	<1/16	<1/16	N/A	<1/16	N/A	<1/16	N/A	<1/16	N/A
		Wing T2	<1/16	N/A	<1/16	N/A	<1/16	N/A	1/16	<1/16	1/16	<1/16	1/16	N/A	1/16	<1/16	1/16	<1/16	<1/16	N/A	<1/16	N/A	<1/16	N/A
6/10/2020	113.4	Point	N/A	N/A	N/A	N/A	1/4	N/A	1/4	N/A	1/4	BU	1/8	BU	1/8	BU	1/8	BU	1/8	1/16	1/8	1/16	5/16	1/16
		Wing T1	<1/16	N/A	<1/16	N/A	1/16	N/A	1/16	N/A	1/16	N/A	1/16	N/A	1/16	<1/16	<1/16	N/A	<1/16	N/A	<1/16	N/A	<1/16	N/A
		Wing T2	<1/16	N/A	<1/16	N/A	<1/16	N/A	1/16	<1/16	1/16	<1/16	1/16	N/A	1/16	<1/16	1/16	<1/16	<1/16	N/A	<1/16	N/A	<1/16	N/A

Note: TGM = Taper Gauge Measurement on that date

Wear = Amount of wear or deformation since first measurement

7.2 NS Frog Hardness Measurements

EWI measured surface hardness on the frog running surface during each of the in-service visits. Hardness measurements were made using a Proceq Equotip 550 Leeb D hardness tester (Figure 96). During the final visit the tester malfunctioned and the results were unusable. Frog hardness was only reported through the January 2020 visit. Hardness measurements were taken on the frog at the same distance from the end of the point as profile measurements were taken. Measurements were taken on both wings and the point, with four individual hardness measurements taken at each location.

Figure 96. Proceq hardness tester (top) and measurements being taken on a repaired frog (bottom)

The Proceq tester statistically analyzed the individual hardness measurements. The mean value for each measurement location and set is shown graphically in Figure 97, Figure 98, and Figure . Measurements were also taken on the automated weld repair outside the running surface. These areas had an average as-welded hardness of 250 BNH.

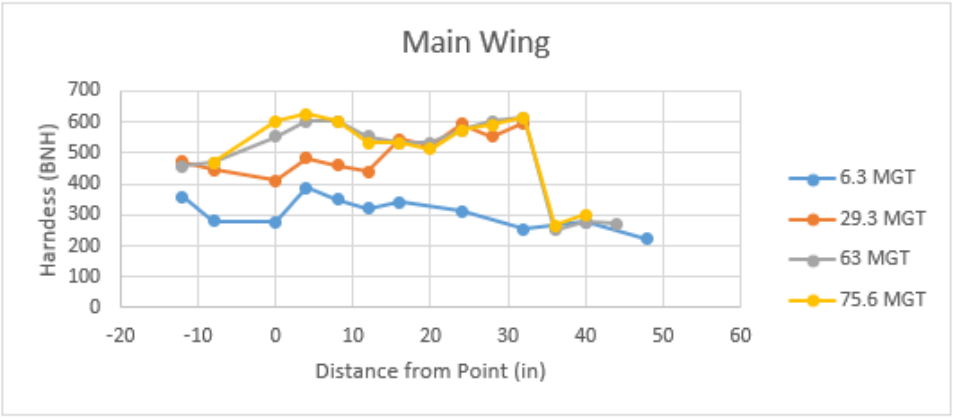

Figure 97. Hardness measurements: NS frog, main wing

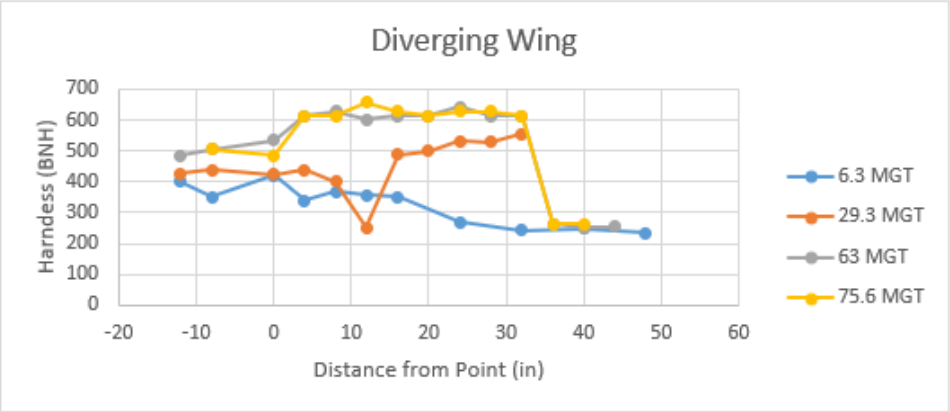

Figure 98. Hardness measurements: NS frog, diverging wing

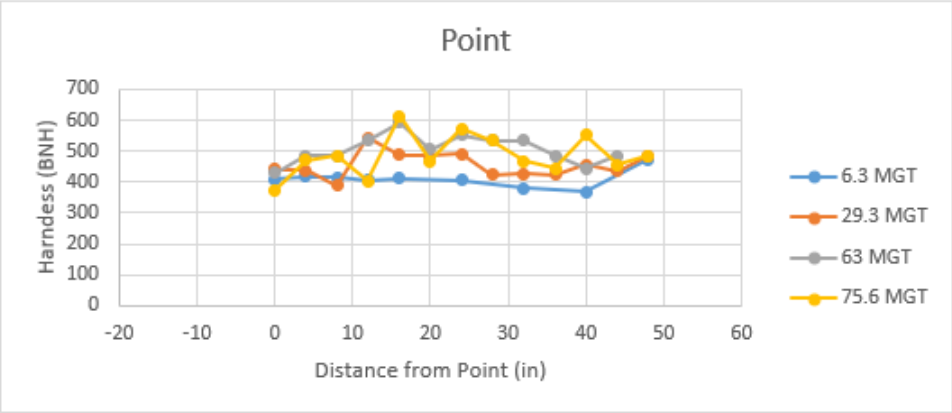

Figure 99. Hardness measurements: NS frog, point

Hardness values taken at the running surface did not reach a stable, work-hardened state as quickly as the previous frogs (Figure 98). (Note: Phase 1 frog labelled TTCI in figure.) Once the hardness level of the automated weld repair reached a stable work hardened range, it averaged around 20 BNH points higher than the highest level measured in previous test frog.

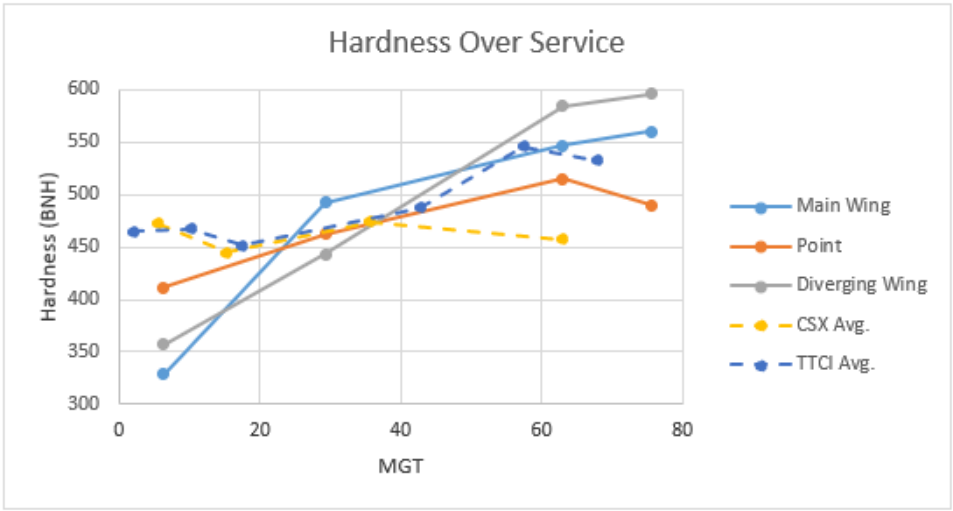

Figure 98. Comparison of work hardening rates

7.3 NS Frog – Field Weld Repairs

The NS frog was field weld-repaired field three times, but only once, during the final visit on June 10, 2020, in the automated weld repaired area. The weld repair in the automated weld repair area was on the point only and had two segments. The larger repaired segment was from 16 to 24 inches from the point and was needed to repair a transverse crack in the point. This area was cut out to a depth of approximately 1 inch, removing the bulk of the crack (Figure 99). The entire crack could not be removed as it ran into the flangeways before stopping. Per the NS welding crew, repairs that require cutting into the flangeway are too time consuming and can lead to further issues. Roughly 1 inch of visible, unrepaired crack was left on each side of the point and into the flangeways. The second segment of repair was located from 8 to 16 inches from the point (labelled wear area in the figure). This is a high-wear area of the point, and the NS welders decided to build up this area while repairing the cracked segment. NS ground down this area slightly and welded two layers of material. NS repaired a third area, located approximately 48 inches from the point, outside the automated weld repair area, to address some shallow but wide pits (Figure 100).

Figure 99. Crack repair area after cut out (left) and unrepaired crack on point and flangeway (right)

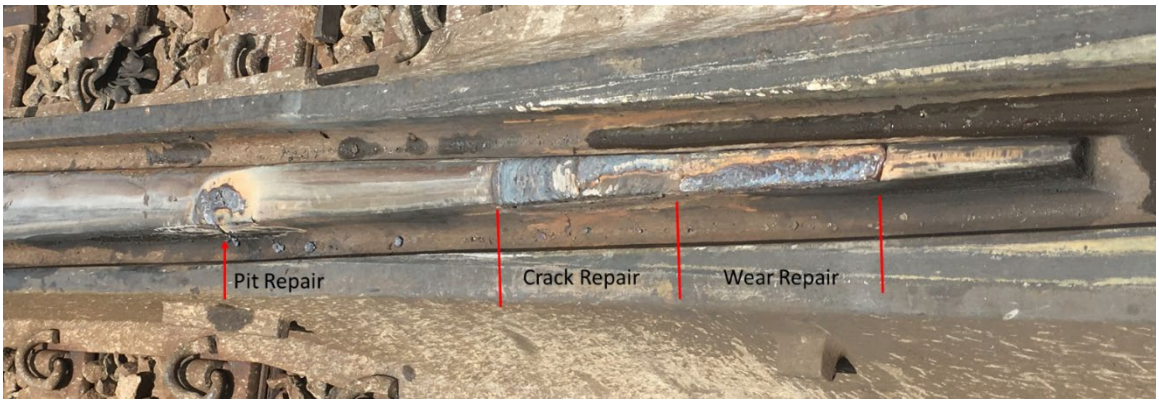

Figure 100. Weld repair segments on point before grinding back to profile

This project concluded at the end of June 2020. At that time, NS planned to continue the use of the automated weld-repaired frog and to maintain it in the normal fashion. With the field weld repair completed during the final visit the frog should have an extend service life.

8. Project Summary and Conclusion

EWI developed and tested a robot-based, automated weld repair process for AMS frogs. The project work included the development of a metal-cored wire for use with GMAW-P and robot motion. These new materials and techniques reduced weld heat input during the repair process while improving weld deposition rates and overall weld quality. EWI also developed a crack mitigation strategy for welds that tie into the frog running surface which has been work-hardened. Researchers repaired and tested two frogs using the new process. One frog was repaired and tested with CSX and the other with NS. All in-track testing of frogs repaired by EWI resulted in a longer service life than the average first-time weld repair, and the performance of the two revenue service frogs exceeded the average service of a new frog before requiring a weld repair.

Key outcomes from this project include:

Metal-Cored Electrode Development

EWI successfully developed a custom metal-cored wire and process parameters that produced mechanical and chemistry properties similar to the repair with flux-cored wire during Phase 1. The lack of slag and extensive inter-pass cleaning when using the metal-cored wire resulted in higher productivity. In addition, the weld beads lay flatter than when using flux-cored wire. This produced more uniform layer thicknesses and better tie-ins than previous weld beads.

CSX Frog Repair

EWI successfully repaired a full-length, #20, flat-top frog utilizing the parameters and approach developed in Phase 1. The parameters and beads were deposited with the same level of stability as during the Task 1 development. For repairs that require long weld bead lengths, spatter collection in the nozzle should be monitored and the nozzle cleaned to ensure it does not become completely blocked over time. However, the use of a copper nozzle and extended contact tip helped to reduce this formation.

CSX Frog Revenue Service Testing

CSX installed the repaired frog in mainline track at Decatur Junction, Alabama. EWI and CSX performed routine inspections of the frog for 13 months. These inspections included a mix of visual inspection, profile measurement, hardness measurement, dye penetrant inspection. CSX completed maintenance grinding as required.

EWI worked with CSX to monitor and test the automated weld-repaired frog while in revenue service. CSX inspected the frog 13 times, measuring wear and maintenance grinding as needed. EWI visited the frog four times while in service, performing PT and surface hardness tests. The automated weld repaired area work-hardened to levels similar to new cast frogs and wore at an acceptable rate. The test frog carried 68 MGT before removal.

CSX Frog Post-Test Analysis

EWI performed post-service UT and PT on the repair areas. Subsurface cracking in the material under the running surface was found with UT. PT verified the depth of visible cracks on the sides of the point and found some surface cracks on the point surface. The cross-sections of the repair were deemed adequate; defect-free weld material had been deposited. Strain bands were found in the microstructure under the running surface where the material had been work-hardened. The breakout which led to the end of the revenue service test was determined to not be caused or accelerated by the automated weld repair.

NS Frog Repair

EWI successfully restored a #20, WBM-conformal, profile frog to service using an automated welding repair process. A combination of localized and general weld repairs was used. Localized repairs were made to areas that had extensive and deep field repairs, creating a solid base over which the general repair could be made. The general repair replaced all the original casting in running surface of the transition area with a higher-grade weld buildup. Advanced robotic path programming was used to place welds efficiently on the complex WBM frog geometry. Temperature and stress management techniques were used where weld beads tied into the existing running surface to mitigate cracking.

NS Frog Revenue Service Testing

EWI worked with NS to monitor and test the automated weld repaired frog in revenue service and witnessed the first field weld repair made on an automated repaired frog. NS inspected and maintained the frog, providing flow removal and weld repairs as needed. EWI visited the NS frog five times while in service, performing wear measurements, PT, and surface hardness testing. Work-hardening of the repaired areas reached a level similar to the adjacent cast material at a slower rate than previous frogs tested in-track. This did not appear to affect the wear of the running surface or the repair's longevity. A weld repair was needed in the automated weld repair after 113.4 MGT of traffic, roughly 112 percent of the average traffic to first weld repair for a new frog or 290 percent of the life of a first-time repaired frog. This frog will continue in service.

8.1 Fully Automated Process Concept

The focus of this program has been to inspire the industrialization and commercialization of the automated frog weld repair process. This was achieved, in part, with the introduction of an in-track, robot-based laser weld repair process by an established rail industry service provider. This process is faster than manual repairs, aided primarily by its low heat input. The lower heat input of the robot-based laser weld repair process eliminates or reduces the hold time required for the frog to cool to below 500°F. Mechanical properties of the robot-based laser weld repair are similar to those of AMS castings and the weld repairs tested by EWI. No data were available indicating the in-track lifespan of this new repair process.

Like the automated weld repair EWI developed, this laser weld repair uses the robot for the welding only. Gouging and grinding of the repair area and post-weld grinding to return the frog to the desired profile is done manually. EWI considers automated frog repair viable for the rail industry in three variants: in-track repair, near-track repair (at a "frog pond"), and in a maintenance, repair, and overhaul (MRO) facility. While the in-track repair has the clear advantages of the frog remaining in service (only being temporarily inoperable), it also has limitations due to track downtime and the size of a repair that can be performed. Weld repair quality is also uncertain due to the uncontrolled environment. The near-track and MRO scenarios allow for a complete restoration of used frogs and take advantage of the efficiencies gained by automating more of the repair process.

8.1.1 Process Workflow

A fully automated process is one that has limited or no operator interactions. This process has generally been used for high-volume, low-mix manufacturing like cars and cell phones, where the incoming parts are held to a high-quality tolerance. In a frog repair situation, the incoming parts may have a known design but the damage from service will be unique to each. Also, special track

work (including frogs) is a low-volume, high-mix product. These two challenges will require the use of technologies and methods that are emerging in the development of large-scale additive manufacturing. A fully automated frog repair could consist of the steps shown in the flow chart below (Figure 101). Individually, all the technologies for these steps exist at an off-the-shelf level of development. Combining them into a single, automated system will require advanced development.

Figure 101. Fully automated frog repair process flow diagram

8.1.2 Repair Cell

The repair cell consists of a single, high-capacity, 6-axis arm robot with a master tool changer attached as the end effector (Figure 102).

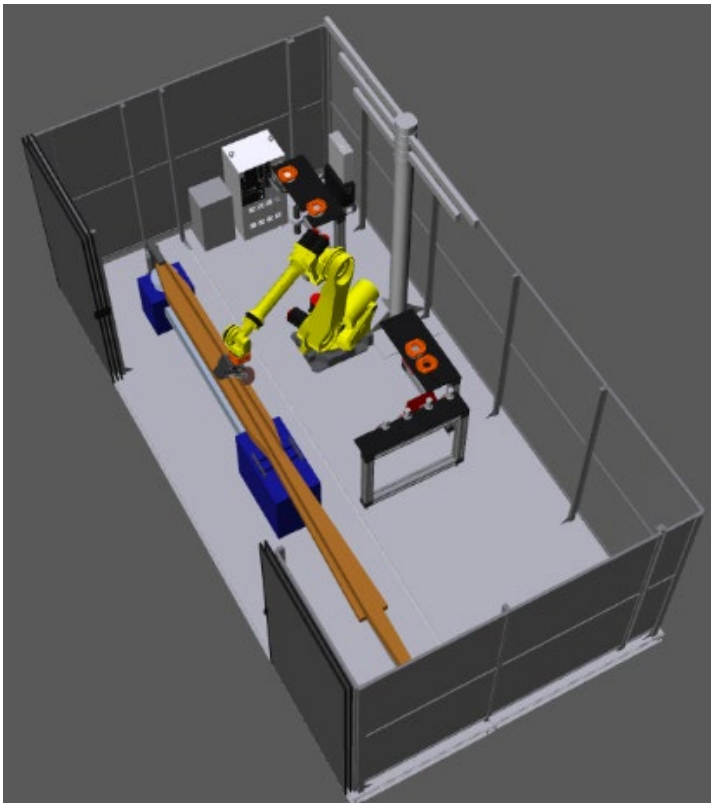

Figure 102. Robot repair cell model

The tool changer allows a single robot to utilize multiple tools and perform all the required weld repair tasks. For example, the robot is used for dimensional inspection by picking up a laser profilometer and scanning the frog. Other tools are available for grinding, plasma gouging, electro-magnetic acoustic testing (EMAT), and a welding torch. This robot cell is designed onto a common steel platform and could be placed directly on a train car or, with some modification, atop a truck trailer for field deployment.

A detailed description of each step and equipment requirements can be found in Appendix A.

9. References

1. Federal Railroad Administration (2017). Weld Repair of Manganese Frogs for Enhanced Performance (Report No. DOT/FRA/ORD-17/01). Washington, DC: U.S. Department of Transportation.
2. Dallos, J. (2017). An Introduction to Pulsed GMAW. Fabtech Inc.

Appendix A. Fully Automated Weld Repair Process – Conceptual Design

A.1 Automated Repair Process Overview

The process for repairing a damaged frog, be it manual or automated, has several steps. By examining the steps taken currently by welding crews on track and the lab-based process used to repair frogs at EWI, an automated repair process was created. EWI envisions the automated frog repair will consist of the steps shown in the flowchart below. (Figure A-1)

Figure A-1. Automated repair process flow diagram

A.2 Automated Repair Process Steps

Below is a description of the steps and some of the specialized equipment needed to perform a fully automated repair on frogs, assumed to take place in an MRO facility. The repair work will be performed in a dedicated robot cell with safety walls to limit human access during operation.

A.2.1 Frog support and distortion control – Custom Frog Fixture

The frog casting will be held in place during the repair with an automated part fixture. The fixture will have three support points – one in the middle and one on each end of the frog. The fixture end supports will be manually adjustable in the distance from the center to account for different frog lengths (Figure A-3). Clamps will hold down the ends to a fixed height.

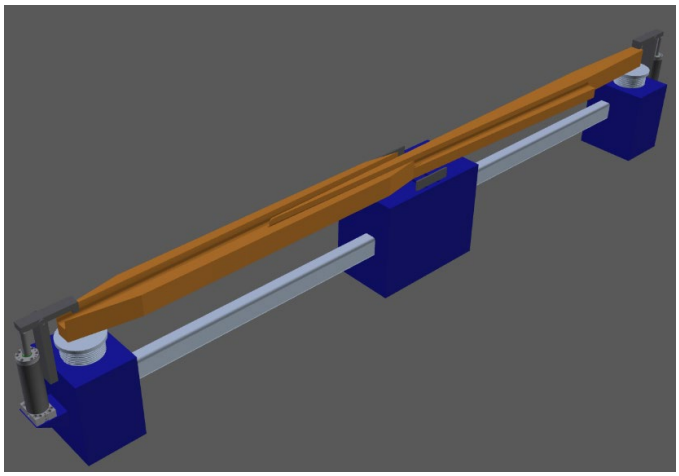

Figure A-2. Part clamping fixture

The center of the frog will be clamped at the sides and a pre-camber set by adjusting the height. A servo-controlled ball screw or hydraulic cylinder will apply the force. This pre-camber counteracts the distortion created by the weld shrinkage and heat. The design of the fixture can be completed by a robotic integrator.

The amount of pre-camber needed for each part could be determined by modeling. Pre- and post-weld dimensions should be tracked to develop a pre-camber/distortion algorithm that is dependent on the volume of repair material deposited.

A.2.2 Wear and surface damage scan – Laser Profilometer

With the frog fixtured, it will be checked for damage and dimensional changes due to wear or impact. The robot will pick up a laser profilometer vision system and scan the frog where damage is commonly found (Figure A-4). Based on typical wear patterns, the outside edges of the frog where the rail wheels do not make contact will be close to the as-manufactured condition. The insides edges bordering the flangeways where the rail wheels make contact will be worn down. By comparing the inside to the outside edges, and profiles of standard AREMA rails, the location and extent of wear will be determined, along with the size of the repair area.

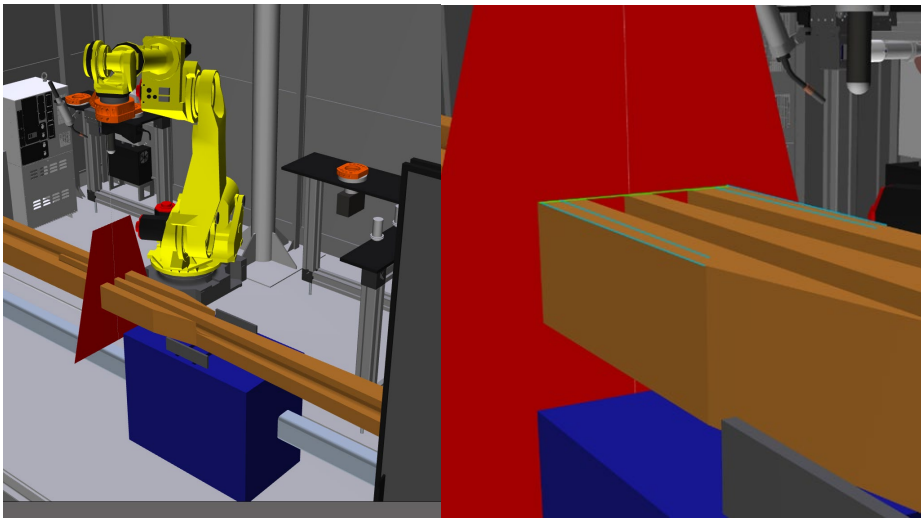

Figure A-3. Laser profilometer scan of the frog section

The laser profilometer vision equipment needed for the surface scan is an off-the-shelf product. The software and methodology for the automated system to determine the repair area from the data created by the surface inspection method needs to be developed. A set of standard repair geometries will need to be developed that cover two or three sizes of repair. One could be a full repair, similar to those conducted by EWI to develop the welding process, where 90 percent of the material in the transition area is removed and replaced. Other smaller repair geometries could be created to fix isolated areas of damage. This would increase efficiency and reduce distortion.

A.2.3 Bulk material removal – Plasma Gouge

Once the repair area has been identified, the damaged section of the rail must be removed. A manual example of this process can be seen in Figure A-5. The repair area to be removed will be based on standardized sizes and cross-sections to make the cutting and welding processes repeatable. To avoid excessive pre-weld preparation, a plasma gouging system is recommended for more precise, cleaner cuts.

Figure A-4. Example of frog after damaged rail section removed

The robot will pick up a plasma torch and begin gouging perpendicular to the rail while moving longitudinally along it (Figure A-6, left). Multiple passes must be made to remove all the required material. The number of passes and robot path plan will need to be developed based on standardized repair sizes and gouging parameters.

Figure A-5. Robotic plasma gouging

The plasma gouging hardware is an off-the-shelf technology (Figure A-6, right), but the process to accurately remove layers of material without removing too much or too little would require development. There are a number of variables regarding travel speeds, current settings, line air pressure settings, standoff, and path requirements that will have to be developed for a given area of repair.

A.2.4 Fine material removal and repair joint preparation – Grinding

After plasma gouging, slag and debris resulting from the process must be removed from the welding area and surrounding surfaces. The robot will pick up the servo grinder and dress the repair areas to create a smooth and even face to build material upon (Figure A-7).

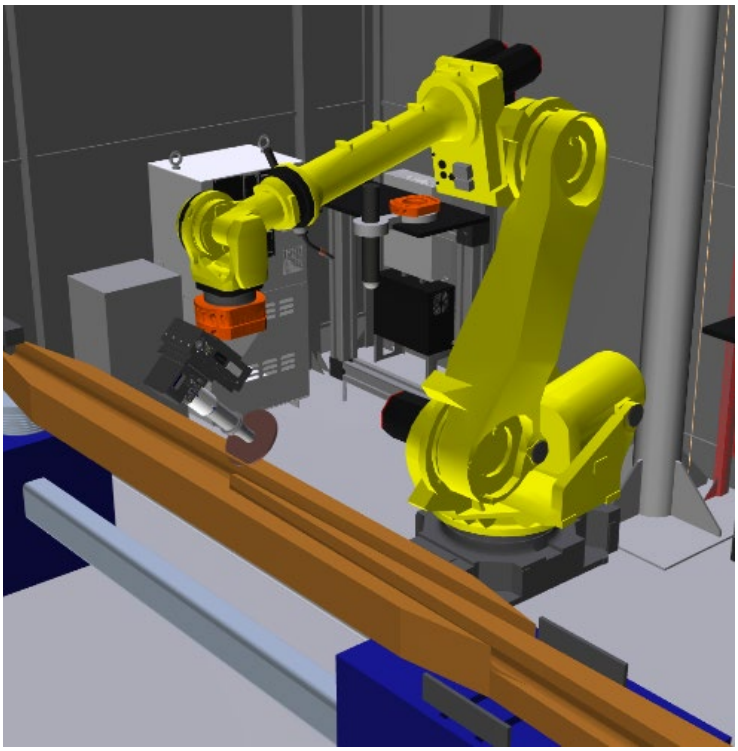

Figure A-6. Robotic grinding example

Since the size of the repairs will be fixed, the grinding path and process variables (including spindle speed, feed rate, forces and grinding media) can be set after development. Intermediate surface scans may be needed to ensure that the repair joint will meet the expected dimensions.

A.2.5 Subsurface damage inspection – EMAT

A nondestructive inspection system is needed to look for subsurface damage before and after the repair is made. An EMAT induces ultrasonic waves into a test object with two interacting magnetic fields. A relatively high-frequency (RF) field generated by electrical coils interacts with a low-frequency or static field generated by magnets to create a Lorentz force in a manner similar to an electric motor. This disturbance is transferred to the lattice of the material, producing an elastic wave. In a reciprocal process, the interaction of elastic waves in the presence of a magnetic field induces currents in the receiving EMAT coil circuit. Disturbances in the waves are indicators of potential issues. This process is conducted without making contact with the parts and without any form of liquid couplant.

After the grinder has smoothed the repair area, the robot will pick up the EMAT sensor (Figure A-8) and inspect for subsurface damage. The sensor will look for any anomalies, such as cracking and inclusions, that may reduce the life of the frog once back in service. If found, gated software will need to determine if the crack indications can be ignored or will require further inspection. If a problem is found, an operator can be flagged for manual inspection or documentation of the presence of underlying damage in the area.

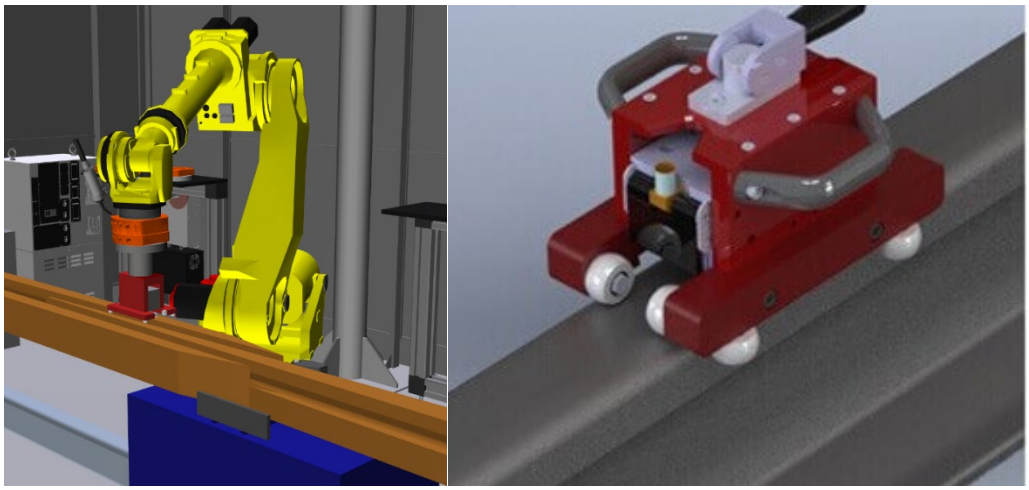

Figure A-7. EMAT sensor carried by robot (left) and manual EMAT sensor (right)

A.2.6 Dimensional restoration – Weld Repair

Once the robot has ground smooth the surface of the weld area, the robot will drop off the grinding head and pick up a welding torch (Figure A-9). The robot will build up the repair areas using path programming generated offline. Multiple weld layers will be required. The repair area temperature will be monitored with strategically placed infrared (IR) sensors, thermocouples applied to the frog, or an IR sensor that can be picked up by the robot. Bead placement strategies will be used to manage repair temperature by skipping to different areas of the frog after each layer or each bead for a more even distribution of heat.

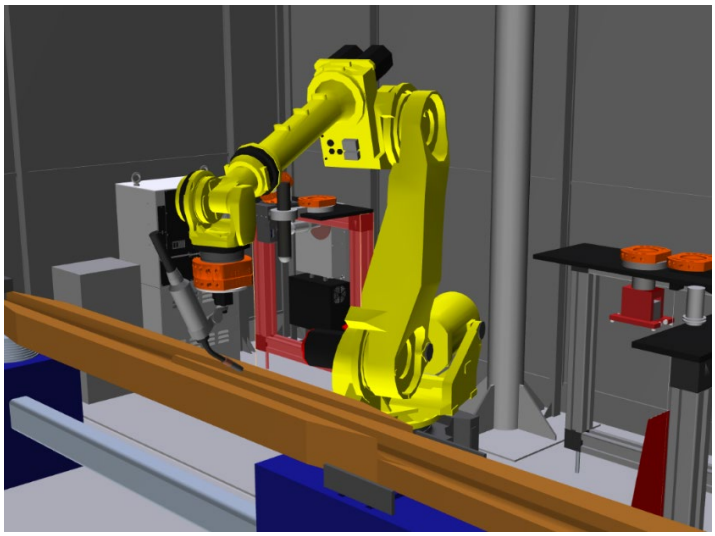

Figure A-8. Robot with welding torch

The welding process will be non-adaptive and based on fixed weld lengths and deposition rates. Weld beads and layer size can be modeled but are not 100 percent predictable. Scanning the repair two or three times during the rebuild process will allow for the path plan to be updated for the actual geometry. A final scan will be made for comparison to ensure that the weld buildup is adequate to return the frog to its original dimensions. Weld process monitoring should be employed to watch for deviations that could predict defects before additional layers are added. Software or applications for existing software would need to be developed to enable the path and process adjustments from the partial-build dimensional scanning.

Once the final dimension scan is complete, the pre-camber will be released by the automated fixture. This will place the ends and the center of the frog at the same level. A final scan will be made of the repair area with the frog in the free state to set the robot path planning for the final steps.

A.2.7 Surface preparation for NDE – Grinding

After the welding is complete, a second grinding operation is needed to smooth the repair surface for NDE inspection. The robot will pick up the servo grinding head and work on the repair areas found in the initial scan. The part does not need to be ground to the exact rail profile to allow NDE – only enough so the sensors do not pick up any false readings. The grinding will focus primarily on the top of the weld. The vision system will be used to verify that enough material has been removed to eliminate surface irregularities that will affect the NDE inspection.

A.2.8 EMAT NDE Inspection

After the weld surface has been smoothed, the robot will pick up the EMAT sensor again and inspect the newly welded areas. The sensor will be looking for any anomalies, such as cracking and lack of fusion, that may cause the buildup of material to fail prematurely in service. If a problem is found, an operator can be flagged for manual inspection. If the anomalies are verified as rejectable, an isolated repair routine can be used to remove the defect and replace the material.

A.2.9 Grind to Profile

After NDE inspection, the rail will be ready to grind to a final profile. The robot will first pick up the vision system and then determine current dimensions of the repair area. This scan of the frog will be compared to a model of a new frog to ensure positive material is present over the entire repair. Standard grinding path plans must be developed to return the repair to acceptable dimensions. Next, the robot will pick up the grinding head and focus on shaping the profile to match the new frog dimensions (Figure A-10).

The robot will use a combination of the vison feedback and positional feedback from the active compliance device mounted between the robot flange and the servo grinding head to determine how to grind the part. By looking for path deviations from a standard profile in the movement of the active compliance device, the robot will be able to “feel” where extra grinding effort is needed to smooth the profile to the correct shape.

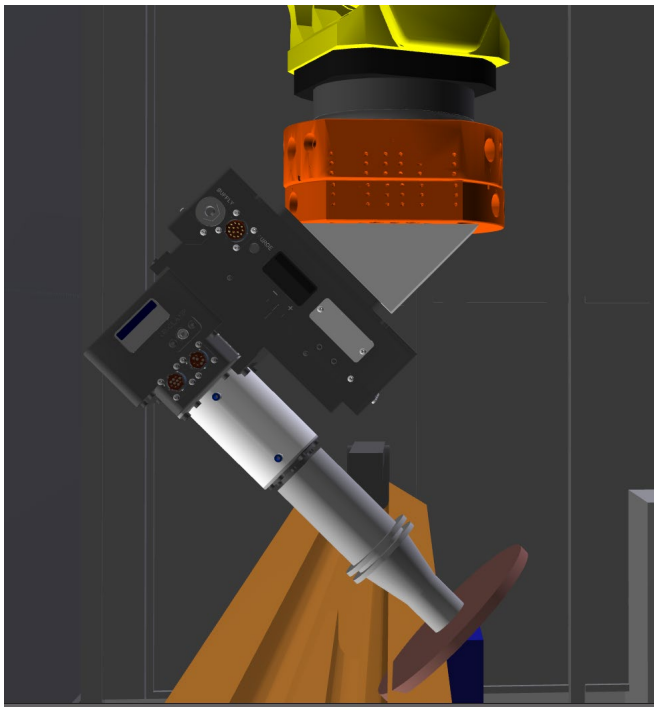

Figure A-9. Robot-mounted servo grinding head with active compliance device

A.2.10 Final Inspection

Vision scans at the 75, 90, and 100 percent complete points will be performed to confirm the profile shape is correct, the part has not been over-ground, and there are no voids in the part. A final report will be generated on the repair after the final scan for documentation purposes.

A.3 Cell Overview

The fully automatic frog repair cell contains all the equipment needed for every aspect of the frog repair operation (Figure A-11). The industrial robotic cell concept consists of a single, industrial, 6-axis articulated arm and flexible fixturing to hold different frog models. The robotic arm is equipped with an automatic tool changer to allow the robot to select the tool for the required process. Around the robot is an 8-feet-tall safety fence with large, front-entry double door and a side maintenance door. The entire system sits on two steel decks for easy transport, relocation, and installation of the cell. The decks are designed with wide lift points for easy movement and transport. The robot controller, cell controls, and all process equipment are located on the steel decks as well. The following is a breakdown of the individual pieces of equipment required.

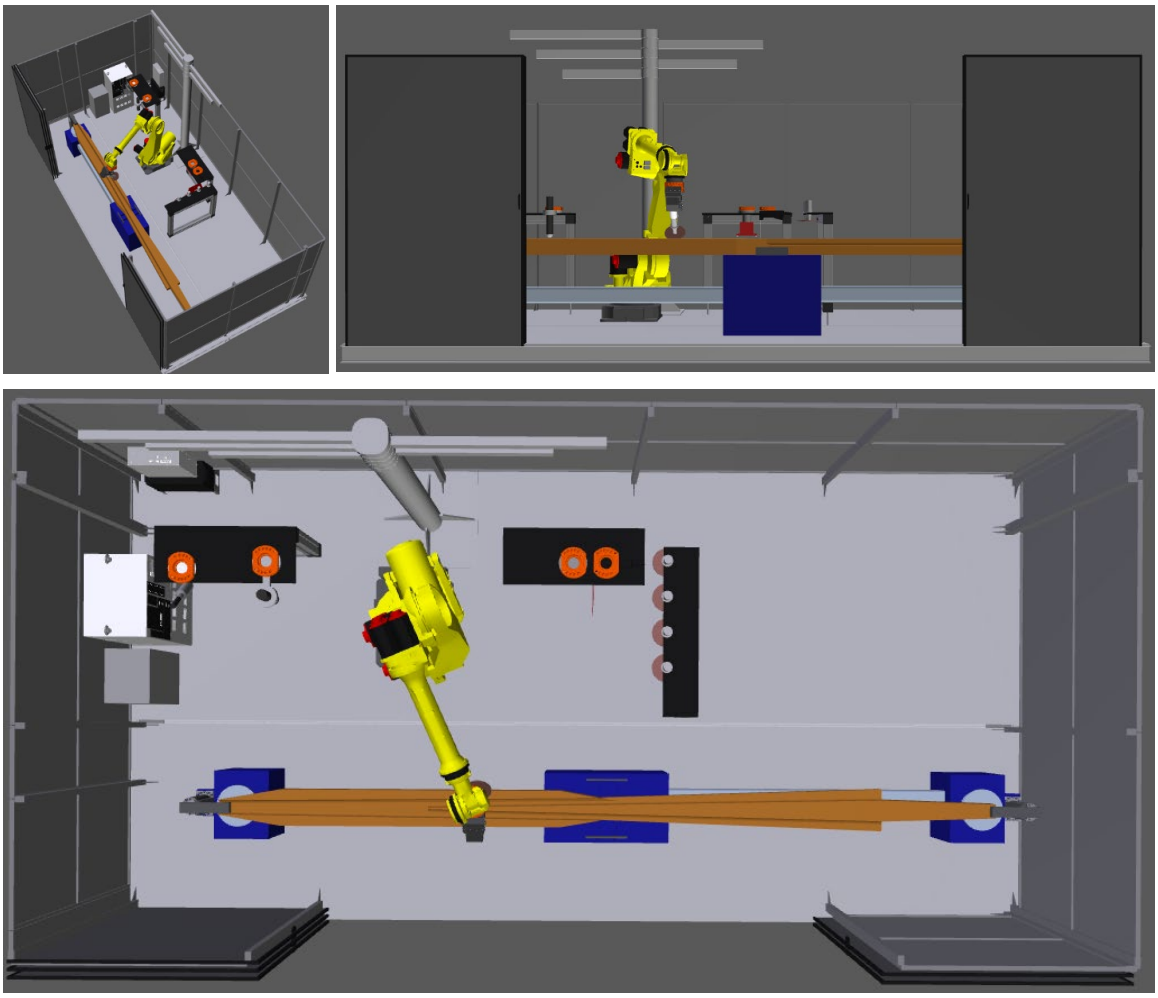

Figure A-10. Automation cell images

A.3.1 Robot

The robot used in this process is a 6-axis articulated arm with a 165-kg weight capacity and a 2.6-m horizontal reach at its furthest point (Figure A- 12). The robot must have discrete and fieldbus I/O. The robot will have a network connection, 24v discrete safety connection, and fieldbus connection back to the main control panel. Multiple pass welding software is required as well as the ability for parallel process programs.

Example robot – Fanuc R2000iC/165F:

- 6 axes of articulation
- Payload: 165 kg
- Repeatability: +-.05 mm
- Reach: 2655 mm
- Ethernet I/P communication
- Arc welding software package

Figure A- 11. Example Robot picture and description

A.3.2 Tool changer

Mounted on the robot will be the master half of a 165-kg capacity tool changer. (Figure A-13 and Figure A-14).There will be five adapter halves of the tool changer mounted to the different process and inspection tools. The tool side adapters and tools will rest on two tooling nests, one mounted on each side of the robot.

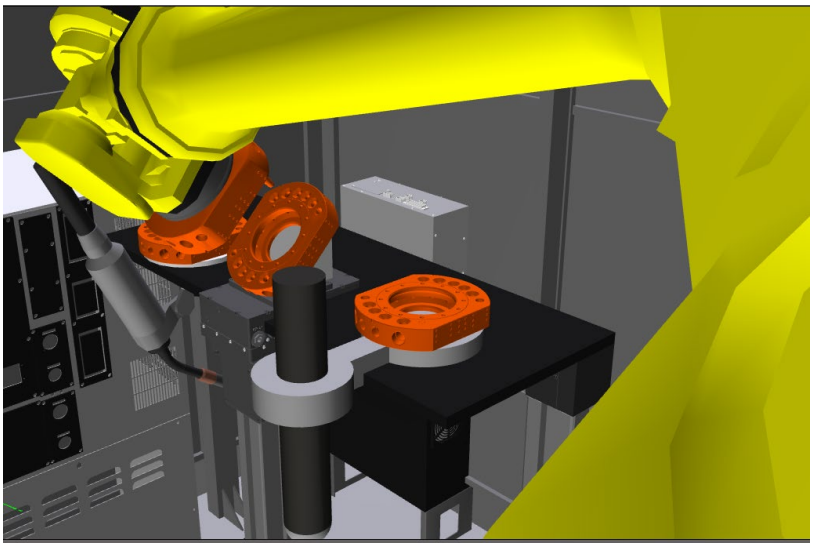

Figure A-12. Robot with tool changer approaching tool for connection

Tool changer example – ATI QC-160:

- Payload limit: 660 lbs
- Static moment capacity xy: 24,000 lbf-in.
- Static moment capacity z: 20,000 lbf-in.
- Positional repeatability: 0.0006 in.

Figure A-13. Example tool changer for robot attachments

The utilities and communications bundles will be supported by a bundle tree with arms overhanging each tool instead of passing through tool changer and add-on modules (Figure A-15). From the arms will be tool balancers to support the load of each process bundle. Sensors will be utilized on the tool nest to determine if a tool is in place for the robot to use.

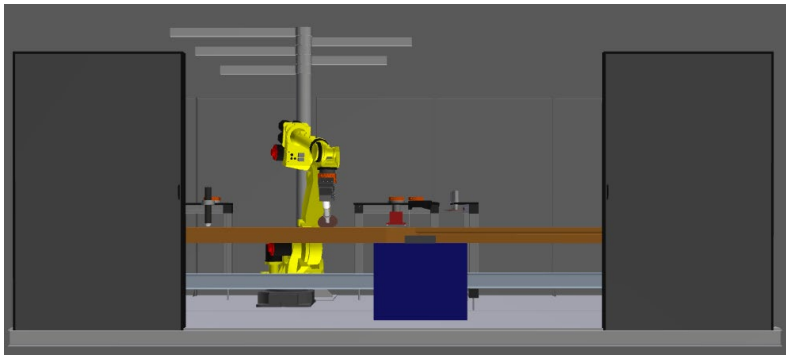

Figure A-14. Tool bundle tree shown behind robot

A.3.3 Vision inspection package

The vision package will take images that are profile cross-sections of the frog track section (Figure A-16). To do this, a laser profilometer will be used with a 20-inch-wide field of view (FOV) at the vertical midrange (Figure A-17). Resolution of the camera will be 3,200 data points or greater, resulting in a horizontal resolution of ≤ 0.15 mm at the midrange of the camera (vertical FOV). The camera system must be able to record and store profile data. These data can be used to build 3D models of the repair area and for comparison to frog models. The camera system should be able to compare the current image being taken to a stored image in the system.

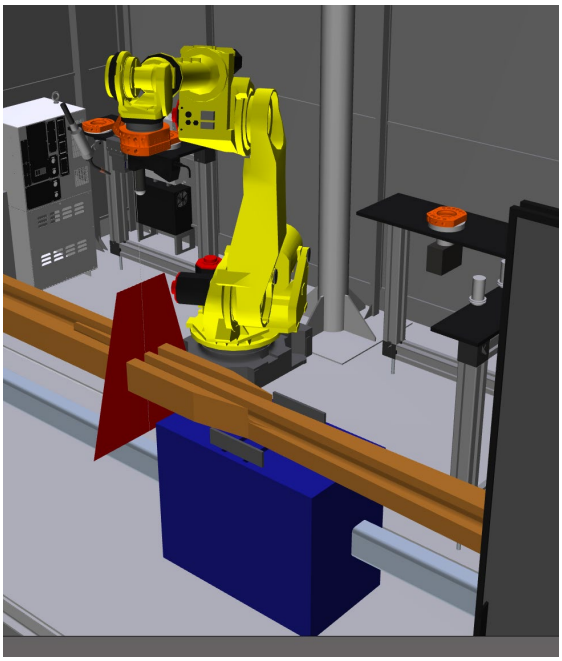

Figure A-15. Laser profilometer vision system being carried by a robot (the red trapezoid represents the FOV)

Example vision system – Keyence LJ-X8900:

- 3,200 points of data in scan
    - Near-side FOV: 580 mm from camera at 300 mm wide
    - Middle of FOV: 980 mm from camera at 510 mm wide
    - Far-side FOV: 1380 mm from camera at 720 mm wide
- Blue laser system w/10 mw output
- 16 KHz data collection rate

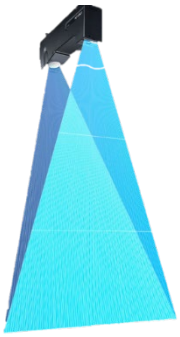

Figure A-16. Example laser profilometer

A.3.4 Plasma gouging system

The plasma gouging system will remove the damaged areas of the rails with a precise path and cut profile. This system consists of the plasma power supply and a mechanized plasma torch (Figure A-18). The power supply must be able to reach 300 amps at 90 percent duty cycle and 280 amps at 100 percent duty cycle. The system must be able to remove greater than 50 lbs an

hour of material and have a built-in CNC interface for connection with automation equipment. The mechanized cutting torch must be water-cooled and rated for 300 amps. The cutting torch will be mounted to one of the tool adapters with the bundle supported by one of the boom arms from the bundle support tree.

Example plasma gouging system – ESAB Deuce Pack:

- Two ESP-150 cutting power supplies
- Rated output: 30A to 280/300A
- Material removal: 77 lbs/hour
- Built-in water cooler
- PT-26 mechanized water cooled cutting torch
- Duty cycle:
  - 100% @ 280A
  - 90% @ 300A
- Gas type: Air/nitrogen, H-35, nitrogen/hydrogen mixtures
- Built-in CNC interface
- Thermal overload switches

Figure A-17. Example plasma gouging system

A.3.5 Grinding System

The grinding system will consist of a servo spindle with a controller and an active compliance device with a controller. (Figure A- 19 and Figure A-20) The 3000-rpm spindle should be a 25 hp (18.6 kW) servo motor with integral tool clamping to perform grinding operations. The spindle should have full speed and torque control and feedback and be designed to use BT40 standard CNC tool holders.

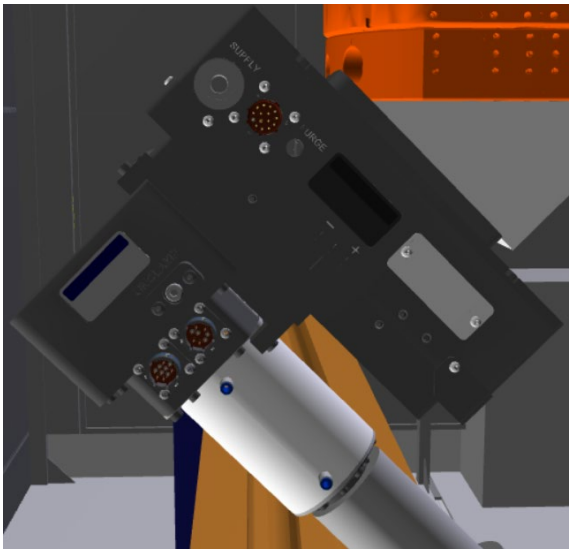

Figure A- 18. Servo spindle and compliance device

The compliance device, when coupled with a controller, should give consistent force regardless of orientation (Figure A-21). The device should have a maximum compliant force of 270 lbs and a linear stroke of 36 mm. Additional features must include automatic payload measurement, acceleration compensation, and variable force based on slide position.

A five-station tool changer with additional CNC tools and grinding wheels will be in the cell for quick change of media.

Example Servo Spindle – Pushcorp STC0325:

- Spindle tool specifications:
  - Power: 25.0 hp (18.6 kW)
  - Contin stall torque: 36.9 lb-ft (50 Nm)
  - Speed range: 0–3,000 RPM
  - Speed regulation: ±2% (reversible)
  - Tool weight: 180 lbs (82 kg) dry
- Collet specifications:
  - Required toolholder: BT40
  - Clamping supply air: Dry, non-lubricated
  - 90 psi (6.2 bar) minimum
  - 100 psi (6.9 bar) maximum

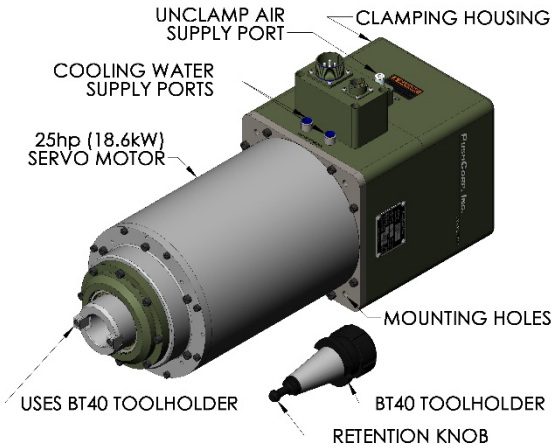

Figure A-19. Example servo spindle for grinding attachment

Example Compliance Device:

- Max applied force: 269.8 lbs (1200 N)
- Force resolution: ±0.8 lb. (±4.0 N)
- Update rate: 2 ms
- Max payload weight: 269.8 lbs (122.4 kg)
- Weight (excluding payload):
  - AFD1240-1 – 79 lbs (35.8 kg)
  - AFD1240-2 – 45 lbs (20.4 kg)
  - AFD1240-3 – 58 lbs (26.3 kg)
- Compliant stroke: 1.4 in. (36 mm)
- Supply air: Dry, 5µm filtered, non-lubricated, 80 psi (5.5 Bar) max
- Required controller: FCUFLEX

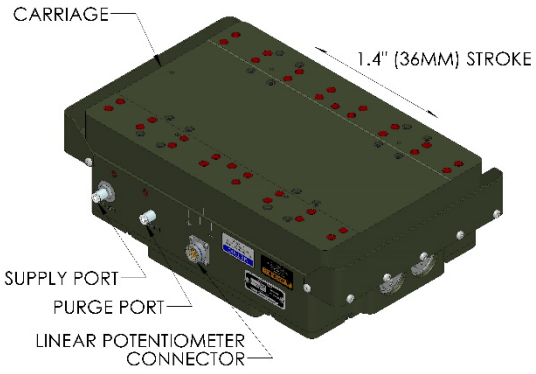

Figure A-20. Example compliance device to allow for precision grinding

A.3.6 Electro Magnetic Acoustic Transducer

The EMAT inspection system consists of a sensor (Figure A-22 and Figure A-23) that will be mounted to one of the tool adapters for the robot and a controller (Figure A-24). The sensor must be able to penetrate 2 inches and travel 1 inch per second. The sensor must have an Ethernet I/P communication and software set up for the automated used.

Figure A-21. Innerspec MRUT EMAT sensor

EMAT sensor example – Innerspec MRUT System:

- Sensor:
  - Wave modes: Lamb, shear vertical
  - 7.25 W x 2.71 H x 8.66 D (in.)
  - 184 W x 69 H x 220 D (mm)
  - Minimum OD: 4 in. (101 mm)
  - Maximum thickness: 0.5 in. (13 mm)

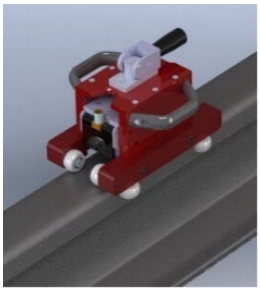

Figure A-22. Example EMAT Sensor

- Controller:
  - Two ultrasonic channels for EMAT applications ranging from 20 kHz to 8 MHz
  - 1,100 Vpp and 6 kW of peak power per channel, 1 to 10 cycles
  - Standard software permits running any EMAT application including normal beam, angled beam, and guided waves.
  - Custom software for MRUT (medium-range UT), LRUT (long-range UT), rail heads, thin welds, and other unique applications.
  - NDT-Web™ user interface and seamless integration with NDT-Link™ portal

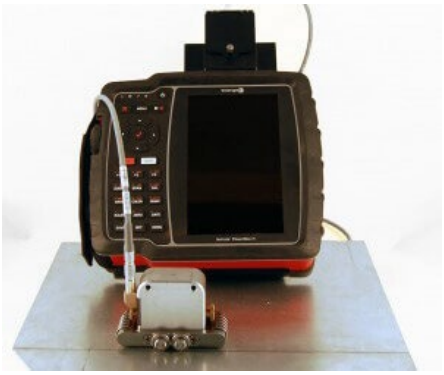

Figure A-23. Example EMAT controller

A.3.7 Welding Equipment

The welding equipment will be primarily GMAW with a minimum of 450 amps at 100 percent duty cycle power supply with an Ethernet I/P communication protocol (Figure A-25). The power supply will have pulse capabilities and be able to run multiple different wave forms. The welding torch and bundle will be a water-cooled configuration rated for 500 amps at 100 percent duty cycle. The wire feeder will be mounted to the boom arm of the bundle support mechanism, and

the boom arm height will be adjustable for easy wire feeder maintenance. The welding torch will be connected to one of the tool changer adapters.

Example welding power supply – Lincoln Power Wave R450:

- Power supply:
  - Rated output:
    - GMAW: 550A/41.5V/40% duty cycle
    - GMAW: 450A/36.5V/100% duty cycle
  - Input current:
    - 40% duty cycle: 37A
    - 100% duty cycle: 27A
  - Output current range:
    - 5–550A
- Wire feeder:
  - Wire feed speed range IPM (m/min):
    - 50–800 in./min (1.3–20.3 m/min)

Figure A-24. Example welding power supply

Abbreviations and Acronyms

ACRONYM	DEFINITION
AMS	Austenitic Manganese Steel
CTWD	Contact Work-to-Tip Distance
CV	Constant Voltage
CVN	Charpy V-Notched
EDM	Electrical Discharge Machined
FCAW	Flux-cored Arc Welding
FRA	Federal Railroad Administration
GMAW	Gas Metal Arc Welding
GMAW-P	Pulsed Gas Metal Arc Welding
MGT	Million Gross Tons
PT	Dye Penetrant Testing
RT	Radiographic Testing
SMAW	Shielded Metal Arc Welding
TTCI	Transportation Technology Center, Inc.
UT	Ultrasonic Testing
WBS	Work Breakdown Structure